ADHESION STUDY OF POLYMERIC MATERIAL

ON GLASS SUBSTRATE

By

MARTIN LEE JIAN HRONG

A project report submitted to the Department of Chemical Science

Faculty of Science

Universiti Tunku Abdul Rahman

in partial fulfillment of the requirements for the degree of

Bachelor of Science (Hons) Chemistry

SEPTEMBER 2018

ABSTRACT

Glass substrate which is made up of mostly silicon had a main disadvantage which is poor adhesion for polymeric material and this could reduce its binding efficiency. Approaches had been done in order to increase the adhesion between polymeric materials and glass substrate. In this study, poly(methyl methacrylate-*co*-acrylic acid) (PMMA-*co*-AA) is synthesized with trimethoxyvinylsilane (TMVS) as the bridging agent between glass substrate and polymeric materials. The PMMA-*co*-AA synthesized had been characterized by particle size analysis (PSA), thermogravimetric analysis (TGA), differential scanning calorimetry (DSC), scanning electron microscopy (SEM), atomic force microscope (AFM), Attenuated total reflectance fourier-transform infrared spectroscopy (ATR-FTIR) and inverted light microscope (IM). The particle size of the polymer synthesized were in the desirable range in between 102 to 108 nm. The result obtained from ATR-FTIR proved that the monomer used were successfully polymerized to from a macromolecule. The side view of the SEM image proved that increasing the concentration of TMVS, increases the thickness of the coated polymer layer on glass substrate due to increase in cross-linking. The peeling test revealed that P(MMA-*co*-AA) with 9 wt% of TMVS shows the best adhesion among other concentration by observing the surface morphology using SEM and AFM. The result shows that, P(MMA-*co*-AA) with 7 wt% of TMVS has the sufficient adhesion strength which gives the highest light harvesting efficiency on the solar cell.

ABSTRAK

Kaca substrat yang kebanyakan diperbuat daripada silikon mempunyai satu kelemahan iaitu kelekatan bahan polimer dan ini merendahkan kecekapan ikatan. Penyelidikan dah banyak dijalankan untuk meningkatkan kecekapan lekatan antara bahan polimer dan kaca substrat. Dalam kajian in, poli(metal metakrilat-*co*-acid akrilat) (PMMA-*co*-AA) telah disintesis dengan TMVS sebagai ejen merapatkan antara kaca substrat dan bahan polimer. PMMA-*co*-AA yang disintesis telah disifatkan oleh analisis size partikel, termogravimetri analisis, kalori pengimbasan kebezaan analisis, mikroskopi electron imbasan, mikroskop berkuatkuasa atom, pemerhatian keseluruhan refleksi spektroskopi inframerah empatier-transformasi dan mikroskop cahaya terbalik. Saiz zarah polimer yang disintesis berada dalam jarak yang diinginkan di antara 102 kepada 108 nm. Hasil yang didapati dari ATR-FTIR terbukti bahawa monomer yang digunakan telah berjaya dipolimerikan pada macromolecule. Pandangan sampingan imej SEM membuktikan bahawa meningkatkan kepekatan TMVS, meningkatkan ketebalan lapisan polimer bersalut pada substrat kaca kerana peningkatan dengan silang silang. Ujian mengupas mendedahkan bahawa P(MMA-*co*-AA) dengan 9 wt% TMVS menunjukkan lekatan yang terbaik di antara kepekatan lain dengan memerhati morfologi permukaan menggunakan SEM dan AFM. Hasilnya menunjukkan bahawa P(MMA-*co*-AA) dengan 7 wt% mempunyai kekuatan lekatan yang mencukupi memberikan kecekapan penyerapan cahaya tertinggi pada solar cell.

ACKNOWLEDGEMENTS

First of all, I would like to express my special appreciation and thanks to my supervisor, Assistant Professor Dr. Chee Swee Yong for providing me advices, patience, guidance throughout my final year project.

I would also like to appreciate the helping from our lab officers, Mr. Seou, Mr. Leong and Mr. Nicholas for their assistant and gentle reminder, and also appreciate my senior, Mr. Goh who gives lots of helps and guidance throughout my project.

A special thanks to my family. Words cannot express how grateful I am to my parents that always support and encourage me all the time. Last but not least, I would also like to say thank you to all my fellow friends who encourage me throughout my project.

DECLARATION

I, Martin Lee Jian Hrong hereby declare that the project report is based on my original work except for the quotation and citations which have been acknowledged. I also declare that it has not been previously and concurrently submitted for any other degree at University Tunku Abdul Rahman or other insititutions.

_____

(MARTIN LEE JIAN HRONG)

APPROVAL SHEET

I certify that, this project report entitled "**ADHESION STUDY OF POLYMERIC MATERIAL ON GLASS SUBSTRATE**" were prepared by MARTIN LEE JIAN HRONG and submitted partial fulfillment of the requirements for the degree of Bachelor of Science (Hons) Chemistry at Universiti Tunku Abdul Rahman.

Approved by,

_____

(Dr. Chee Swee Yong) Date : _____

Supervisor

Department of Chemical Science

Faculty of Science

University Tunku Abdul Rahman

FACULTY OF SCIENCE

UNIVERSITI TUNKU ABDUL RAHMAN

Date : _____

PERMISSION SHEET

It is hereby certified that **MARTIN LEE JIAN HRONG** (ID No.: **14ADB04637**) has completed this thesis entitled "**ADHESION STUDY OF POLYMERIC MATERIAL ON GLASS SUBSTRATE**" under the supervision of Dr. Chee Swee Yong from Department of Chemistry, Faculty of Science.

I hereby give permission to my supervisor to write and prepared manuscripts of these research findings for publishing in any form to UTAR community and public.

Yours truly,

_____

(MARTIN LEE JIAN HRONG)

TABLE OF CONTENTS

LIST OF TABLES

LIST OF FIGURES

LIST OF ABBREVIATIONS

AA	Acrylic acid
AFM	Atomic force microscope
APS	γ-aminopropyltriethoxysilane
APTS	3-acryloxypropyltrichlorosilane
ATR-FTIR	Attenuated total reflectance fourier-transform infrared spectroscopy
B	Boron
BF	Bamboo fiber
B_2O_3	Boric oxide
^oC	Degree celcius
CaO	Calcium oxide
$-CH_3$	Methyl group
cm	Centimeter
DSC	Differential scanning calorimetry
EB	Electron beam
EPOLA	Epoxidized palm oil acrylate
FTIR	Fourier-transform infrared spectroscopy
IM	Inverted light microscope
KPS	Potassium persulfate
LDI	Lysine based diisocyanate

$-OCH_3$	Methoxy group
-OH	Hydroxyl group
OH^-	Hydroxide ion
m	Meter/mass
M	Molar concentration
MA	Maleic anhydride
mg	Milligram
mL	Millilitre
MMA	Methyl methacrylate
mN	Millinewton
MPa	Mega Pascal
MPS	γ -methacryloxypropyltrimethoxysilane
Na^+	Sodium ion
Na_2O	Sodium oxide
NiTi	Nickel titanium
nm	Nanometer
PAA	Poly(acrylic acid)
PBS	Poly(butylene succinate)
PETIA	Pentaerythritol Triacrylate
PLA	Poly(lactic acid)
PMMA	Poly(methyl methacrylate)
PMMA-*co*-AA	Poly(methyl methacrylate-*co*-acrylic acid)
PSA	Particle size analyzers

PSD	Particle size distribution
PVC	Polyvinyl chloride
SAM	Self-assembled monolayer
SCA	Silane coupling agent
SDS	Sodium dodecyl sulfate
SEM	Scanning electron microscopy
Si	Silicon
SiO_2	Silicon dioxide
T_d	Decomposition temperature
TEA	Triethylamine
T_g	Glass transition temperature
TGA	Thermogravimetric analysis
TiO_2	Titanium dioxide
TMVS	Trimethoxyvinylsilane
TSC	Total solid content
UP	Unsaturated polyester
UV	Ultraviolet
V	Volume
VTES	Vinyltriethoxysilane
VTMOS	Vinyltrimethoxysilane
wt%	Percentage by weight

CHAPTER 1

INTRODUCTION

1.1 Glass substrate

Most of the glass produced commercially are made of silicon (Si). Silicon is one of the most abundant resources that could be found naturally in the earth's crust about 28 % by mass. Silicon is found mainly in sands, stone, gravel and granite. Owing to the abundancy of silicon, it is used as a raw material for making products such as window glass and kitchenware in view of its transparency and its capability to withstand high heat. Silicon is a group 14 element consisting of four valence electron on the outer shell occupying the outer s and p orbital. Therefore, silicon rarely occur in a pure state (Si) but mostly in combined form such as silicon dioxide (SiO_2) (Rsc.org, 2018).

Glass is a non-crystalline amorphous solid because lacking of orderly pack structure and long-range order characteristic if it is present in crystalline structure. The phenomena that causes the formation of amorphous structure are due to supercool effect. The raw materials are subjected to high temperature where they start to fuse together. During cooling, unstable solid are form due to shortage of time for the crystallization process and the formation of stable nucleation sites. Thus, glass exist as a disordered arrangement, but still cohesive to form rigid structure (Gibbs, 1996).

There are many types of glasses being made in this present-day by differing the composition of materials in glass production or by varying the rate of cooling to achieve the specific application. The abundance of silicon makes it easily available in the market in large quantity and the cost of the raw material is low. Besides, silicon is known to be a non-toxic element to both human being and the environment.

1.2 Silane coupling agent

Silane coupling agents are compounds usually consist of two different type of functional groups which is capable of forming strong chemical bond between organic and inorganic materials. Silane coupling agents are widely used because they are capable in binding organic materials to different polarity materials such as inorganic silica and alumina surface. Silane coupling agent are compatible almost with any organic polymer. The application of silane coupling agent as adhesion promoter shows improvement in the physical properties of composite materials such as adhesion on metal and glass, and resin-coated and painted metal (Sterman and Marsden, 1966).

For this study, trimethoxyvinylsilane (TMVS) was used as an adhesion promoter. The general formula of silane coupling agent usually possess two types of functional group. Figure 1.1 shows the general formula of a silane

coupling agent. The X group for TMVS is a methoxy group (-OCH_3). The methoxy group bonds chemically to the glass substrate through the condensation reaction with an active hydroxyl group (-OH) on the glass surface. The reaction yield a stable Si-O-Si bond with water as the by-product. The organofunctional group of TMVS is a vinyl group which is responsible for reacting with the polymer sample. The vinyl group can react with the unsaturated component of polymer through the free radical initiated polymerization reaction forming a stable C-C single bond (Faghihi and Shojaei, 2009).

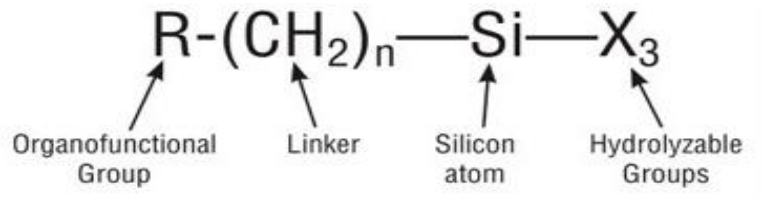

Figure 1.1: General formula of silane coupling agent (Gelest.com, 2018)

Silane coupling agent is added to treat the surface of the substrate so that polymer are able to bind firmly on the surface. The modification of substrate surface is maximized when the number of the coupling agent that reacts with the surface substrate and the number of reachable active hydroxyl group site increases. Figure 1.2 shows the effectiveness of silane coupling agent binding on the inorganic substrate. Different kind of substrates have different degree of interaction with the coupling agent which depends on the concentration of hydroxyl group exists on the substrate and type of hydroxyl present (Gelest.com,

2018). As listed in Figure 1.2, silane coupling agent is an excellent adhesion promoter for glass substrate. Therefore, silane coupling agent are suitable to be use as an adhesion promoter between polymer and glass substrate.

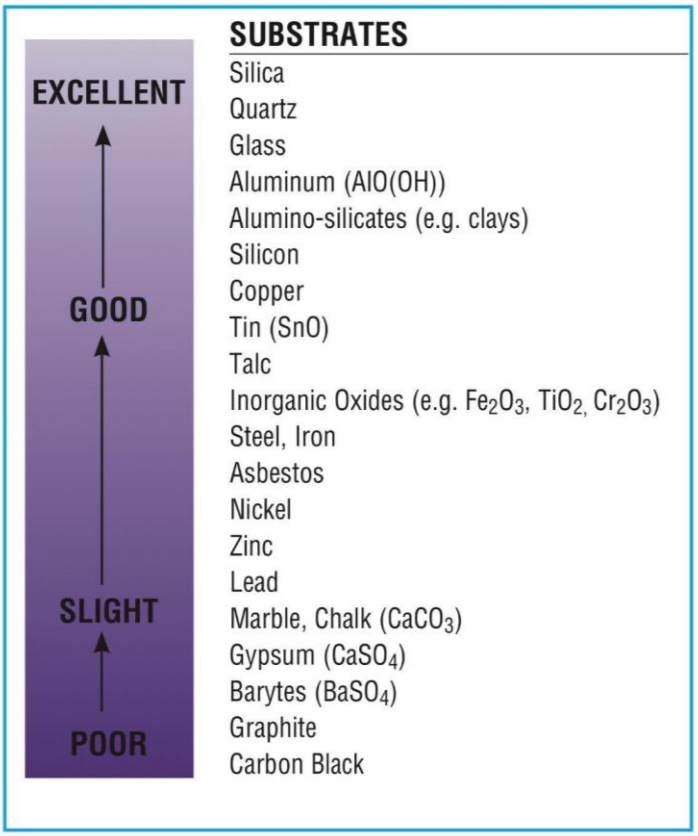

Figure 1.2: Effectiveness of silane coupling agent on inorganic substrate (Gelest.com, 2018)

1.3 Polyacrylate composite

Polymerization of acrylic ester monomers produce polyacrylates which are widely used in industry due to it high adhesion, transparency and fast curing

speed. In recent years, polyacrylates find its application in areas such as automotive products, leather finishing, adhesives tape and steel corrosion prevention. However, there are some major drawbacks that limit it applications such as wide molecular weight distribution, poor solvent resistance and poor mechanical properties. To improve the applications of polyacrylate, methods have been developed to control the chain length and molecular weight of polyacrylate, which subsequently determine the physical and mechanical properties of the polyacrylate (Wu et al., 2015).

1.3.1 Monomer

Monomer is the building block for polymer, where monomers are joined by covalent bond to form a large molecule network. The monomers used for this study are acrylic acid (AA) and methyl methacrylate (MMA). AA is a carboxylic acid molecule with a vinyl group attach to the carbonyl group while MMA is an ester with an extra methyl group ($-CH_3$) attach on the carbon of the vinyl group. For this study, emulsion polymerization will be carried out using MMA and AA as monomer to synthesize poly (methyl methacrylate-*co*-acrylic acid) [P(MMA-*co*-AA)]. Table 1.1 show the molecular structure of both the monomers.

Table 1.1: The molecular structures of MMA and AA

Monomer	Structure
Methyl methacrylate (MMA)	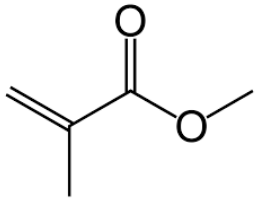
Acrylic acid (AA)	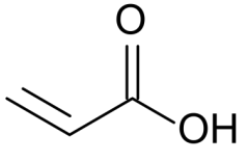

1.3.1.1 Methyl methacrylate (MMA)

Methyl methacrylate is largely produced from methacrylic acid as raw materials through acetone cyanohydrin route. The present of methyl group on the vinyl group causes the polymer chain to have certain degree of steric strain that prevent the chain to form a close dense packing which result in the formation of rigid and tough polymer. Besides, MMA have a high transparency of visible light and ultraviolet radiation properties compare to other monomer which find it usage in the manufacturing of LED light guide panels and lens caps to maximize the light emitting properties and energy saving (Hadi, Rahayu and Danu, 2013).

1.3.1.2 Acrylic acid (AA)

Acrylic acid (CH_2=CHCOOH) is a carboxylic acid with a vinyl group connected to the carbonyl carbon forming an unsaturated carboxylic acid. Acrylic acid is present in liquid form with colorless and pungent smell. Most of the acrylic acid are produced using vapor phase oxidation of propylene process. The oxidation process involved two reactors using two different catalysts, in the first reactor propylene was converted to acrolein which then completing the reaction in the second reactor to convert acrolein to acrylic acid (Laskowski, 1998). The monomer are widely used to synthesize copolymer and homopolymer including elastomer, adhesives, plastic and coating.

1.3.2 Homopolymer

When a single type of monomer are involve in polymerization reaction, the end product form a macromolecule where all the monomers are linked together to form a long polymer chain with a three-dimensional networks. The macromolecule that make up of one type of monomers are widely known as homopolymer (Polymer with the same repeating unit as the monomer used). Homopolymers find its usage when the crystallinity of the polymers is important for certain application because homopolymer is able to pack better compared to copolymers. (Andrews and Kazama, 1967).

1.3.3 Copolymer

Copolymer consists of two or more monomers reacting together through polymerization reaction to form a three-dimensional macromolecule network. Recently, copolymer have been widely used in many industries because copolymerizing different monomer gives an excellent improvement in the chemical and physical properties. Copolymer can be categorized by the arrangement of the monomers, since more than one type of monomers are involved. It is categorized as alternating copolymer, random copolymer, grafted copolymer and block polymer.

1.4 Emulsion polymerization

Emulsion polymerization is a method of conducting the polymerization reaction of a monomer usually in aqueous (water) medium. This type of emulsion polymerization is an oil-in-water emulsion where the monomer (organic) as the dispersed phase and water (inorganic) as the continuous phase. Emulsion polymerization reaction is widely used in many production industries such as paints, textile coating and adhesives applications because it is more preferred to organic solvent-based products due to the absent of solvent in the products and thus is more environmental friendly (Asua, 2004).

The basic components for the emulsion polymerization are monomer (MMA and AA) as reactant, water as the solvent for reaction medium, thermal initiator (potassium persulfate) to initiate the free-radical in monomer for radical polymerization reaction and emulsifier (sodium dodecyl sulfate) as surfactant for stabilizing the emulsion preventing the polymer particle to coagulate. This reaction is a type of radical polymerization by which polymer are formed by consecutive addition of free-radical monomers. At the end of the reaction, termination of radical takes place to end the growing polymer chain.

The advantages of using emulsion polymerization reaction are higher rate of polymerization to yield high molecular weight polymer with low polydispersity, low viscosity polymerization emulsion which facilitates monolayer coating and using water as solvent which enables better heat control because water has higher heat capacity compared to organic solvent. However, the disadvantages are separation of emulsifier from the polymer are often difficult and removal of emulsifier would cause coagulation. Besides, emulsifier would lower the transparency properties of the polymer. In view of this, the amount of emulsifier added should be sufficient for the purpose only (Asua, 2004).

1.5 Problem Statement

P(MMA-*co*-AA) are widely used as anti-reflective film, protective film, adhesives and etc. The major drawbacks of P(MMA-*co*-AA) in the application is that the coating suffer a low adhesion on silicon substrate because both material are not compatible with each other. The glass substrate is an inorganic material whereas the polymer is an organic materials. The hydrophobic nature of polymer causes low wettability on hydrophilic glass surface. Wettability is referred to the tendency of the polymer to spread or adhere to the glass substrate.

Therefore, a strong and stable adhesion must be present between the P(MMA-*co*-AA) and glass substrate in order to overcome the high photon energy from sunlight which is capable to break the bond at the interface and gives strong weathering resistance for outdoor purpose. In this study, silane coupling agent is added as an additive to modify the surface of the glass substrate. The adhesion between two different material increases in the present of silane coupling agent due to its capability to react with organic and inorganic material.

1.6 Objectives

The objectives of this study are stated below:

1. To synthesize [P(MMA-*co*-AA)] with TMVS as a coupling agent through emulsion polymerisation.
2. To study on the relationship between the concentration of TMVS incorporated into the polymer and its corresponding effect on the adhesion of the polymeric material on glass substrate.
3. To characterize the P(MMA-*co*-AA) with TMVS using total solids content, particle size analyzer, scanning electron microscopy (SEM), thermogravimetric analysis (TGA), attenuated total reflectance fourier-transform infrared spectroscopy (ATR-FTIR) analysis, differential scanning calorimetry (DSC), inverted light microscopy and Atomic force microscopy (AFM).

1.7 Scopes of study and limitation

In this study, P(MMA-*co*-AA) is synthesized using emulsion polymerization with MMA and AA as monomers. During emulsion polymerization, different amount of TMVS (1, 3, 5, 7 and 9 wt%) will be incorporated into the polymer. The solvent used is distilled water which forms

an oil-in-water emulsion which is stabilized by the addition of sodium dodecyl sulfate (SDS) as surfactant. Potassium persulfate (KPS) which serve as a thermal initiator will be used to initiate free radicals for polymerization reaction to occur.

The emulsion polymer will be coated onto hydroxylated glass substrate using dip coating technique. The emulsion polymer is diluted to 20 mg/L with distilled water for the coating process. The coated glass slide was placed in an oven for the curing of the polymer coating. The coated glass slide will be tested with peeling test with adhesive tape and the surface morphology will be study under an inverted light microscope with the magnification power of 400X. The effect of TMVS on P(MMA-*co*-AA) coating on glass substrate will be studied.

Besides that, several characterization tests will be carry out to determine the characteristic of the polymer produced, which include total solids content, particle size analyzer, thermogravimetric analysis (TGA), attenuated total reflectance fourier-transform infrared spectroscopy (ATR-FTIR) analysis, scanning electron microscopy (SEM), differential scanning calorimetry (DSC), inverted light microscope and Atomic force microscope (AFM).

There are some limitation in this study, increasing the amount of TMVS might not increase the adhesion between P(MMA-*co*-AA) and glass substrate proportionally as expected. Excessive amount of TMVS may decrease its chance to attach to P(MMA-*co*-AA) because TMVS might also interact among

themselves through the unsaturated double bond (vinyl group) in the present of free radical initiator. Therefore, the suitable amount of TMVS incorporated into P(MMA-*co*-AA) will be determine in this project.

CHAPTER 2

LITERATURE REVIEW

2.1 Silane coupling agent

Chemical bonding between organic materials and inorganic surface has long been developed for protective coating on various metal and glass surface. However, major drawback of dissimilar materials and weak resistance toward water causes the loss of adhesion strength of the organic materials on inorganic surface. Therefore, the need of new bonding technique arose in the mid 1900 to improve the adhesion strength and the resistance toward different weathering effect. Today, the most commonly use coupling agent for polymer and inorganic substrate are silane based coupling agent (Plueddemann, 1991).

2.1.1 Type of silane coupling agent

Through years of researching on the adhesion between polymer and glass substrate, many types of coupling agent with different functional groups have been developed for polymer with different functional groups. Owing to the wide variety of coupling agent, it is applied in many areas such as anti-reflective coating, adhesion and etc. Silane coupling agent is known for having bifunctional groups which may react with two dissimilar materials by acting as a bridge to connect both the materials together. The general formula of silane

coupling agent is R-$(CH_2)_n$-Si-X_3 (n = 1, 2, etc) where R is an organofunctional group and X represent alkoxy group (Xie et al., 2010). Table 2.1 shows the commercially available coupling agent.

Table 2.1: Commercially available coupling agent (Kalita and Netravali, 2015).

No.	Functional group	Chemical formula	Applicable polymers
1	Vinyl	CH_2=CHSi$(OC_2H_5)_3$	unsaturated polymers
2	Chloropropyl	Cl$(CH_2)_3$Si$(OCH_3)_3$	Epoxy, epoxide
3	Epoxy	$(C_3H_5O)O(CH_2)$Si$(OCH_3)_3$	Elastomers, epoxy,
4	Methacryl	(C_3H_5)COO(CH_2)3Si$(OCH_3)_3$	Unsaturated polymers,
5	Amine	$H_2N(CH_2)_3$Si$(OC_2H_2)_3$	Phenolic, nylon, epoxies
6	Phenyl	C_6H_5Si$(OCH_3)_3$	polystyrene
7	Mercapto	HS$(CH_2)_3$Si$(OCH_3)_3$	Almost all resin
8	phosphate	$C_6H_{10}O_8Ti.{}_2H_4N$	Polyolefin, polyester,

2.1.2 Reaction of silane coupling agent

According to Plueddemann (1991), both ends of the silane coupling agent are capable of undergoing two different chemical reactions, either simultaneously or separately. Silane coupling agent is a compound that can be handled easily when all the conditions are controls properly. The R groups can be replaced without altering the X group, or the X group may be modified while retaining the R group. If the X group is modified in an aqueous environment, the R groups are simultaneously hydrolyzed forming free hydroxyl group. Chemical reactions of the X group may precede application to a surface or may take place at a surface after silylation. The type of organofunctional group to be used is determined by its compatibility with the polymer, while for hydrolysable group are only intermediates for the formation of silanol groups which facilitate its bonding to glass substrate.

As reported by Hertl (1968), the reaction mechanism between the alkoxy groups on the coupling agent with the non-hydrogen bonded hydroxyl group of silica on the glass substrate was known as the condensation reaction. The rate determining step for the reaction to occur is determined by the physical absorption of the alkoxy group onto the hydroxyl group of silica on the glass substrate and the reachability of the hydroxyl group. Before condensation occurs, the alkoxy groups are hydrolyzed by water to produce silanol and alcohol as by-products.

According to Jörg (2017), organofunctional group has the capability to react with an appropriate polymer depending on the functional group present on the polymer. Large number of polymer with different functional groups can be tailored as a function of the polymer matrix to be used. Table 2.1 shows the different types of organofunctional group which are suitable for the polymeric materials. Silane can form a Self-Assembled Monolayer (SAM) on the glass substrate surface with one layer molecule. Nowadays, they have various applications in the areas of reinforced composites, coatings, adhesives, paints, inks and elastomers.

For this study, silane coupling agent is used as an adhesive promoter to increase the adhesion of P(MMA-*co*-AA) on the surface of glass substrate. The coupling agent used was TMVS where the organofunctional group, R is a vinyl group and the alkoxy group, X is a methoxy group. The three hydrolysable methoxy group in the TMVS are hydrolyzed with three water molecules to produce three free hydroxyl groups with three methanol molecules as by-products. In emulsion polymerization, water is used as the solvent medium which promotes the hydrolysis process (Xie et al., 2010). Figure 2.1 below shows the hydrolysis reaction of TMVS to silanol.

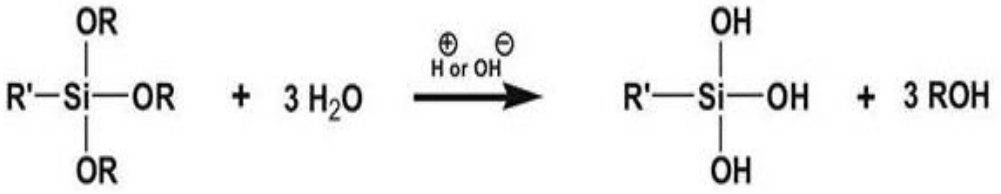

Figure 2.1: Hydrolysis of Trimethoxyvinylsilane to silanol (Xie et al., 2010)

According to Simal, Demonceau and Noels (1999), the organofunctional group of TMVS is capable to react with unsaturated polymeric materials. During the free radical polymerization reaction, the vinyl group on the coupling agent react with MMA and AA monomer to form P(MMA-*co*-AA) when TMVS is incorporated. The reaction take place through the unsaturated carbon double bond in the presence of KPS as thermal initiator to initiate the free radical molecules. Figures 2.1 – 2.6 show the mechanism of free radical polymerization of MMA, AA and TMVS and the chemical structure of P(MMA-*co*-AA) incorporated with TMVS.

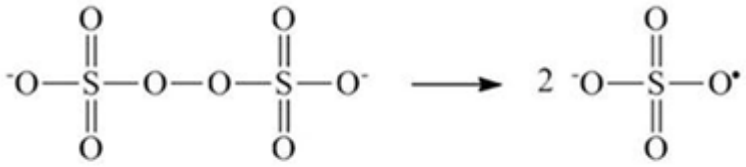

Figure 2.2: Formation of free radical by homolytic reaction of potassium persulfate

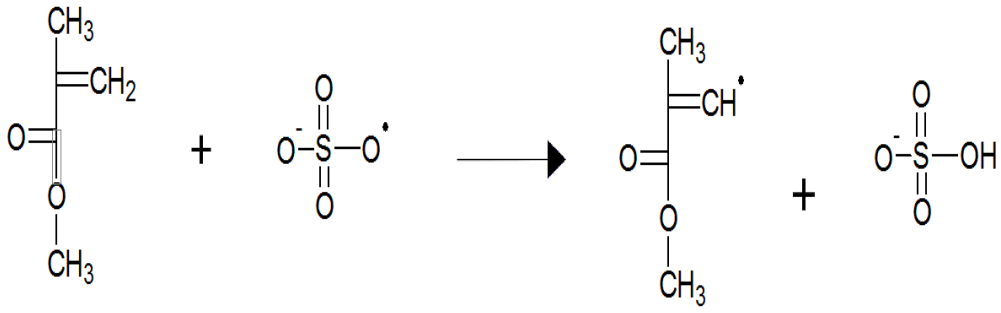

Figure 2.3: Abstraction of hydrogen form MMA to form free radical MMA

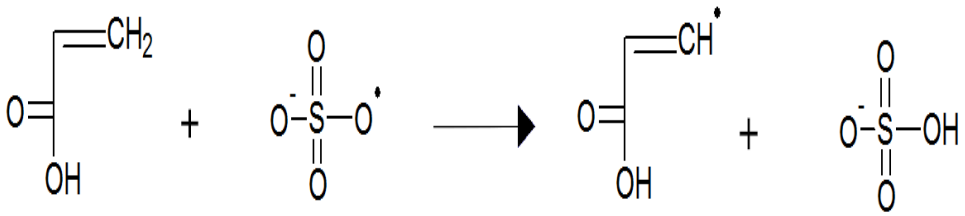

Figure 2.4: Abstraction of hydrogen from AA to form free radical AA

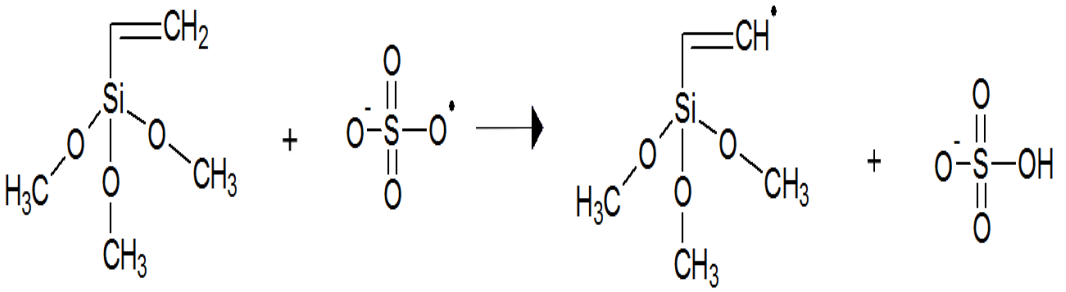

Figure 2.5: Abstraction of hydrogen form TMVS to form free radical TMVS

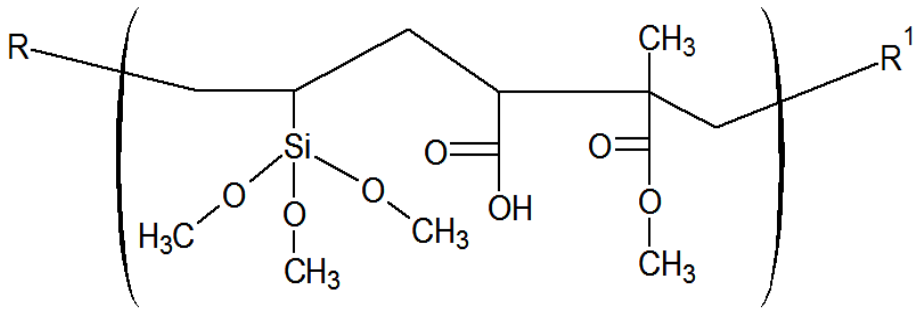

Figure 2.6: Chemical structure of P(MMA-*co*-AA) incorporate with TMVS

2.2 Effect of incorporation of silane coupling agent into polymeric matrix

According to Kaynak, Celikbilek and Akovali (2003), they found some of the silane coupling agent used were able to improve the interface between the treated rubber particles and epoxy matrix. The result obtain revealed an increase in tensile strength and elastic modulus values while a slight decrease in the toughness value of the sample produced. The rubber particles and epoxy matrix are usually incompatible with each other which lead to a poor interfacial and adhesion strength. The rubber particles treated with silane coupling agent showed some improvement in the tensile strength and the elastic modulus values of the system. Four out of the seven types of silane coupling agent used in the study showed significant results in the tensile strength and elastic modulus: methyltrimethoxysilane shows an increase of 7.0% on the tensile strength and 3.03% on the elastic modulus compare to the untreated sample; 3-aminopropyltriethoxysilane shows an increasing value of 15.7% on the elastic modulus value and 15.3% on the tensile strength; hexadecyltrimethoxysilane shows the highest increase in value of 17.1% in the elastic modulus and a slight decrease of 5.3% in the tensile strength; lastly, octadecyltrimethoxysilane shows an increase of 10.1% in the elastic modulus value and 18.5% in the tensile strength. However, silane coupling agent also shows to cause a slight decrease in the toughness of the sample. This is mainly due to the incompatibility of the rubber particles with epoxy matrix. The rubber particle which is hydrophobic has a poor bonding with the hydrophilic epoxy matrix. Increasing in adhesion lead to an improvement in tensile strength and elastic modulus value.

As reported by Nachtigall, Cerveira and Rosa (2007), organosilane as coupling agent is widely use as surface modifier for polypropylene/wood-flour composites. The treated surface shows significant improvement in the water-absorption behavior, tensile properties and thermal degradation properties as compared to the untreated polypropylene/wood-flour composites and polypropylene modified with maleic anhydride. The use of vinyltriethoxysilane (VTES) as coupling agent proved that silane show higher reactivity toward polypropylene chains compared to maleic anhydride (MA). In the study, same molar concentration of VTES and MA were used (1.54 mol %). The result obtain shows an increase in the concentration of functional group attached to the polymer chain for VTES with 0.84 mol % higher than the MA treated system (0.88 mol % for VTES and 0.04% for MA). Treatment with MA produced a lower concentration of functional group attach to the polymer chain, due to its low miscibility in non-polar substance. As VTES is less polar than MA, it can mix better with polypropylene. Thus, it allows higher degree of functionalization despite its bulkiness. Besides, the tensile strength for pure polypropylene and for the composition containing 30 wt% of wood fiber were 23 MPa and 15 MPa respectively. The result showed that the addition of wood fiber restrict the reinforcing effect, due to the incompatibility of both materials resulting in low interfacial adhesion. The tensile strength increased up to 28 MPa when the coupling agent was added. The material incompatibility between both materials was eliminated through the establishment of strong interaction with the bifunctional coupling agent as the interface between wood fiber and polymeric materials.

According to Park and Jin (2001), γ - methacryloxypropyltrimethoxysilane (90 wt%, MPS) with γ-aminopropyltriethoxysilane (10 wt%, APS) were applied for surface treatment of glass fibers to study on the adhesion, contact angle, critical stress intensity factor and mechanical interfacial properties. FT-IR spectroscopy was used to observe the glass fiber before and after the hydrolysis of the silane coupling agent. The FT-IR spectra before the hydrolysis of MPS/APS shows a strong peaks at 2947 and 819 cm^{-1} which shows the presence of Si-CH_3 group of MPS. For APS, the primary amine functional group shows peak at 3421 and 3371 cm^{-1} while peaks at 943 and 820 cm^{-1} are observed due to the presence of Si-OC_2H_5 which is the hydrolysable group of APS. After hydrolysis, the peptide bonding interaction occurs between –N-H of APS and C=O of MPS causes the decrease of intensity in C=O peak. Besides, two new peaks are present at 3367 and 1032 cm^{-1} due to –OH and Si-OH group respectively. According to the contact angle measurement, the glass fiber that was treated with silane showed an increase in surface free energy, due to hydrogen bonding between coupling agent and glass fiber which plays an important role to improve the degree of adhesion at the interface of the system. The result reveal the total surface free energy showed an increase to a maximum at 0.2 wt% of MPS/APS present. This indicates that treatment with silane coupling agent leads to a change in the surface of the glass fiber and results in the increase in hydrophilic properties. Critical stress intensity factor at 0.2 wt% silane-treated composites was the highest at about 3.98 $MPa \cdot m^{1/2}$ due to the present of peptide bond. Moreover, the mechanical interfacial properties decreases above 0.2 wt% of silane concentration due to the excessive amount of silane forms a weak physisorption boundary layer.

Lee and Wang (2006), stated that incorporation of lysine based diisocyanate (LDI) coupling agent into poly(lactic acid) (PLA) and poly(butylene succinate) (PBS) on bamboo fiber (BF) to improve the interfacial adhesion, tensile strength and water resistance properties. The melting point remains constant after the addition of LDI but the heat fusion of both composite system decreases. The thermal degradation temperature test showed that composite with LDI have a higher degradation temperature than composite without LDI and biodegradability of both composite with LDI using Proteinase K and Lipase PS showed a delayed in degradation. Figure 2.7 shows the SEM micrographs of the surface morphology of PBS and PLA/BF composite with and without the addition of LDI. Figure 2.7 (A) and (C) show clearly that most of the polymeric matrix was peeled off from the BF and creates a large visible gap. The findings proved that the interaction between BF and polymeric matrix was very weak in the interfacial adhesion due to the incompatibility of the materials. For the tensile strength test, PLA-BF composite show an increase of tensile strength from 29 to 42 MPa while Young's modulus increased from 2666 to 2964 MPa after the addition of LDI. Also for PBS/BF composites increases from 21 to 34 MPa while for Young's modulus not much changes were observed. Both composite shows an improvement in thermal degradation temperature after the addition of LDI because cross-linking between the BF and polymeric matrix has resulted in the increase of degradation temperature.

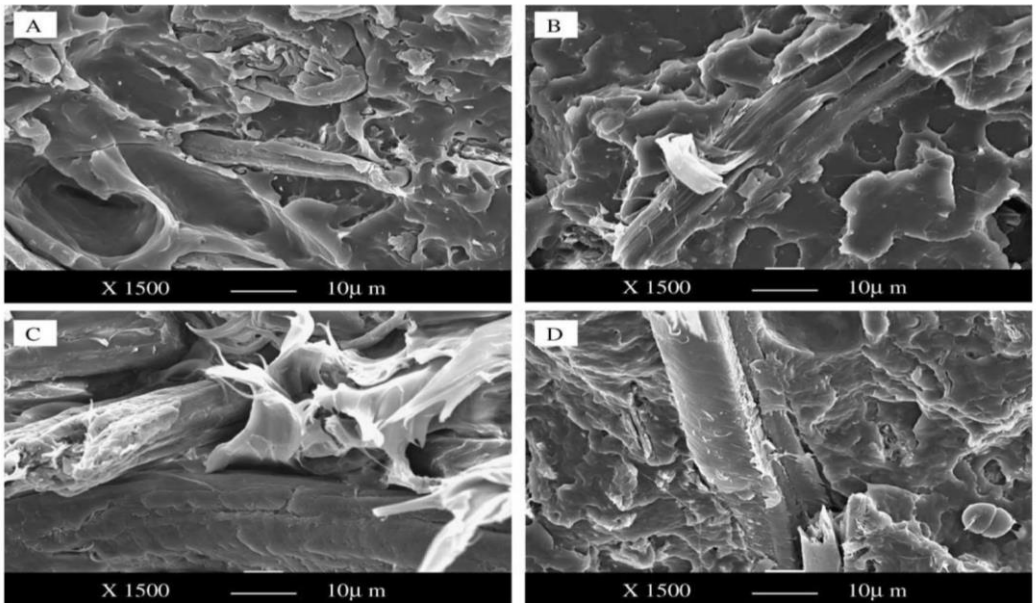

Figure 2.7: SEM micrographs of PLA/BF (70/30) composite without (A), or with LDI (N-C=O content, 0.65%) (B), and PBS/BF (70/30) composite without (C), or with LDI (N-C=O content, 0.65%) (D).

As reported by Smith et al. (2004), the surface of nickel titanium (NiTi) alloy modified with silane coupling agent shows an improvement of 100% in interfacial adhesion compared to the untreated system. The amount of carbon and oxygen content for the modified and unmodified surfaces are observed using X-ray Photoelectron Spectroscopy. The result obtained shows the oxygen content for the unmodified NiTi surface are predominantly presence in the form of TiO_2 while the modified NiTi surface with silane coupling agent such as 3-acryloxypropyltrichlorosilane (APTS) and trimethoxysylylpropylmethacryate (MPS) are predominately in the Si-O-Si and Si-O-Ti bond which proved chemical bonding occurred between the NiTi surface (polar) with the polymeric materials (non-polar). The peeling test was done to characterize the adhesion properties. The result obtained shows modified surface with APTS and MPS coupling agent have an increase of roughly 85 to 90 % on the average maximum

adhesion strength compared to the unmodified surface. Figure 2.8 shows the average maximum adhesion strength. The improved adhesion prolong the life time and the overall strength of the composite system. Thus, debonding and peel off were reduced with a precise control on the composition of the composite system.

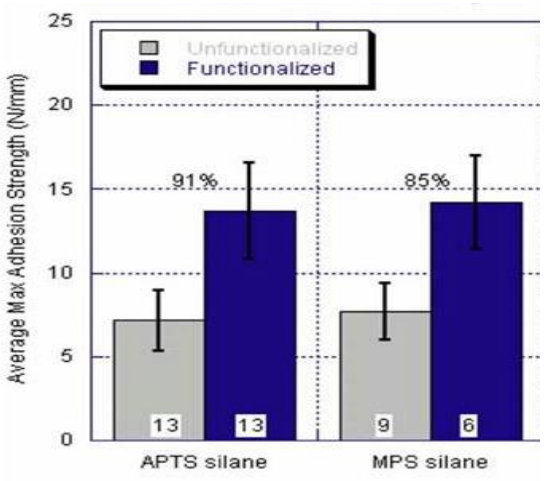

Figure 2.8: Comparison of the adhesion strength of modified and unmodified surface with APTS and MPS silanes.

According to Chand and Dwivedi (2006), research had been conducted to study on the abrasive resistance properties of jute fiber reinforced polypropylene composites with and without the grafting of silane coupling agent. SUGA abrasion tester have been used to study on the effect of composites after jute fiber was grafted with maleic anhydride as adhesion enhancer. The advantages of using reinforcing thermoplastic composites with natural fiber are low cost and availability of natural fiber in large quantity. But debonding occurs between the fiber and polymeric materials within a certain period due to low

wettability and adhesion properties. Natural fiber are a polar material which lead to poor wettability with the polymeric materials due to its high affinity toward water. The results shows that treated jute fiber reinforced polypropylene composites have an increase in tensile strength of around 2 MPa and an increase in elongation properties by 2.0% compared to untreated jute fiber reinforced composition. The major reason for the improvement of the tensile strength and elongation properties are enhancement of fiber matrix adhesion and stress transfer through interface via silane coupling agent. The improved tensile strength also resulted in the reduction in the amount of natural fiber being peel off and lesser fiber-matrix debonding.

2.3 Effect of curing process

Curing process is widely used in many industry for the purpose of converting a viscous liquid into a strong rigid amorphous packing materials through increasing the amount of cross-linking. The curing process generally result in higher elasticity, tensile strength, resistance toward high temperature exposure and peel off properties. Many types of curing process have been developed. The common ones are heat curing, ultraviolet radiation, electron beam and incorporation of chemical additives (Oh et al., 2016).

As reported by Monticelli et al. (2006), the bond strength of the coupling agent is strengthen after the air-drying process. The result shows air-drying at different temperature (21^{o} and 38^{o}C) gives different microtensile bond strength. For air-drying of sample at 38^{o}C, a significant increase in bond strength ($p < 0.001$) was observed with microtensile bond strength of 11.6 MPa for glycidoxipropyltrimetil-oxisilane and 11.7 MPa for γ-trimethoxysilyilpropylmethacrylatesilane/4-methacryolxyethyltrimellitate anhydride. For 3- methacryloxypropyltrimethoxy-silane no different were observed when air-drying for 21^{o} and 38^{o}C. The use of silane proved to enchance the bond strength by increasing the wettability of the fiber surface and facilitate diffusion of the composite resin to the remaining space in the fiber. Two phase were present which are the loosely bound physisorbed layer and stable bounded chemisorbed layer on the fiber surface. Besides that, introducing heat to the composite system increases the rate of condensation reaction and forming a tightly packed system via the coupling agent on to the fiber surface. During condensation process, solvent are present as by-product which could affect the adhesion of the coupling agent on to the fiber surface. The air-drying process helps in the removal of solvent and excess silane which is loosely bound.

In a study by Said et al. (2013), it was found that crosslinking occurred within the nano-particle with silane coupling agent as modifier. The formation of crosslinking was due to the exposure of ultraviolet (UV) and electron beam (EB), thus producing a significant modification effect on the viscoelastic properties of the composites system. Figure 2.9 shows the weight loss of materials during the abrasion test. The result proved that coating cured with UV

showed a better resistance toward abrasion compared to the coating cured with EB. The curing process of EB is relatively more uniform compare to UV. The EB curing have a uniform hardness, thus it have a weaker shock resistance which lower down the abrasion resistance properties.

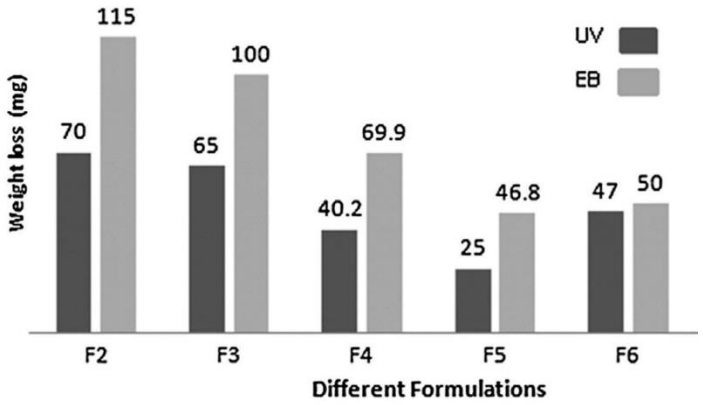

Figure 2.9: Abrasion resistance of radiation (UV/EB) cured coatings

According to Liu et al. (2001), the interaction of methacryloxypropyltrimethoxysilane (MPS) with fumed silica and poly(methyl methacrylate) (PMMA) composite system with and without curing process have been studied. It was found that the silane coupling agent methacryloxypropyltrimethoxysilane (MPS) was removed after being washed with methanol, but with curing in the vacuum at 25^{o}C, the MPS was firmly adsorbed and remained intact with the composite system. It was also found that drying at 110^{o}C for 2 hours result in the removal of loosely bound MPS while increasing the amount of firmly bound MPS. The result from thermogravimetric analysis (TGA) shows a loss of weight firstly in between 50^{o} and 150^{o} C, secondly between 350^{o} and 425^{o}C. The first weight loss were due to the loosely

bound silane and increased with increasing amount of MPS. The composite system that was dried in 110^{o}C for 2 hours in 1 atm, showed only one weight loss in TGA which that occurred between 320^{o} to 425^{o}C. The table 2.3 shows the comparison of composite system curing at 25^{o}C in vacuum and 110^{o}C in 1 atm. The result obtain revealed that curing at 110^{o}C have a lesser weight loss percentage around 1 to 3 % compared to the sample cured at 25^{o}C in vacuum

Table 2.2: Comparison of composite system curing at 25^{o}C in vacuum and 110^{o}C

Curing condition	Silanated silica	Total weight lost %	Loosely adsorbed %	Firmly adsorbed %
25^{o}C in vacuum	1% MPS in ethanol	0.96	0.37	0.59
	5% MPS in ethanol	3.65	1.39	2.26
	1% MPS in acetone	2.05	1.2	0.85
	5% MPS in acetone	6.94	5.56	1.38
Curing at 110^{o}C	1% MPS in ethanol, 110^{o}C	0.69	NA	0.69
	5% MPS in ethanol, 110^{o}C	2.6	NA	2.6
	1% MPS in acetone, 110^{o}C	1.3	NA	1.3
	5% MPS in acetone, 110^{o}C	2.6	NA	2.6

2.4 Factors affecting the adhesion

2.4.1 Number of alkoxy group in silane

According to Miller and Berg (2003), silane coupling agent with different number of alkoxy groups but the same organofunctional group were tested on the adhesion strength on glass beads. It was found that the silane with mono-alkoxy group have a low adhesion strength while for di- and tri-alkoxy groups an increase of adhesion strength were observed. The mono-alkoxy silane shows no significant changes on the adhesion with the untreated glass beads because only one bonding could take place for one silane. While for di- and tri-alkoxy groups more than one bonding were present to condense with other available silanes on the surface or with neighboring silane groups. Thus, the vertical condensation give an addition advantage to bind strongly together forming a strong coating.

2.4.2 Solubility of silane coupling agent in aqueous

Most of the silane coupling agent are known to be insoluble in aqueous phase, but upon hydrolysis of alkoxy group to form hydroxyl group it become soluble in aqueous phase. In order for the alkoxy group to be hydrolyze, the silane coupling agent needs to be in contact with the water molecule. This criteria makes silane coupling agent very difficult to be hydrolyze in aqueous

phase and slow reaction rate in organic phase as well. The common method used to speed up the rate of hydrolysis is by shaking it with acidified water till a clear solution is obtain. Addition of emulsifying agent, can further increase the rate of hydrolysis. The mechanism of acid catalyzed hydrolysis were initiated by the attacking the oxygen on the alkoxy group by hydronium ion. Then, SN_2 reaction take place to displace the leaving group with water. The result obtained by Plueddemann showed that acid catalyzed hydrolysis have a higher rate of first step hydrolysis compared to base catalyzed hydrolysis. Table 2.3 shows the rate of hydrolysis at different pH.

Table 2.3: Hydrolysis of silane coupling agent in acetone-water (Blum et al., 1991)

R-group of coupling agent	Acetone-water ratio	pH	k (s^{-1})
Methacryloxypropyltrimethoxysilane	10:1	1.0	Fast
	10:1	3.9	0.38
	5:1	4.5	0.95
Vinyltrimethoxysilane	10:1	1.0	Fast
	5:1	4.5	3.3
	5:1	3.6	3.5
γ-glycidoxypropyltrimethoxysilane	5:1	4.5	0.63
	5:1	3.6	2.0
	1:1	3.6	Fast

CHAPTER 3

METHODOLOGY

3.1 Chemicals

In this study, emulsion polymerization technique was performed to synthesize P(MMA-*co*-AA). Emulsion polymerization is a technique based on the oil-in-water emulsion principle where the monomers act as the discontinuous phase while the water act as the continuous phase with surfactant stabilizing the emulsion solution. Table 3.1 shows the chemicals and materials that was used for emulsion polymerization and Table 3.2 shows the chemical used for cleaning the glass substrate.

Table 3.1: Chemicals used for emulsion polymerization

Chemical	Function	Producer
Methyl methacrylate	Monomer	DAEJUNG
Acrylic acid	Monomer	Merck
Potassium persulfate	Thermal Initiator	Sigma-Aldrich
Sodium dodecyl sulfate	Emulsifier	Systerm®
Trimethoxyvinylsilane*	Additives	Merck

* Trimethoxyvinylsilane is a coupling agent used as adhesion promoter

Table 3.2: Chemicals used for the cleaning of glass substrate

Chemical	Function	Producer
30 % Ammonia solution	Reducing agent	R&M Chemicals
Hydrogen peroxide	Oxidizing agent	Systerm®

3.2 Procedure

To study the adhesion of polymeric material on glass substrate, three major procedures were performed. Firstly, to carry out emulsion polymerization to synthesis P(MMA-*co*-AA) with the incorporation of TMVS as additive. Secondly, to coat glass substrate with polymeric material using dip coater. Lastly, to study the adhesion between polymeric material and glass substrate.

3.2.1 Synthesis of P(MMA-*co*-AA) by emulsion polymerization technique

Emulsion polymerization technique was used to synthesize P(MMA-*co*-AA). Table 3.3 below shows the amount of chemicals and materials used for emulsion polymerization. Sodium dodecyl sulfate ($NaC_{12}H_{25}SO_4$) was added to act as an emulsifier to form a stable emulsion system. Potassium persulfate

($K_2S_2O_8$) was added to act as a thermal initiator to promote the formation of free radical to initiate the polymerization process. For this study, different amount of TMVS was added as additive to the emulsion polymer.

Table 3.3: Ingredients for emulsion polymerization

Materials	**Quantity (g)**
Distilled water	390.00
Sodium dodecyl sulphate (30%)	6.00
Potassium persulfate	0.70
Methyl methacrylate	95.00
Acrylic acid	5.00
Trimethoxyvinylsilane	Vary from 1.0 to 9.0 wt%

In the beginning, 200 mL of water and 0.600 g of SDS solution was added to the reactor flask. The reactor flask was heated up to 75^{o}C in the water bath. Then, 12.5 mL of the initial monomer and 0.35 g of initiator KPS were added at the same time. After 15 minutes, the remaining monomers with SDS and KPS were added into the reactor flask dropwise for an hour. Next, the polymerization reaction was allowed to carry on for another 2 hours before the reaction was stopped. The product was cooled at room temperature for about 30 minutes. The P(MMA-*co*-AA) was then transferred to a plastic bottle and kept for further study.

3.2.2 Treatment of glass substrate

The glass substrate used for the coating of polymeric material was cleaned with distilled water under ultrasonication for about 30 minutes. The glass substrate were then immersed into a mixture with the composition of distilled water: hydrogen peroxide: 30 % ammonia solution in a ratio of 5: 1: 1 and heated at 67 °C and washed for 30 minutes in order to hydrophilize its surface. Then, the glass substrate was taken out to dry in a vacuum oven at 60 °C. The treated glass substrate were ready to be used for coating (Wang, Liu and Liu, 2017).

3.2.3 Dilution of polymer emulsion

The emulsion polymer was diluted to a concentration of 20 mg/mL by diluting it with distilled water to 100 mL in a 100 mL volumetric flask. The polymer emulsion was then undergone ultrasonication for 30 minutes to achieve a homogeneous emulsion polymer. After that, the polymer emulsion was used to coat on the glass substrate using a dip coater.

3.2.4 Testing on the adhesion of P(MMA-*co*-AA) on glass substrate

The adhesion of the polymeric material on glass substrate was tested using the peel adhesion method. This method give an indication of how easy a polymeric material can be peel off from the glass substrate. For this study, adhesive tape was used as the peeling aid. In the beginning, half of the coated glass substrate was pressed with the adhesive 3M tape. The adhesive tape was even out using a ruler to ensure no air pocket were present between the adhesive tape and glass substrate (Kendall, 1971).

The adhesive tape was peeled at 180^{o} parallel to the adhesive tape that was still adhere to the glass substrate. The peeling process was carried out in a rapid and complete manner to ensure no residue leftover was on the glass substrate which would cause discrepancy in the result obtained (Kendall, 1971). Then, the peeled glass substrate was viewed under inverted microscope to study its surface morphology. Two sampling point were scanned for each of the unpeeled and peeled sample.

The result obtained from inverted microscope was used to determine the concentration of TMVS in polymer that would achieve the best adhesion between the polymeric material and glass substrate by comparing the peeled and the unpeeled result. The emulsion polymer variant with the best adhesion would be used to further study its effect on the light harvesting efficiency of solar cell coated with the polymer nanospheres.

3.2.5 Power output measurement of solar cell

The same treatment were used to treat the solar cell as for the preparation of glass substrate before coated with P(MMA-*co*-AA). The same dilution emulsion technique were used for the preparation of emulsion solution. Solar cell was coated with polymer using a dip coater.

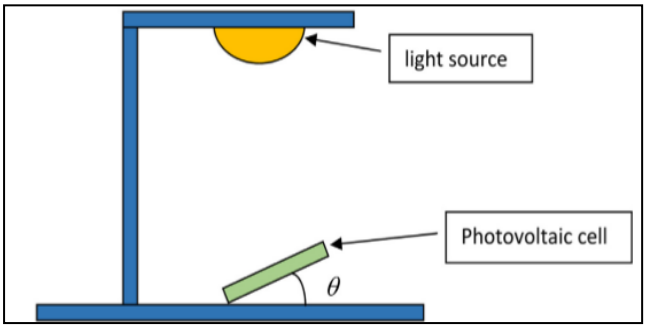

Figure 3.1: A diagrammatic representation of experimental setup for solar cell power output measurement (Lee et al., 2017)

The voltage and current of the solar cell coated with P(MMA-*co*-AA) were measured using multimeter under a white fluorescent light source. The setup is crucial and thus the distance between the light source and solar cell was fixed at a constant distant of 5 cm (Lee et al., 2017). The obtained current and voltage readings were used for calculation of the power output using the formula below:

$$Power\ (mW) = current(mA) \times Voltage(V)$$

3.3 Characterization

The P(MMA-*co*-AA) synthesized was characterized using total solids content, particle size analyzer, thermogravimetric analysis (TGA), attenuated total reflectance fourier-transform infrared spectroscopy (ATR-FTIR) analysis, differential scanning calorimetry (DSC), inverted light microscopy, Atomic force microscopy (AFM) and scanning electron microscopy (SEM).

3.3.1 Total solids content

The total solids content is a quantitative measurement to determine the amount of total solids present in the emulsion of fixed amount of emulsion polymer solution (1 mL) were measured into an evaporating dish with micropipette. Before that, the empty evaporating dish was weighed to obtain its mass. Then, the evaporating dish with 1 mL of solution were put into the vacuum oven for 3 hours at 60^{o}C until a constant weight was obtained. Heating in the oven evaporate all unreacted monomer and solvent (water) from the sample solution. The remaining solid residue is known as total solids of the sample solution. For every sample, the step is repeated twice to obtain an average value to ensure the result obtained is accurate (Schneider et al., 2002). The equation 3.1 shows the calculation of total solids contents of 1 mL of solution.

$$\text{Total solids content} = \frac{m1-m2}{v1}$$

where m1 and m2 represent the weight of evaporating dish with dried sample, mg and weight of empty evaporating dish, respectively. v1 represents the volume of the sample solution used, 1 mL. The final value obtain will have the unit of mg/ mL.

3.3.2 Particle size analyzers

The polymer nanosphere size of the synthesized P(MMA-*co*-AA) nanosphere was measured using a Particle Size Analyzers. This instrument is a very useful tool because it provides the information on the particle size, average particle size and the distribution of particle size. Before subjecting the polymer emulsion for measurement, it was sonicated for 15 minutes. This was to ensure that polymer particles in the emulsion sample were well dispersed and homogenous for the analysis. Before measuring the emulsion polymer, the refractive index of the polymer must be measured beforehand. The parameters and the refractive index were set into the computer system and measurement was proceed (Eshel et al., 2004).

3.3.3 Attenuated total reflectance fourier-transform infrared spectroscopy (ATR-FTIR) analysis

The P(MMA-*co*-AA) in powder form and the monomer used for the synthesis were subjected to ATR-FTIR analysis in the range between 4000 cm^{-1} and 400 cm^{-1}. The prepared emulsion of P(MMA-*co*-AA) was dried in the oven to remove the solvent (water and methanol) in the emulsion because the presence of solvent would interfere the peaks given by the polymer. Before performing the analysis of P(MMA-*co*-AA) powder, it was dried in an vacuum oven at 60^{o}C to remove the water, moisture and solvent that is trap in the polymer. The drying process was to ensure no unnecessary peak present in the IR spectrum.

3.3.4 Thermogravimetric analysis (TGA)

The thermal stability of P(MMA-*co*-AA) with the incorporation of TMVS were analyzed and compared with the control P(MMA-*co*-AA). About 5 mg of dry sample was weighed into an alumina crucible for the analysis. Nitrogen gas was purged throughout the scan to reduce thermo-oxidative degradation. The sample was heated from 25^{o}C to 600^{o}C with a heating rate of 20 ^{o}C/min (Alkan, Aksoy and Anayurt, 2015).

3.3.5 Differential scanning calorimetry (DSC)

The P(MMA-*co*-AA) with the incorporation of Trimethoxyvinylsilane were analyzed with DSC to determine its glass transition temperature, T_g and compared with the control P(MMA-*co*-AA). About 3 mg of the dried sample was weighed into an aluminium pan and scanned from 25^{o}C to 160^{o}C with a heating rate of 20^{o}C/min under inert atmosphere of nitrogen gas purging (Alkan, Aksoy and Anayurt, 2015).

3.3.6 Inverted light microscopy

The important features of an inverted microscope is the location of the light source which is placed above the stage while for normal microscope it is below the stage. It is a useful tool because of its capability in producing clear image in a short time. Inverted microscope was used to study the surface morphology. Images at 100, 400 and 1000 of magnification power were captured and studied.

3.3.7 Atomic force microscopy (AFM)

AFM is a useful tool in the study of surface morphology of the materials tested. Image captured using AFM give a good magnification and clear image

of the surface of the materials tested. The AFM image was used to characterized the P(MMA-co-AA) synthesized. Besides that, the 3-dimensional image of AFM gives the characteristic, packing of the polymer on glass substrate and the shape of the polymer synthesized (Adhikari, 2013).

3.3.8 Scanning electron microscopy (SEM)

SEM is a common and useful tool in the study of the surface topography and composition of a substance. It is a tool that can give a good magnification and clear image of the surface of materials tested. SEM was used to characterize the surface morphology of the P(MMA-*co*-AA) synthesized in the study. Top view and side view SEM images of 20000, 50000 times of magnification power were captured and studied (Khursheed, 2006).

CHAPTER 4

RESULTS & DISCUSSION

4.1 Total solids content

Table 4.1 shows the average total solid content for each polymer sample being synthesized. The values obtained for all the polymer sample were within the acceptable range around 200 to 210 mg/mL. The result obtained were further used to calculate the volume needed for diluting the polymer emulsion.

Table 4.1: The average total solid content for each P(MMA-*co*-AA) sample with and without the incorporation of TMVS.

Polymer sample	1st trial (mg/mL)	2nd trial (mg/mL)	3rd trial (mg/mL)	Average (mg/mL)
Polymer	202.0	209.0	205.7	205.57
Polymer with 1 wt% of TMVS	210.1	204.0	203.8	205.97
Polymer with 3 wt% of TMVS	198.4	200.5	198.2	199.03
Polymer with 5 wt% of TMVS	205.8	207.8	206.0	206.53
Polymer with 7 wt% of TMVS	211.1	209.5	210.3	210.3
Polymer with 9 wt% of TMVS	201.6	202.0	204.8	202.8

4.2 Particle size analysis

The synthesis of P(MMA-*co*-AA) through emulsion polymerization technique was subject to analysis using the particle size analyzer (PSA) for the determination of the particle size. Table 4.2 below shows the average particle size of the P(MMA-*co*-AA) nanosphere without and with the incorporation of different concentrations of TMVS.

Table 4.2: Average particle size of synthesized P(MMA-*co*-AA) with and without the incorporation of TMVS

Polymer sample	Particle size (nm)
Polymer	102
Polymer with 1 wt% of TMVS	108
Polymer with 3 wt% of TMVS	108
Polymer with 5 wt% of TMVS	108
Polymer with 7 wt% of TMVS	105
Polymer with 9 wt% of TMVS	105
Average size	106

Table 4.2 shows the average particle size for each P(MMA-*co*-AA) synthesized with and without the incorporation of TMVS. The average particle sizes of the polymer synthesized with different amount of TMVS show a range from 102 to 108 nm, giving an average particle size of 106 nm. The result shows that incorporation of different amount of TMVS during the emulsion polymerization process does not affect the outcome of the polymer size synthesized. To govern the size of the polymer synthesized, some parameters were kept constant such as the speed of stirring during polymerization (rotation per minute), the polymerization reaction time, amount of thermal initiator (KPS) and emulsifier (SDS) used (Lee et al., 2017).

Figure 4.1 shows the particle size distribution (PSD) of the P(MMA-*co*-AA) synthesized. The particle synthesis have a distribution range from 52 to 240 nm with the average particle size of 106 nm. The distribution range of the polymer obtain were considerable wide with a difference of 188 nm between the largest and the smallest polymer that can be found in the emulsion. There are a few factor affecting the PSD of polymer chain, the major factor were initial initiator amount, the method of monomer addition and the amount of emulsifier (Sood, 2003).

The growth of polymer chains involves two stages which are the nucleation stage and the growth stage. To obtain a narrow range of PSD from the nucleation stage to growth stage, a few factors are needed to be considered such as the amount of initiator, emulsifier and rate of monomer addition. High

amount of initiator with sufficient amount of emulsifier result in a narrow PSD. Besides, controlling the rate of monomer addition control the polymerization of the polymer chain such that all the polymer chains obtained result in narrow PSD. Thus, by shortening the nucleation period and lengthening the growth stage, the distribution will be narrower (Sood, 2003).

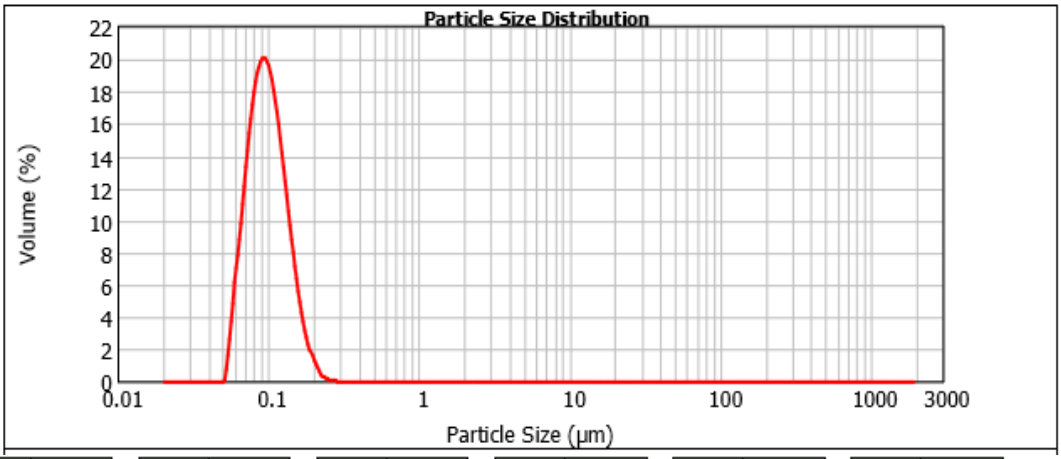

Size (µm)	Volume In %	Size (µm)	Volume In %	Size (µm)	Volume In %	Size (µm)	Volume In %	Size (µm)	Volume In %	Size (µm)	Volume In %
0.010	0.00	0.105	15.76	1.096	0.00	11.482	0.00	120.226	0.00	1258.925	0.00
0.011	0.00	0.120	11.64	1.259	0.00	13.183	0.00	138.038	0.00	1445.440	0.00
0.013	0.00	0.138	7.20	1.445	0.00	15.136	0.00	158.489	0.00	1659.587	0.00
0.015	0.00	0.158	3.62	1.660	0.00	17.378	0.00	181.970	0.00	1905.461	0.00
0.017	0.00	0.182	1.41	1.905	0.00	19.953	0.00	208.930	0.00	2187.762	0.00
0.020	0.00	0.209	0.33	2.188	0.00	22.909	0.00	239.883	0.00	2511.886	0.00
0.023	0.00	0.240	0.06	2.512	0.00	26.303	0.00	275.423	0.00	2884.032	0.00
0.026	0.00	0.275	0.00	2.884	0.00	30.200	0.00	316.228	0.00	3311.311	0.00
0.030	0.00	0.316	0.00	3.311	0.00	34.674	0.00	363.078	0.00	3801.894	0.00
0.035	0.00	0.363	0.00	3.802	0.00	39.811	0.00	416.869	0.00	4365.158	0.00
0.040	0.00	0.417	0.00	4.365	0.00	45.709	0.00	478.630	0.00	5011.872	0.00
0.046	0.00	0.479	0.00	5.012	0.00	52.481	0.00	549.541	0.00	5754.399	0.00
0.052	3.02	0.550	0.00	5.754	0.00	60.256	0.00	630.957	0.00	6606.934	0.00
0.060	8.00	0.631	0.00	6.607	0.00	69.183	0.00	724.436	0.00	7585.776	0.00
0.069	13.56	0.724	0.00	7.586	0.00	79.433	0.00	831.764	0.00	8709.636	0.00
0.079	17.35	0.832	0.00	8.710	0.00	91.201	0.00	954.993	0.00	10000.000	
0.091	18.05	0.955	0.00	10.000	0.00	104.713	0.00	1096.478	0.00		
0.105		1.096	0.00	11.482	0.00	120.226	0.00	1258.925	0.00		

Concentration:	Span :	Uniformity:	Result units:
0.1089 %Vol	0.780	0.243	Volume

Specific Surface Area:	Surface Weighted Mean D[3,2]:	Vol. Weighted Mean D[4,3]:
63.5 m^2/g	0.094 um	0.102 um

d(0.1): 0.068 um d(0.5): 0.097 um d(0.9): 0.144 um

Figure 4.1: The result of P(MMA-*co*-AA) on the particle size distribution

Figure 4.2 shows the SEM image of the P(MMA-*co*-AA) coated on the glass substrate with the magnification of 50000 times. The SEM image reveals that the polymer coated on the glass substrate have a high amount of coverage with a random distributed arrangement. The PSD observed on the image were mostly in the range of 70-150 nm. Based, on the result obtain form particle size analysis approximately 83.56% of the polymer particles synthesized are in the range of 70-150 nm. The SEM image proves that the polymer particles are mostly in the range of 70-150 nm.

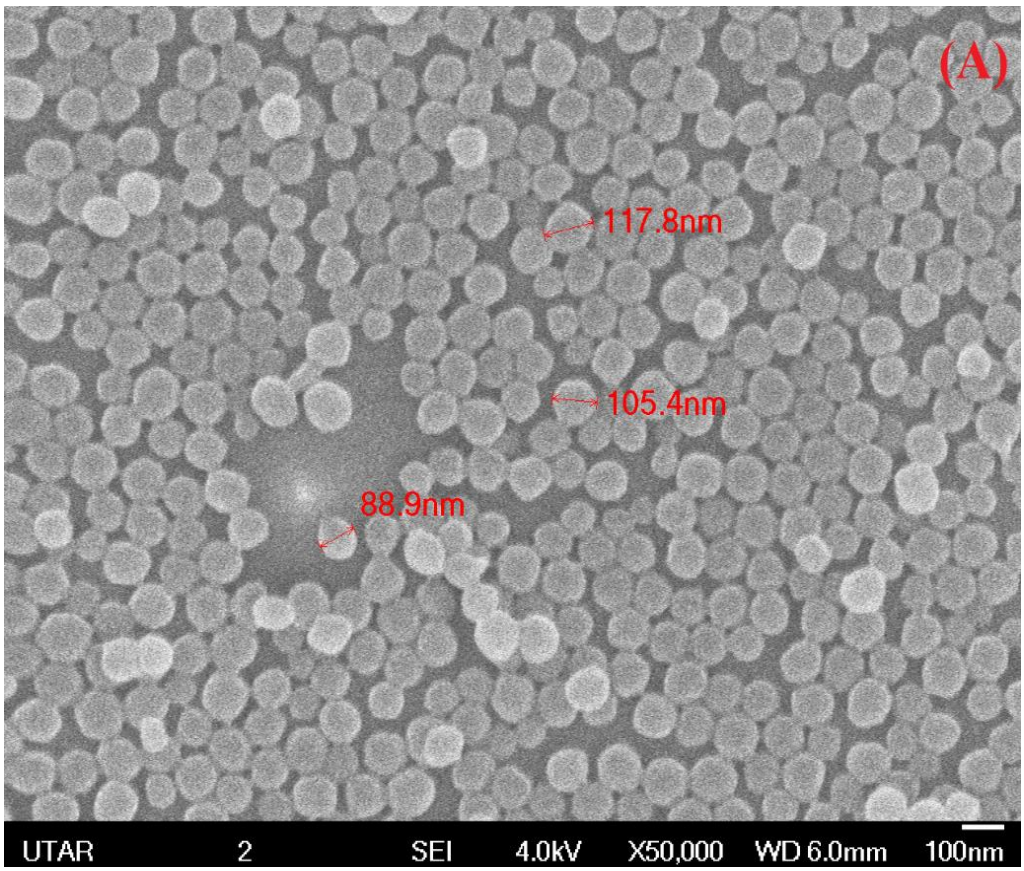

Figure 4.2: SEM image of the glass substrate coated with P(MMA-*co*-AA) with the magnification of 50000.

4.3 Attenuated Total Reflectance Fourier-Transform Infrared spectroscopy (ATR-FTIR) analysis

The functional groups present in P(MMA-*co*-AA) structure with and without the incorporation of TMVS were studied with ATR-FTIR. Table 4.3 are the extracted data from the IR spectra of AA, MMA and P(MMA-*co*-AA). All IR spectra were scan from 4000 to 400 cm^{-1}.

Acrylic acid (CH_2=CHCOOH) is a carboxylic acid with a vinyl group connected to the carbonyl carbon forming an unsaturated carboxylic acid. The hydroxyl group (–OH) attached to the carbonyl absorb between 2500-3300 cm^{-1} with a strong and broad peak. The observed –OH peak are 3045 cm^{-1} which extended and covering the peaks appearing in between 2500-3300 cm^{-1} thus overlapping the C-H stretching peak. The C-O single bond also causes absorption in the finger print region at 1000-1300 cm^{-1}. The observed C-O peak were 1295 cm^{-1}. Besides, stretching of carbonyl group also cause peak in between 1670-1820 cm^{-1} with a strong intensity. Owing that the carbonyl group are part of the acid, it would have a relatively lower wavenumber because carboxylic acid group does not present in free-state but rather hydrogen bonding with other carboxylic acid. Lastly, the observed peak at 1634 cm^{-1} are cause by the stretching of C=C group with a medium intensity (Coast et al., 1996).

Table 4.3: IR Spectral data of MMA, AA and P(MMA-*co*-AA)

Sample	Wavenumber (cm^{-1})	Type of vibration
MMA	2956	CH_3 stretching
	1721	C=O stretching
	1636	C=C stretching
	1438	CH_3 bending
	1159	C-O stretching
AA	3045	O-H stretching
	1698	C=O stretching
	1634	C=C stretching
	1295	C-O stretching
P(MMA-*co*-AA)	3557	O-H stretching
	2995,2951	CH_3 stretching
	1726	C=O stretching
	1450,1388	CH_3 bending
	1149	C-O stretching
P(MMA-*co*-AA) with TMVS	3557	O-H stretching
	2995,2951	CH_3 stretching
	1726	C=O stretching
	1450,1388	CH_3 bending
	1149	C-O stretching
	988	Si-O-Si stretching
	842	Si-O-Si bending
	482	Si-O-Si rocking

MMA is an ester of AA with a methyl group replacing the hydrogen atom on the hydroxyl group of AA. The C=O group of an ester functional group have a theoretical absorption range of 1725-1700 cm^{-1}. The value obtain were 1721 cm^{-1} which considerable at a higher wavenumber compare to AA due to the electronegative oxygen withdrawing effect. The absorption at 1159 cm^{-1} were due to the present of C-O single bond group which proved the present of an ester group. Besides that, the unsaturation of carbon double bond present in MMA were proved by the peak present at 1636 cm^{-1}. At the left side of the spectrum appears a peak at 2956 cm^{-1} which is cause by the stretching of CH_3 while the bending of CH_3 present at the finger print region at 1438 cm^{-1} (Wang et al., 2001).

The IR spectrum obtained from the P(MMA-*co*-AA) show some similarity between MMA and AA spectrum because some of the functional group were not reacted after the polymerization reaction. The strong and broad peak observed at 2800-3600 cm^{-1} were peak form the hydroxyl group of AA. The two peaks observed at 2997 and 2952 cm^{-1} were due to the stretching of the C-H bond form the methyl (CH_3) in the MMA compound. Strong and sharp peak present at 1731 cm^{-1} were cause by the present of carbonyl (C=O) group contributed by MMA and AA. The CH_2 and CH_3 form both MMA and AA show bending vibrational at 1458 cm^{-1}. While on the finger print region peak were observed at 1149 cm^{-1} for C-O single bond. Besides that, no peak were found between 1680-1640 cm^{-1} which is cause by the C=C from MMA and AA because during the emulsion polymerization the carbon double bond were all

reacted to form a polymer chain. Thus, forming new single C-C bond which link all the monomer together (Liu and Du, 2006).

The IR spectrum obtained from the P(MMA-*co*-AA) with the incorporation of TMVS show additional peak compared to P(MMA-*co*-AA) sample only. Firstly, the present of broad peak were observed which is due to hydrolyze of Si-OCH_3 to Si-OH bond at 3530 cm^{-1} and OH bond form the AA. By comparison, the polymer with the TMVS shows a broader peak range form 3600-2800 cm^{-1}. Besides that, some of the neighboring Si-OH bond could undergo condensation to form Si-O-Si bond with water as by-product. Peak at 1075 cm^{-1} were observed which is cause by the stretching of Si-O-Si bond while bending were seen at 800 cm^{-1}. Moreover, 400 cm^{-1} were observed which is due to the rocking vibration of Si-O-Si bond. The vinyl group on the TMVS were not seen on the spectrum ranging from 1680-1620 cm^{-1}. It proved that the vinyl group were reacted and becoming a part of the polymer chain. The absent of C=C and present of Si-OH proved that the TMVS were successfully incorporated into the polymer chain and present of hydrolysable Si-OH group indicate that there is available active site for the condensation reaction of silane coupling agent onto the free hydroxyl glass substrate.

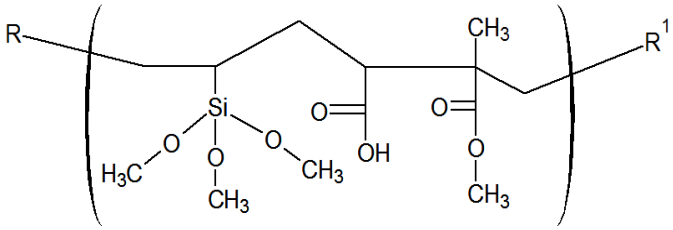

Figure 4.3: The general structure of P(MMA-*co*-AA) with the incorporation of TMVS

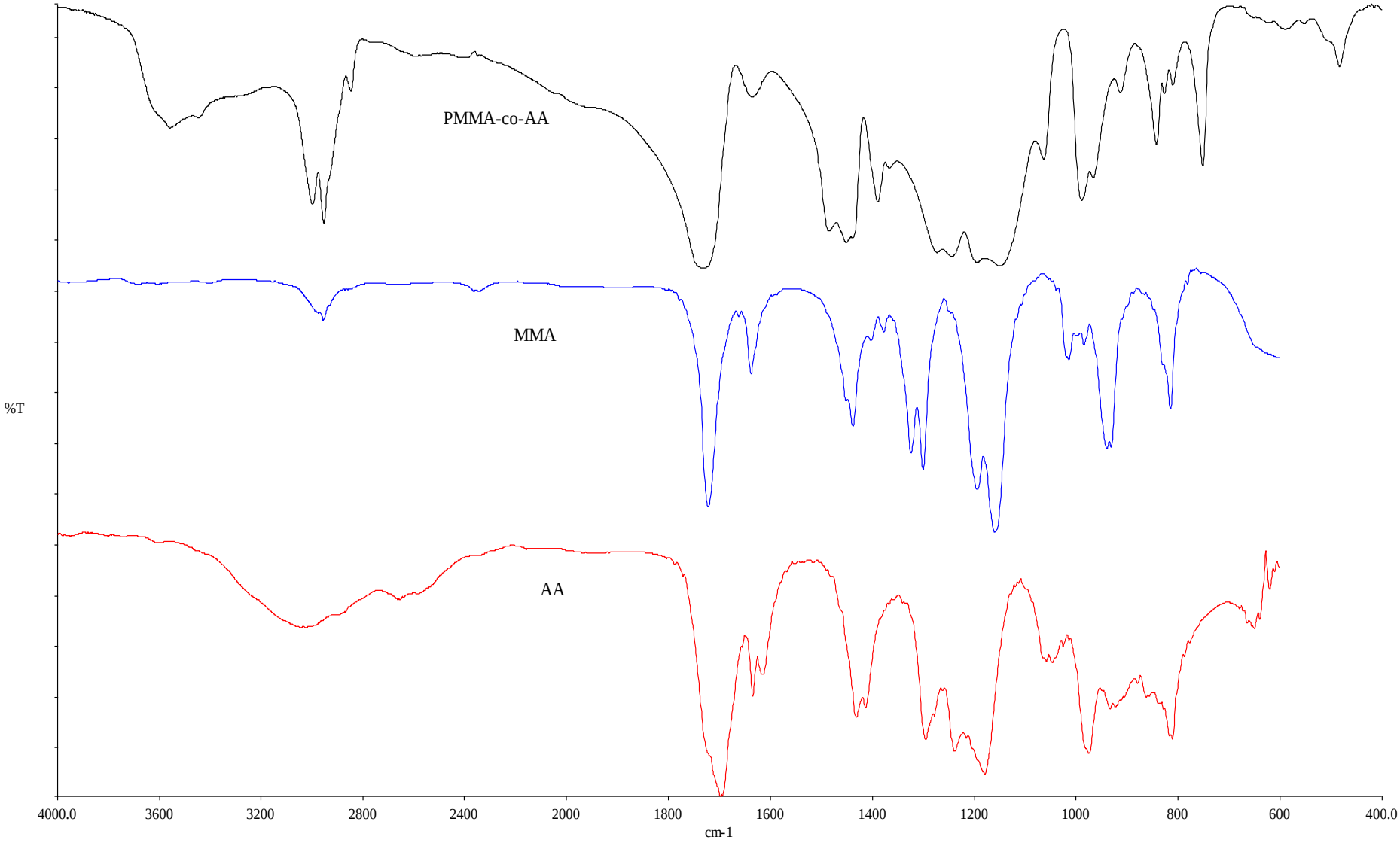

Figure 4.4: Comparison of FTIR spectrum of MMA, AA and P(MMA-*co*-AA)

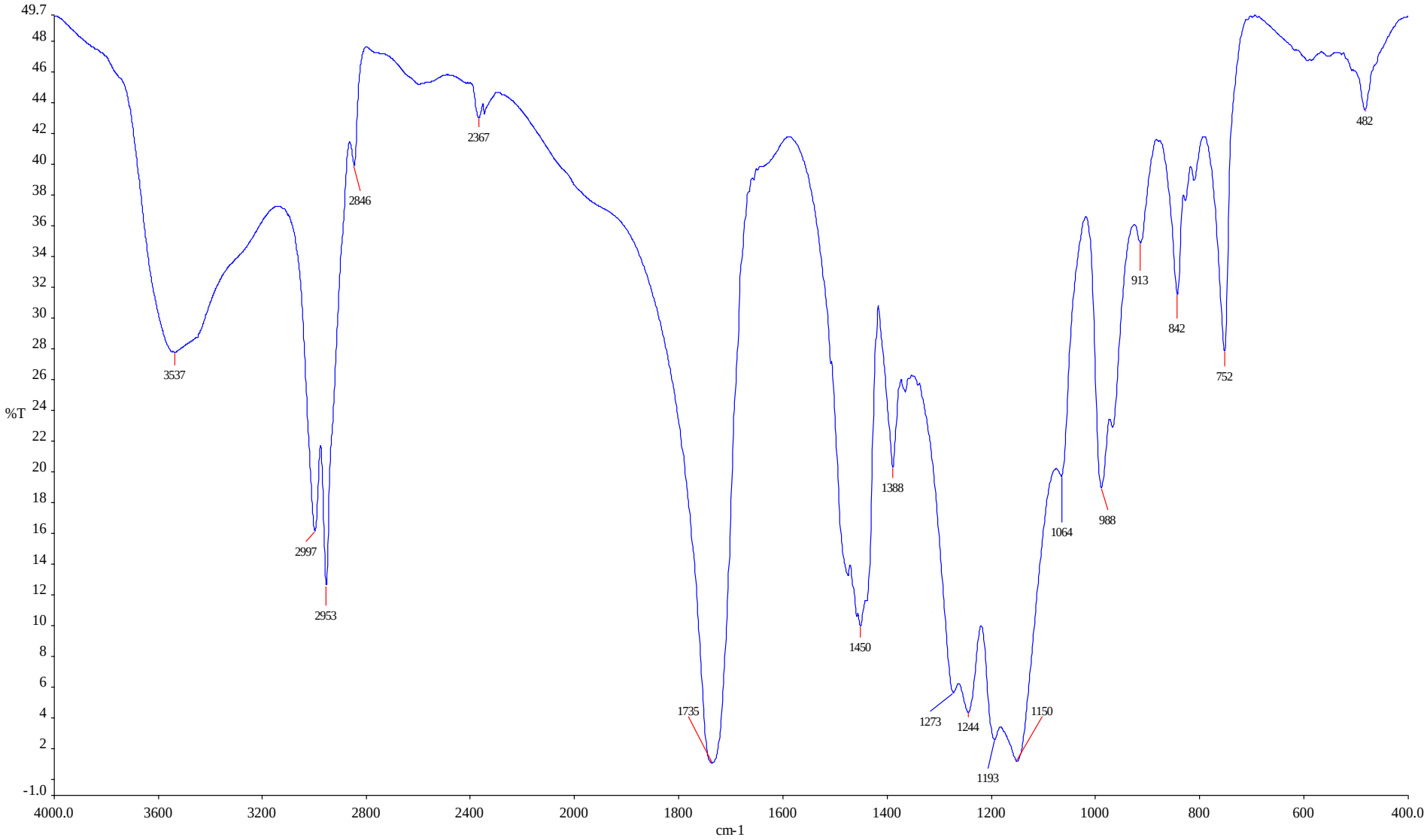

Figure 4.5: FTIR spectrum of P(MMA-*co*-AA) with the incorporation of TMVS

4.4 Thermogravimetric analysis (TGA)

TGA is a method use to analyze the mass of a substance over a period of time as the temperature increases. Exposing the polymer to high temperature will cause the polymer to degrade and changes in properties. This analysis provide physical and chemical information. Table 4.4 shows the degradation temperature and % residue after degradation.

Table 4.4: Degradation temperature and percentage of residue after degradation of the polymer sample

Sample	Degradation temperature, T_d (°C)		Percentage of residue after degradation (%)	
	1st degradation	2nd degradation	1st degradation	2nd degradation
Polymer	186.85	389.00	98.73	11.30
Polymer (1 wt% TMVS)	193.20	390.46	98.19	6.33
Polymer (3 wt% TMVS)	189.42	387.04	98.59	10.96
Polymer (5 wt% TMVS)	189.07	386.83	98.92	9.23
Polymer (7 wt% TMVS)	193.68	387.50	98.83	7.70
Polymer (9 wt% TMVS)	193.20	388.72	97.18	19.65

The result obtained for P(MMA-*co*-AA) with and without the incorporation of TMVS shows two degradation temperature, T_d. The first degradation occurred at 103.73°C with the inflection temperature at 186.85°C for P(MMA-*co*-AA). According to Moharram and Khafagi (2006), homo-polymer of PAA clearly show the first degradation occur at 156.8°C and end at 225.3°C with the maximum degradation at 196.89°C. The first degradation of PAA were reported to be cause by the removal of AA side chain by the decarboxylation reaction. Besides that, as reported by Gałka, Kowalonek and Kaczmarek (2013), homo-polymer of PMMA also show the first degradation at 180°C which were caused by the head-to-head linkages (H-H) depolymerization. Therefore, the first degradation were mainly cause by the removal of side chain AA as compare to the depolymerization of MMA. The percentage of residue left after first degradation is 98.73%.

As the temperature increases, second degradation is observed around 257.98°C with the inflection temperature at 389.00°C. For homo-polymer PAA, degradation occur at 301°C and stops at 476.1°C, with a maximum degradation at 372.36°C. The last degradation is the major cause of the degradation of polyacrylic anhydride with the weight loss of 55.87 wt% (Moharram and Khafagi, 2006) whereas for PMMA degradation also occur at 350-400°C due to the scission of the backbone polymer chain of the side group methoxycarbonyl. Therefore, the weight loss is due to breakdown of the polymer backbone, which causes a large weight lost compare to the first degradation. The percentage of residue left after second degradation is 11.30%.

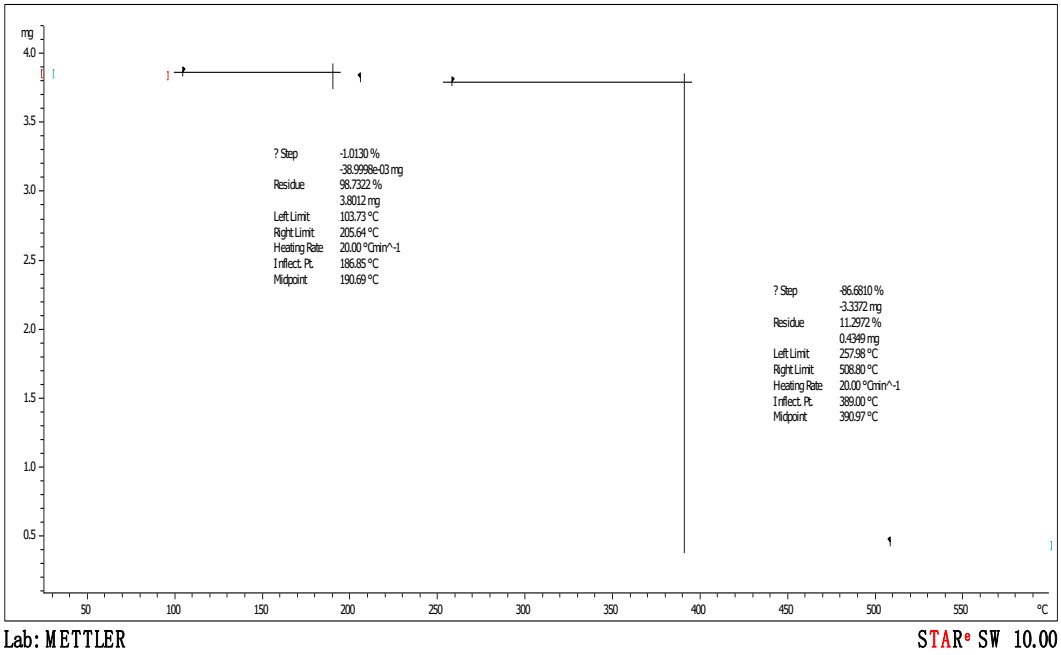

Figure 4.6: The thermogram of TGA for P(MMA-*co*-AA) sample

The thermogram obtained for P(MMA-*co*-AA) with the incorporation of 9 wt% TMVS shows two thermal degradation steps as well. The first degradation started at 156.02°C to 280.58°C with the inflection point at 193.20°C. Then, while the temperature continues to increase, the second degradation started at 298.58°C to 537.47°C with the inflection point at 388.72°C. The residue remained in the first and second degradation were 97.18% and 19.65% respectively. Both the degradation patterns occur for P(MMA-*co*-AA) with TMVS and the P(MMA-*co*-AA) without TMVS were similar.

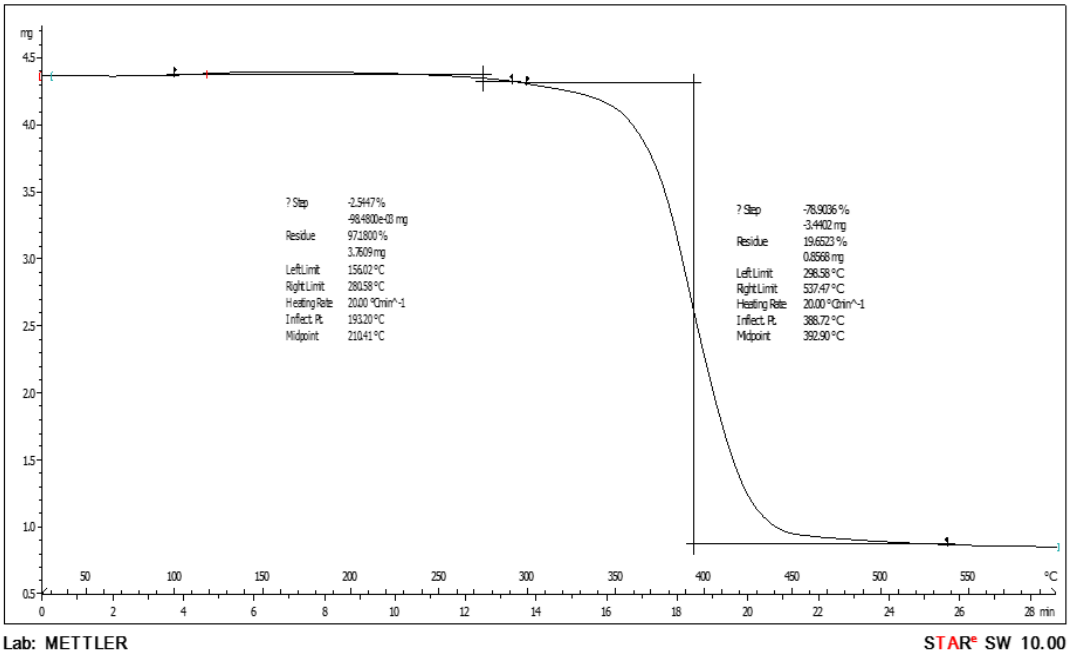

Figure 4.7: TGA thermogram of P(MMA-*co*-AA) with 9 wt% of TMVS

It was observed that the incorporation of TMVS into the polymer does not affect its T_d. Even though there is a few degrees of difference for the first and second degradation temperatures. The amount of TMVS added into the polymer emulsion is considerably negligible because there is only small difference and changes occur to the thermal properties of the polymer synthesized. The results obtained also confirm the fact that the polymers synthesized are able to withstand the outdoor condition under hot sunlight exposure.

4.5 Differential scanning calorimetry (DSC)

DSC was used to determine the glass transition temperature, T_g for each of the polymer sample. Table 4.5 shows the result for the T_g obtained from the P(MMA-*co*-AA) with and without the incorporation of TMVS.

Table 4.5: Glass transition temperature (T_g) of the polymer samples

Sample	Glass transition temperature, T_g (°C)
Polymer	110.31
Polymer (1 wt% TMVS)	111.43
Polymer (3 wt% TMVS)	112.19
Polymer (5 wt% TMVS)	114.84
Polymer (7 wt% TMVS)	115.88
Polymer (9 wt% TMVS)	118.42

The thermogram of P(MMA-*co*-AA) reveal that the T_g occurred at 110.31°C while the T_g for P(MMA-*co*-AA) with 9 wt% of TMVS occurred at 118.42°C. The results exhibit an increasing trend in T_g as the amount of TMVS increases. The T_g range from 110.31°C to 118.42°C with a difference of 8.11°C. This provide an evident that with the incorporation of TMVS, the T_g of the polymer samples increases.

As reported by Shefer and Gottlieb (1992), the degrees of crosslinking in the polymer network affect the elastomer properties because the elasticity of the polymer materials require high amount of crosslinking between polymer chains for proper functioning. Study on the network structure found that, crosslinking decreases the mobility of the polymer system while expecting the increase in the T_g value. The results show that as the amount of TMVS increases, the T_g of the polymer sample increases as well. For P(MMA-*co*-AA), the T_g obtained was 110.31°C which is lower compare to the polymer sample with TMVS because the silane coupling agent were capable to act as a good crosslinking agent. TMVS is able to link polymer chains to form a closely packed structure which results the increase of T_g.

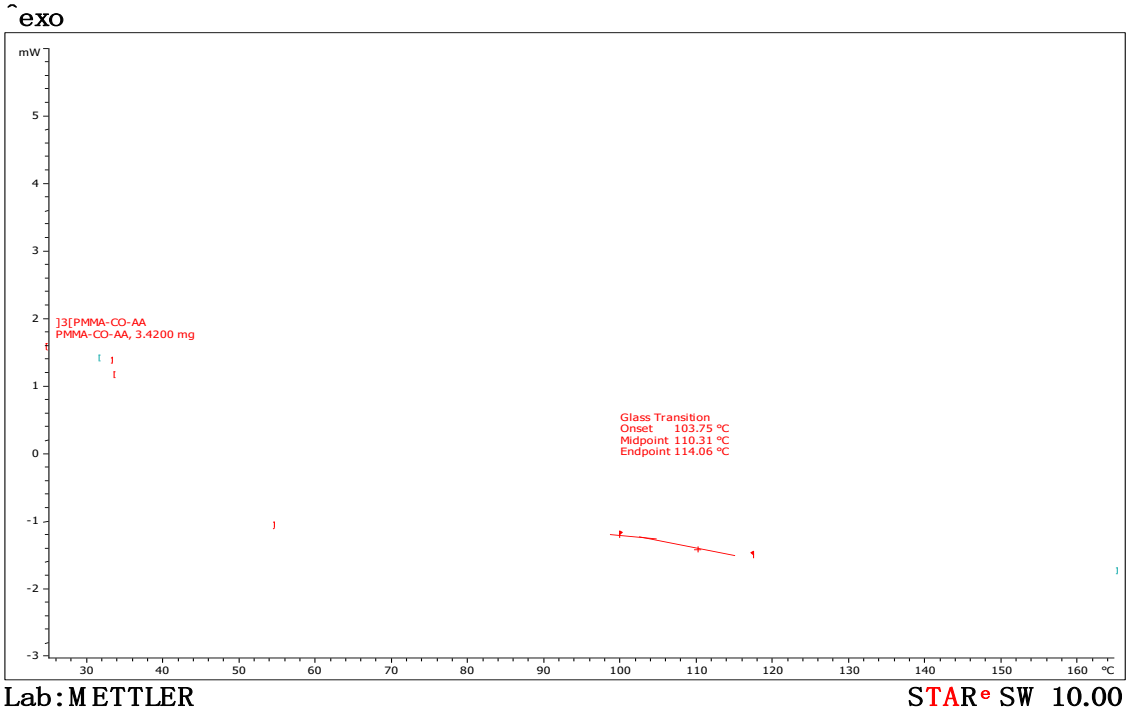

Figure 4.8: The thermogram of DSC for P(MMA-*co*-AA) sample.

The P(MMA-*co*-AA) with 9 wt% TMVS shows the T_g occurred at 118.42 ^oC which have the highest T_g value compare to the rest of the polymer samples with lower amount of TMVS. The presence of TMVS promotes increasing number of crosslinking between the polymer chains. The hydroxyl group of TMVS would interact with polymer chains through condensation reaction to form a stable Si-O-Si bond with water as by-product. The increase of crosslinks also increases the T_g. Besides that, a trend was observed that the T_g increases as the amount of TMVS increases. The reason was owing to the increasing number of hydroxyl group present on the polymer chain. Which result in higher occurrence of cross linking among the polymer chains.

Figure 4.9: DSC thermogram of P(MMA-*co*-AA) with 9 wt% of TMVS

4.6 Peeling test

The peeling test was carried out by peeling the coated polymer on the glass substrate with 3M adhesive tape. After the removal of the tape, the glass substrate was subjected to be viewed under an inverted light microscope with 400 times of magnification. The peeling step was repeated several times to determine the adhesion strength of the coating. The result was captured and shown in Figure 4.10 (a)-(f) and 4.11 (a)-(f). The images on the left show the coated glass substrates before peeling while those on the right show the coated glass substrates after the peeling process. Two sets of samples were prepared, the first set was cured in the vacuum oven at 60^{o}C for one hour whereas the second set was cured at room temperature.

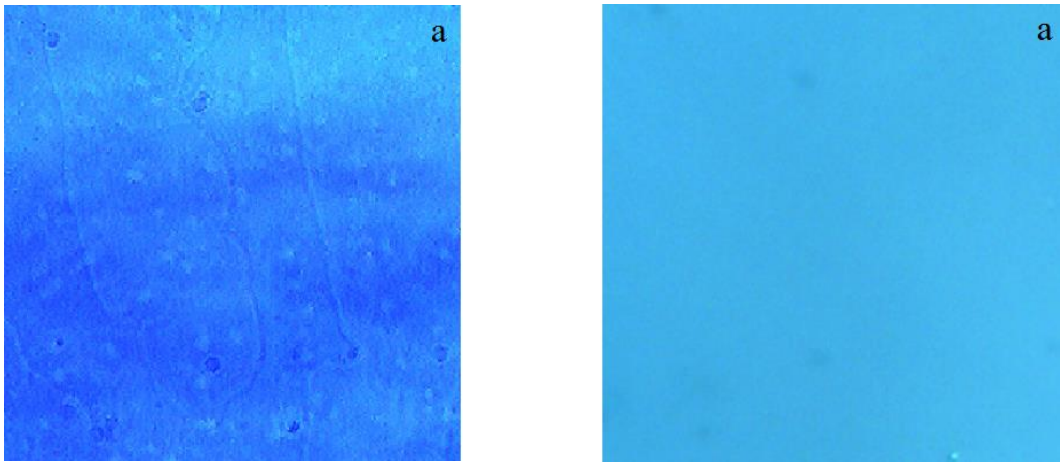

Figure 4.10: Microscope images of polymer on glass substrate (with curing at 60^{o}C in vacuum oven) before and after peeling test (a) blank (without TMVS) (left: before; right; after)

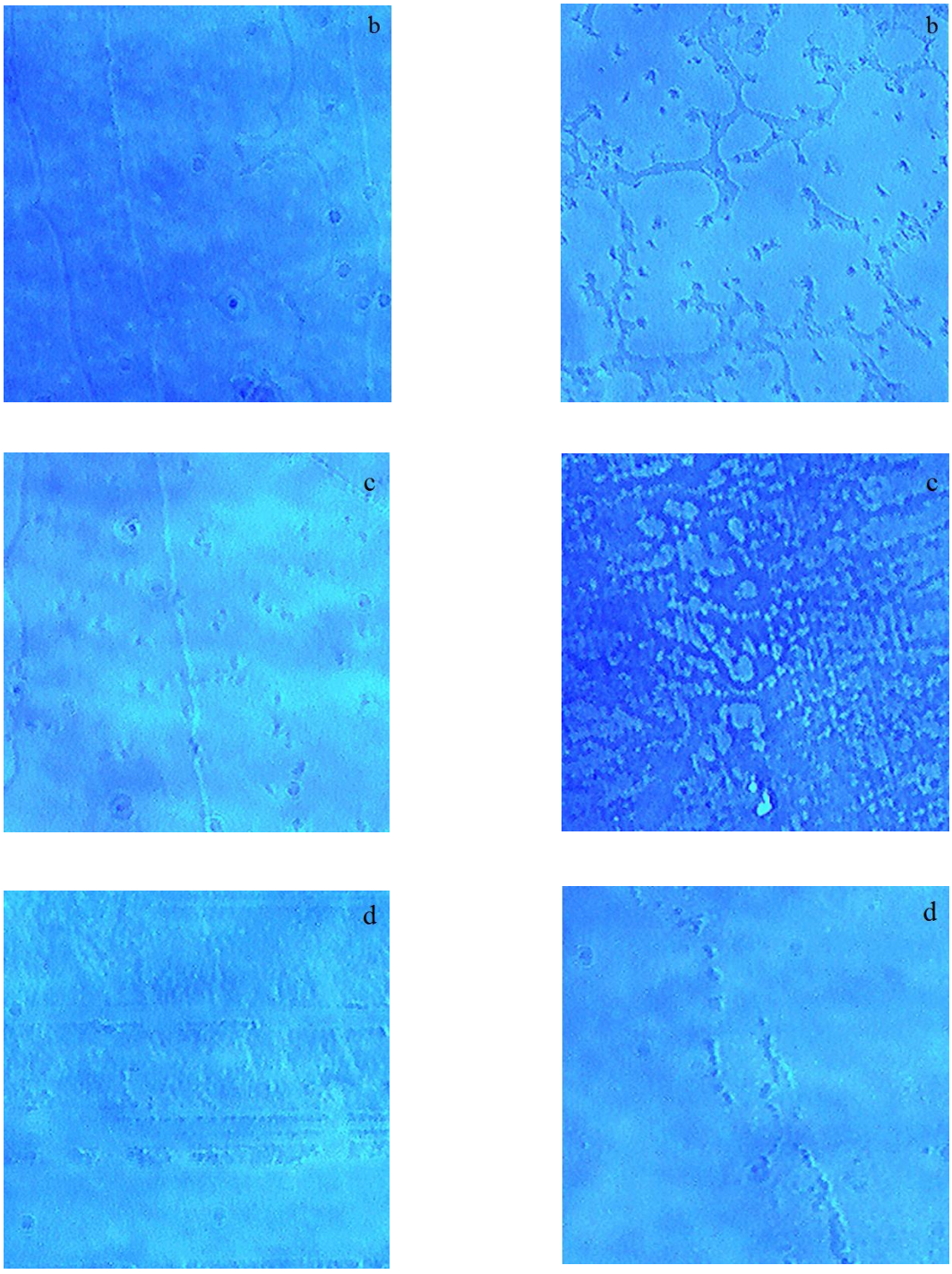

Figure 4.10: Continue microscope images of polymer on glass substrate (with curing at 60^{o}C in vacuum oven) before and after peeling test (b) polymer with 1 wt% of TMVS; (c) polymer with 3 wt% of TMVS; (d) polymer with 5 wt% of TMVS (left: before; right; after)

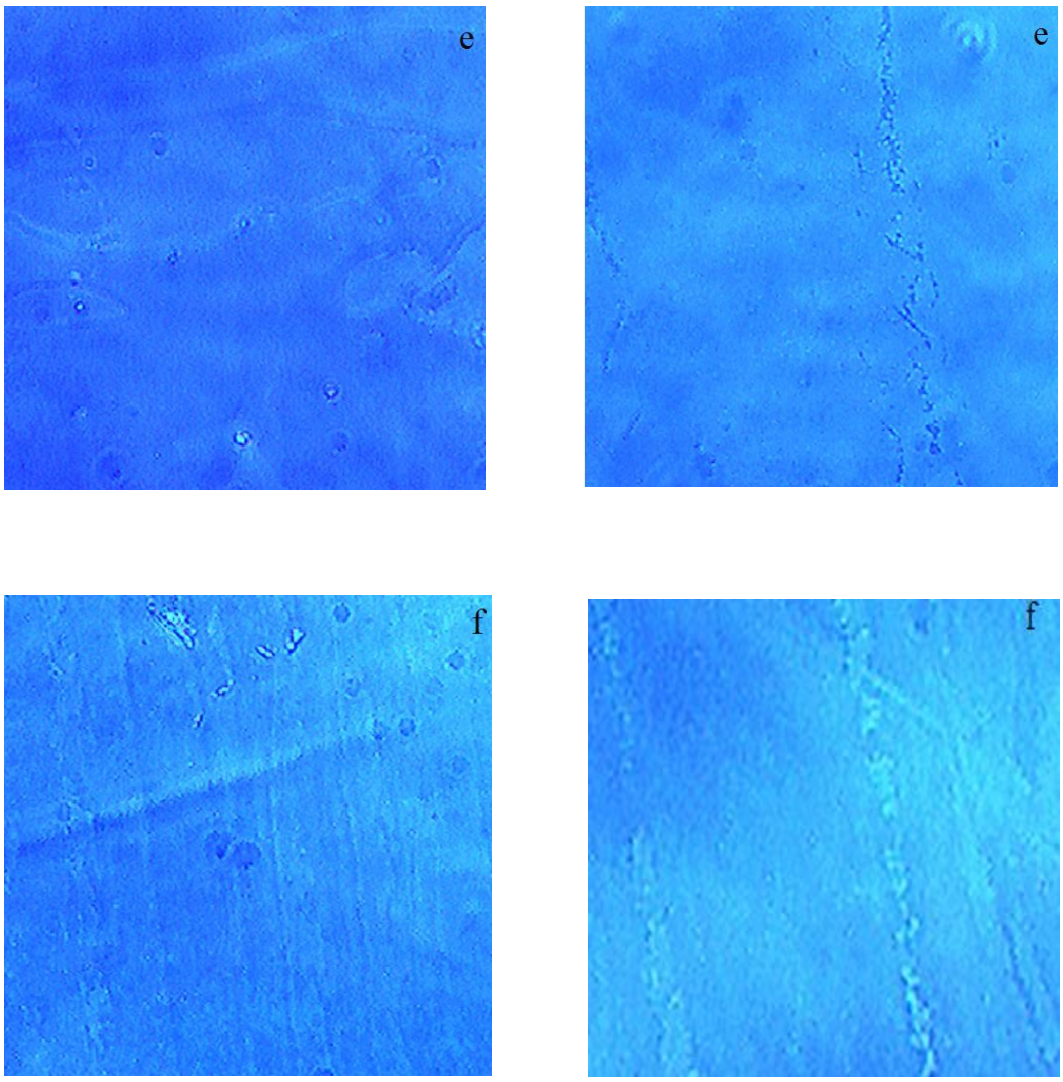

Figure 4.10: Continue microscope images of polymer on glass substrate (with curing at 60^{o}C in vacuum oven) before and after peeling test (e) polymer with 7 wt% of TMVS; (f) polymer with 9 wt% of TMVS

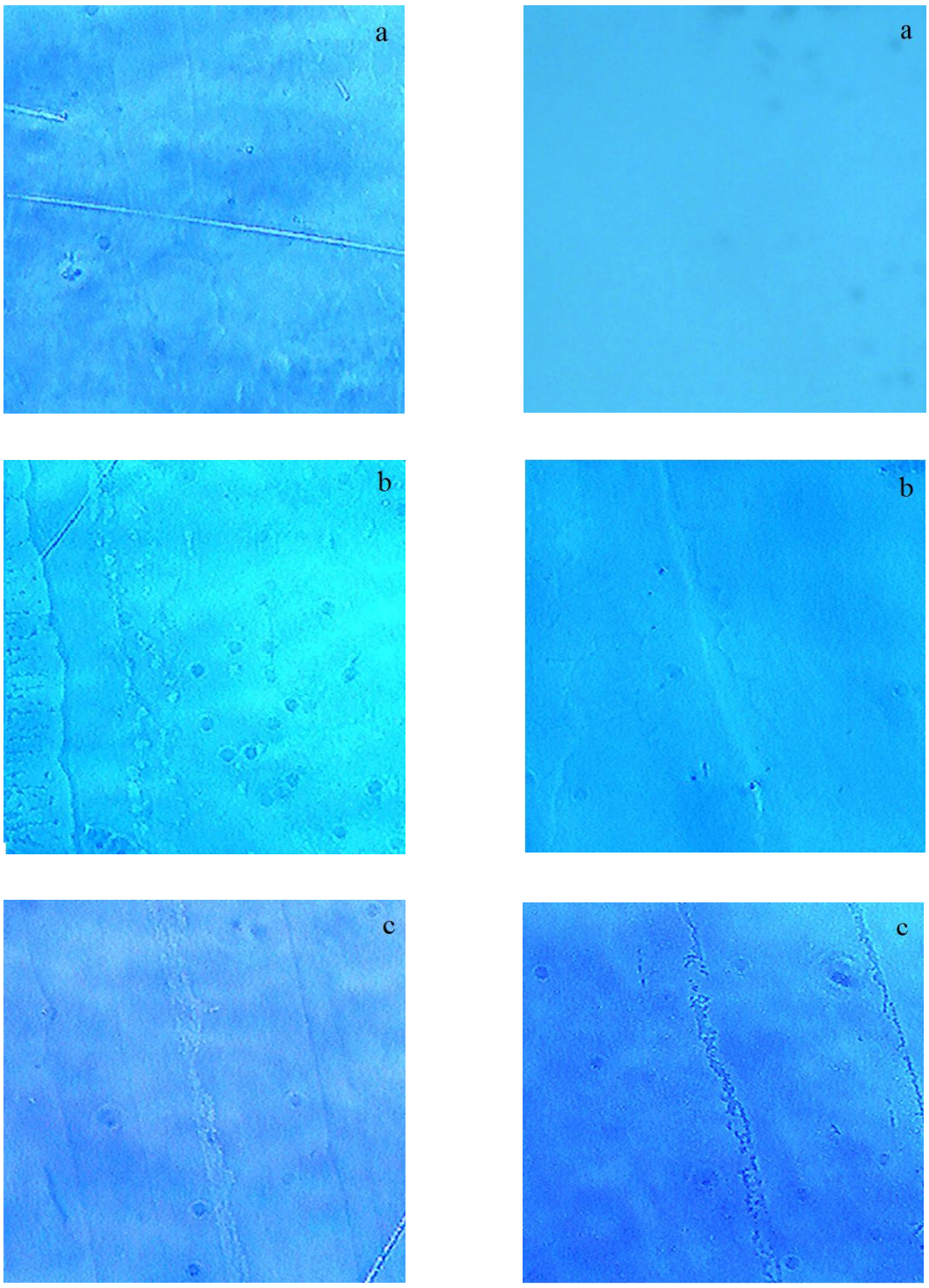

Figure 4.11: Microscope images of polymer on glass substrate (with curing at room temperature) before and after peeling test (a) blank (without TMVS) (left: before; right; after) (b) polymer with 1 wt% of TMVS; (c) polymer with 3 wt% of TMVS

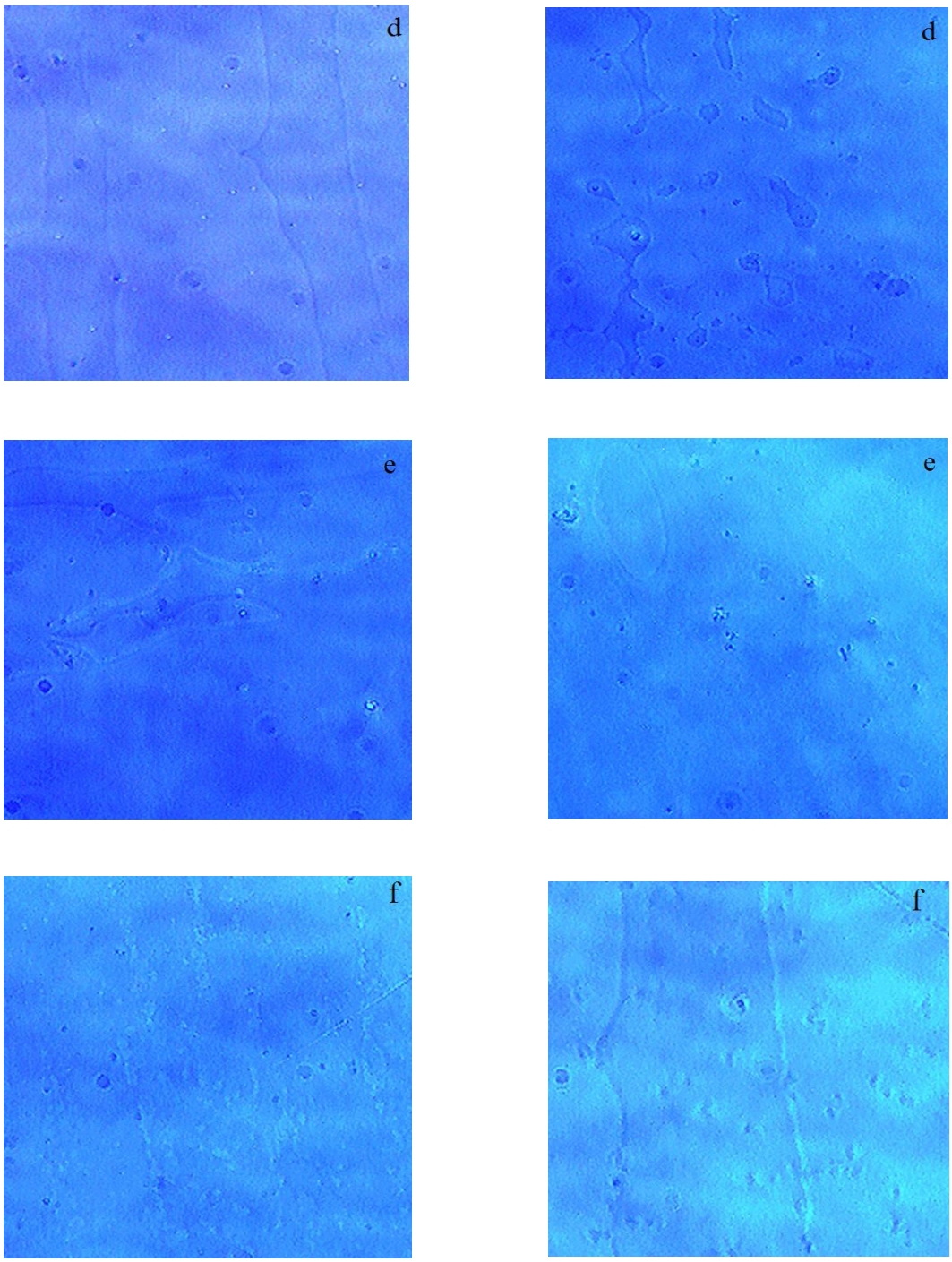

Figure 4.11: Continue microscope images of polymer on glass substrate (with curing at room temperature) before and after peeling test (d) polymer with 5 wt% of TMVS; (e) polymer with 7 wt% of TMVS; (f) polymer with 9 wt% of TMVS

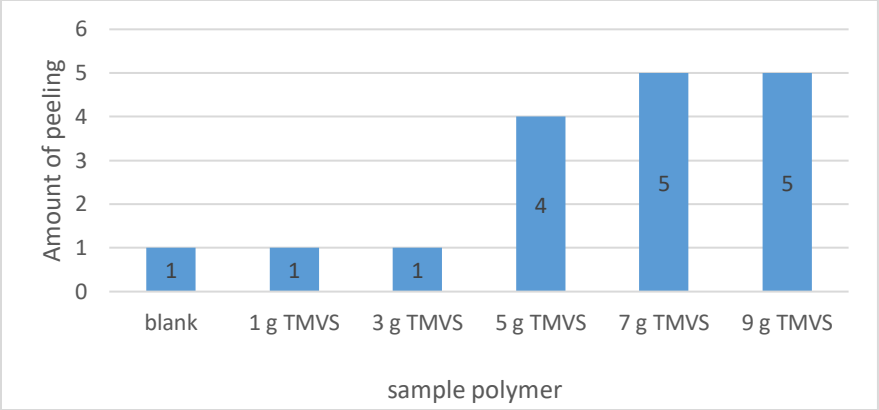

Figure 4.12: Graph of the number of time of peeling versus the polymer sample with curing at 60°C in vacuum oven.

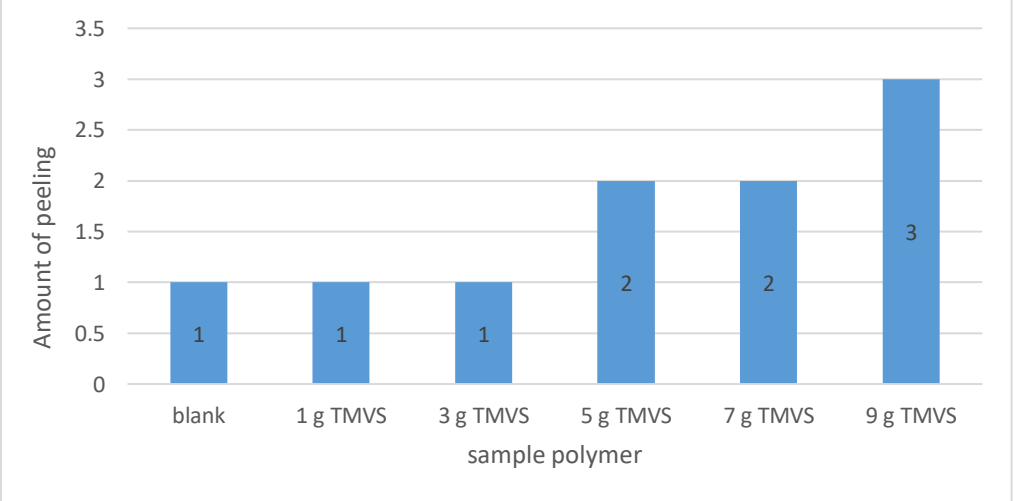

Figure 4.13: Graph of the amount of peeling versus the polymer sample with curing at room temperature.

The peeling test was repeated till defect on the polymer coating was observed. Figure 4.12 and 4.13 show the results on the number of peeling was done on the sample before defect was observed. It was found that the sample cured in vacuum oven at 60^{o}C have better adhesion strength on the glass substrate compared to the set of sample that were cured at room temperature. The cured set show a better resistance toward being pull-off from the glass substrate because more peeling is done on polymer (5 wt%, 7 wt% and 9 wt%) for the defect to be observed.

The coating of the polymer with and without the incorporation of TMVS on the glass substrate were all similar to each other before the peeling test. It was observed that the polymer on the glass substrate form a multilayer due to the interaction of Si-OH bond between polymer forming cross-linking. The interaction between polymer with TMVS and glass substrate are through the Si-O-Si bond and Si-O-C bond while for polymer without TMVS the interaction between polymer and glass substrate through the hydrogen bonding (-OH form AA segment and –OH form glass substrate). It was observed, that the polymer without TMVS does not adhere onto the glass substrate well because the polymeric materials are organic material while the glass substrate are inorganic material. Thus, both materials are incompatible with each other.

The polymer with TMVS shows a gradual increase in adhesion strength as the amount of TMVS increases. Therefore, the number of time of peeling increases

as the amount of TMVS increases. For polymer with 1 wt% and 3 wt% of TMVS, cracking and defect were seen after the first peeling because of lesser interaction between polymer and glass substrate. On the other hand, the polymer with 7 wt% and 9 wt% of TMVS show to give good adhesion because of it resistance toward pull-off with 5 times of peeling. The polymer with 7 wt% and 9 wt% TMVS consist of large amount of Si-O-Si bond between polymer and glass substrate/polymer. Therefore, it increases the adhesion and cohesion force of the system.

4.7 Atomic force microscopy (AFM)

The Figure 4.13 shows the AFM images of the surface after peeling test for the set with curing in vacuum oven at 60^{o}C. Image in Figure 4.14 (a) show that polymer without the incorporation of TMVS result in the weakest adhesion because no polymer were retain after the peeling test. Image in Figure 4.14 (b) and (c) after one peeling resulted in some defects seen between polymers. The polymer with 1 wt% and 3 wt% of TMVS show that the composite have insufficient Si-O-Si bond between the glass substrate and TMVS per polymer chain which results in weak adhesion. Image in Figure 4.14 (d) after the fourth peeling, the polymer remain intact with the formation of small island with lesser defect compare to images (b) and (c). Lastly, images in Figure 4.14 (e) and (f) after the fifth peeling show a better overall result with the least gap formation. For the polymer with 9 wt% TMVS it

shows a better adhesion when compared to the one with 7 wt% TMVS because the polymer layer remain intact with a thicker polymer layer. Therefore, the result obtained shows that increasing the concentration of TMVS in the polymer samples increases the adhesion between the polymer and glass substrate due to the formation of chemical bond between both materials. Thus, polymer sample with incorporation of 9 wt% of TMVS show the strongest adhesion.

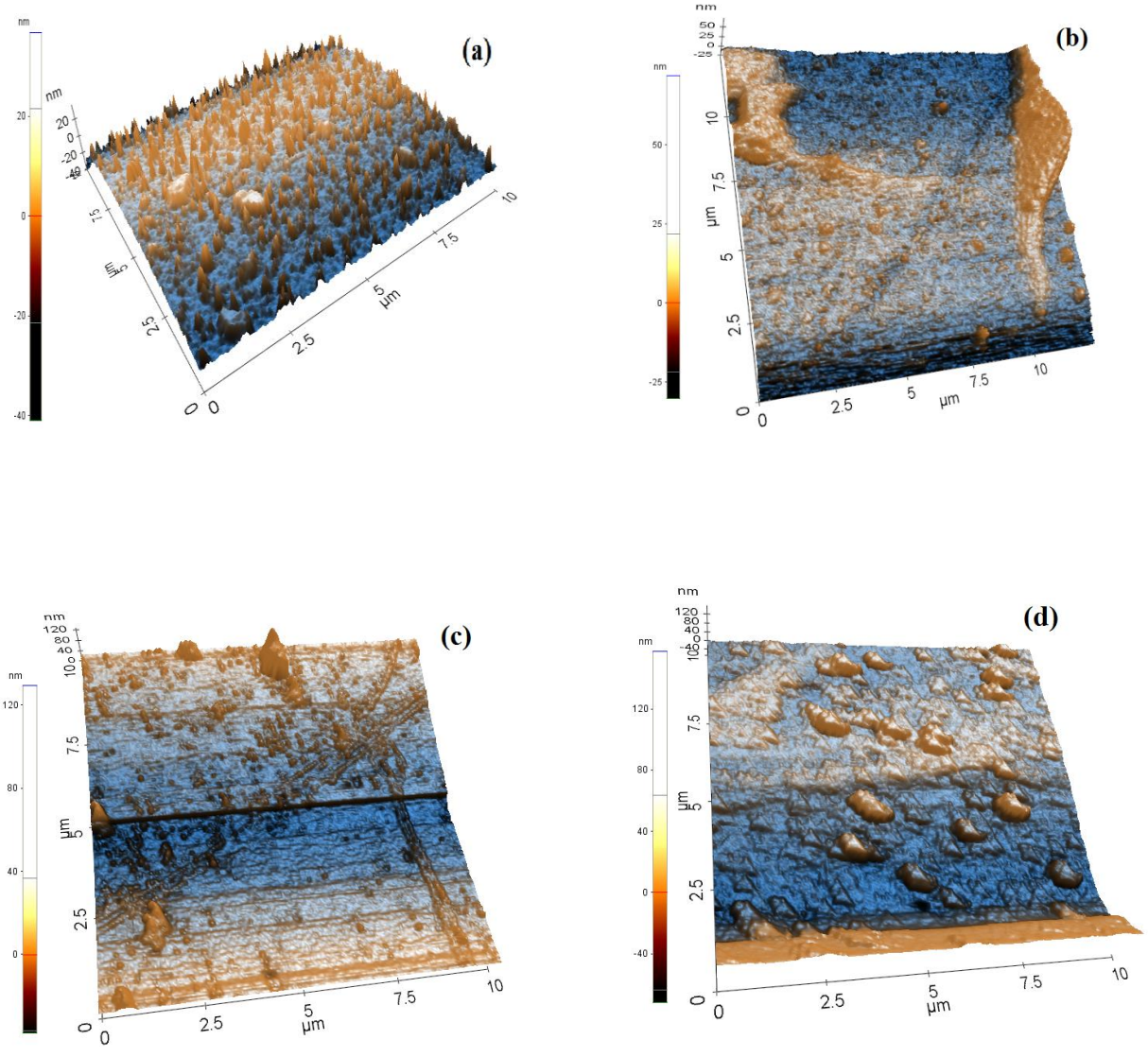

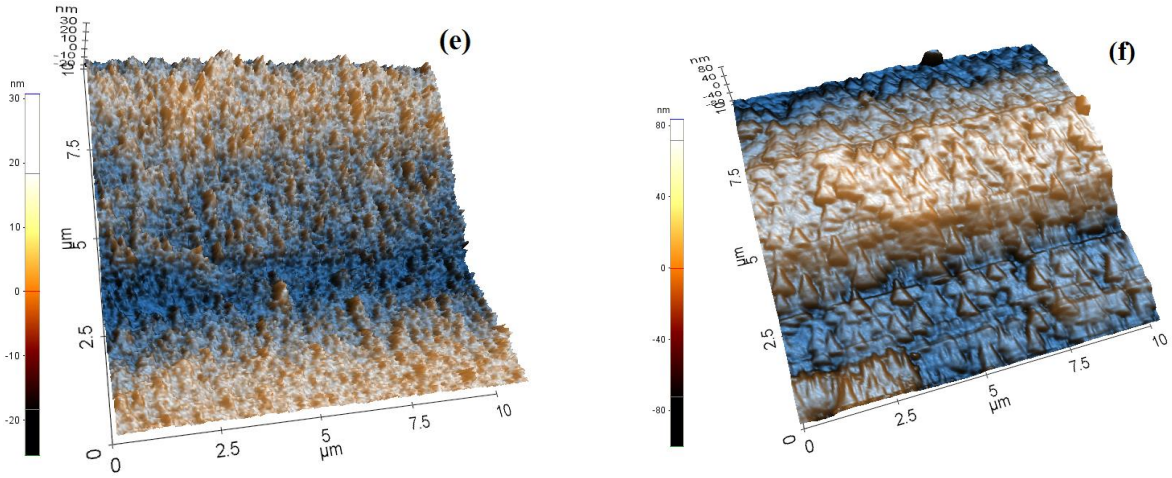

Figure 4.14: AFM images of P(MMA-*co*-AA) coating on glass substrate after peeling (a) blank (without TMVS) (b) polymer with 1 wt% of TMVS; (c) polymer with 3 wt% of TMVS; (d) polymer with 5 wt% of TMVS; (e) polymer with 7 wt% of TMVS; (f) polymer with 9 wt% of TMVS

4.8 Scanning electron microscopy (SEM)

Table 4.6 shows the thickness of P(MMA-*co*-AA) coated on the glass substrate. The results reveal that the thickness of the P(MMA-*co*-AA) coating increases steady according to the increase of the concentration of TMVS as predicted before. The polymer without the incorporation of TMVS have the thinness coated layer of 0.070 µm while for the polymer with the incorporation of 9 wt% of TMVS have the thickest coated layer of 0.263 µm. The thickness between the thinness and the thickest are in range of 0.193 µm.

Table 4.6: Thickness of coated P(MMA-co-AA) on glass substrate.

Sample	Thickness (µm)
Polymer	0.070
Polymer with 1 wt% TMVS	0.085
Polymer with 3 wt% TMVS	0.136
Polymer with 5 wt% TMVS	0.197
Polymer with 7 wt% TMVS	0.225
Polymer with 9 wt% TMVS	0.263

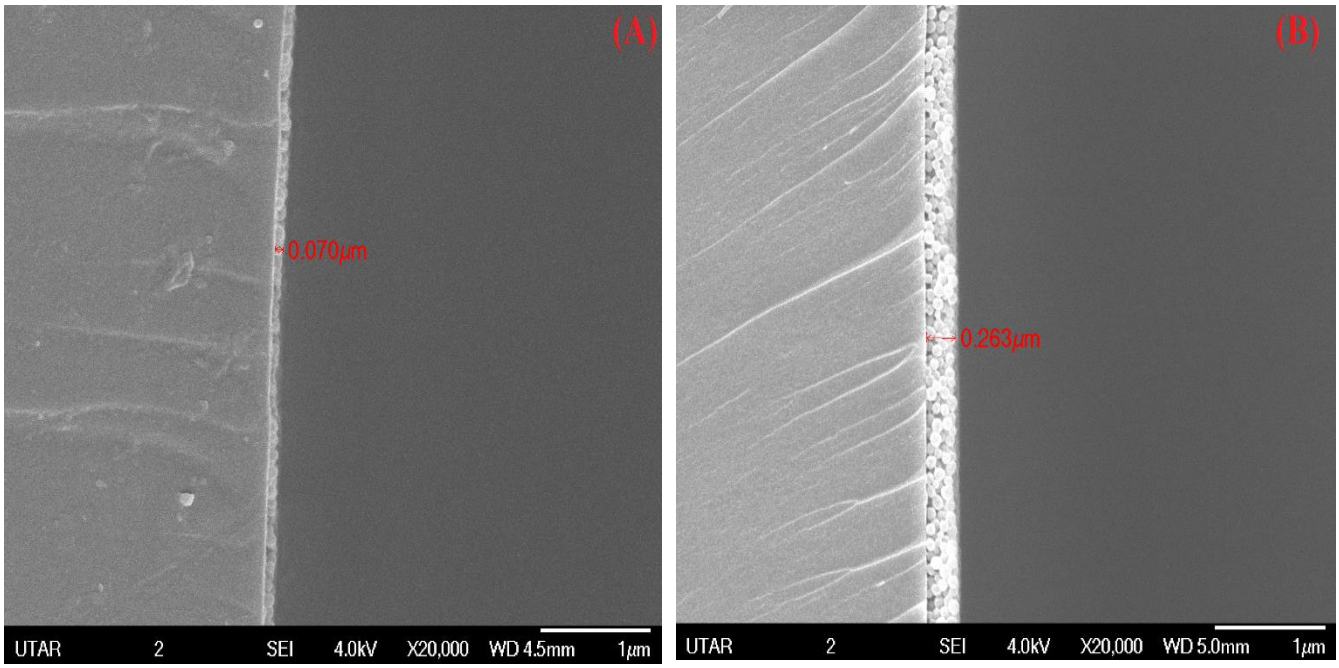

Figure 4.15: The coated P(MMA-*co*-AA) on glass substrate view under SEM with the magnification of 20000. (A) P(MMA-*co*-AA) (B) P(MMA-*co*-AA) with incorporation of 9 g of TMVS.

The major factor which causes the different range of thickness on the coated P(MMA-*co*-AA) on the glass substrate is due to the amount of TMVS incorporated into the synthesis of polymer. The different amount of TMVS incorporated into the polymer would have different degree of cross-linking between polymers. The higher cross-linking present between the polymers particles increases the thickness of the coating because higher TMVS present in the polymer increases the chance of interaction between the polymer particles.

The results obtain show that, P(MMA-*co*-AA) in the absent of TMVS have the thinnest coated layer on the glass substrate because the degree of cross-linking is the least compared with those samples with the incorporation of TMVS. This indicates that, the P(MMA-*co*-AA) does not possess the cross-linking properties as no TMVS was added into it. The thickest coated layer were present in the polymer with the highest concentration of TMVS (9 wt%). The high amount of TMVS in the polymer increases the hydrolysable –OH group to be directed to the exterior surface of the polymer particle which would increase the chance of cross-linking between the polymer particles through the condensation process. The results obtain form the SEM images provide an evident of crosslinking based on the surface morphology of the polymer with different concentration of TMVS. Therefore the increase in the thickness of the polymer coating is due to the increase in the degree of cross-linking.

4.9 Light harvesting efficiency of solar cell under fluorescence light

The solar cells coated with the P(MMA-*co*-AA) with and without the incorporation of TMVS were tested on the voltage, current and power to determine their light harvesting efficiency. Table 4.7 summarizes the result of the power output of the coated solar cell after multiple peeling test.

Figure 4.16 shows the graph of power output of a solar cell before and after the peeling test was carried out. The power output of the solar cell coated with P(MMA-*co*-AA) was compared in the graph. The six bare solar cell to be used was illuminated under the light source and generates 4.31, 4.67, 3.86, 4.63, 4.90 and 4.00 mW respectively. The solar cell with coating of P(MMA-*co*-AA) illuminated under the light source shows a generated power of 9.784 mW with an increment of 126.9%. The enhancement of light harvesting efficiency was due to the anti-reflective layer of the coating of P(MMA-*co*-AA). This reduces the amount of light being reflected away from the surface. Therefore, enhancing the light trapping efficiency of the solar cell consequently increased the creation of charge carrier in the form of electrons and holes, thus enhanced the power output. The peeling test shows a gradual decrease in the power output for each peeling was done (Table 4.7). The power output of solar cell after fourth peeling was 7.57 mW which shows a decrease of 51.37% compared to the result before peeling was done. This shows that most of the P(MMA-*co*-AA) layer has been removed from the surface of the solar cell after the fourth peeling process.

Table 4.7: Current, voltage and power measured from coated and uncoated solar cell samples

Condition of coating	Power output of solar cell (mW)					
	Polymer control	**Polymer with 1 wt% TMVS**	**Polymer with 3 wt% TMVS**	**Polymer with 5 wt% TMVS**	**Polymer with 7 wt% TMVS**	**Polymer with 9 wt% TMVS**
Before coating	4.31	4.67	3.86	4.63	4.90	4.00
After coating	9.78	10.77	8.58	8.83	8.97	6.03
1^{st} peeling	9.16	10.17	8.26	11.15	12.66	8.26
2^{nd} peeling	8.50	9.45	7.77	9.71	10.53	7.46
3^{rd} peeling	7.86	8.89	7.43	8.89	9.78	6.88
4^{th} peeling	7.57	8.57	7.09	7.64	9.02	6.20

Table 4.8: Percentage increment of solar cell efficiency

Condition of coating	Percentage increment of solar cell efficiency (%)					
	Polymer control	**Polymer with 1 wt% TMVS**	**Polymer with 3 wt% TMVS**	**Polymer with 5 wt% TMVS**	**Polymer with 7 wt% TMVS**	**Polymer with 9 wt% TMVS**
After coating	126.9	130.54	122.26	90.73	83.25	50.7
1^{st} peeling	112.5	117.75	113.91	140.87	158.9	106.5
2^{nd} peeling	97.2	102.36	101.29	109.82	115.0	86.6
3^{rd} peeling	82.2	90.27	92.58	92.03	99.7	72.1
4^{th} peeling	75.5	83.51	83.74	65.05	84.2	55.1

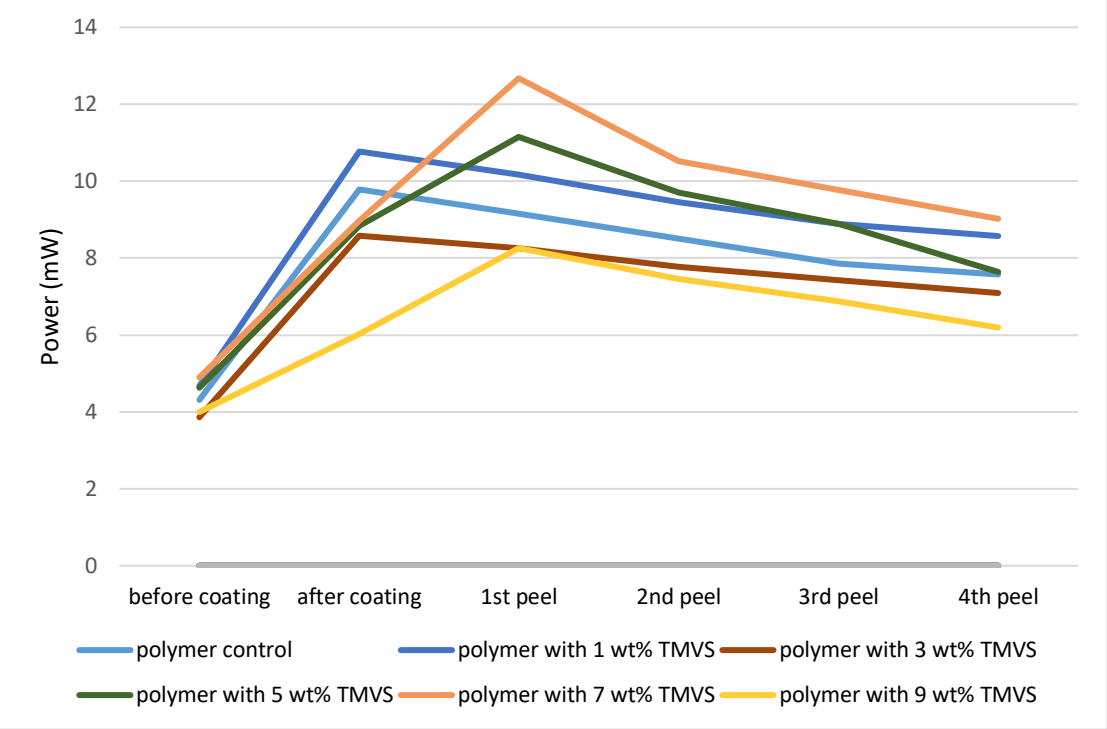

Figure 4.16: Graph of the number of peeling versus the power output of the solar cell

The solar cell with coating of P(MMA-*co*-AA) with 1 and 3 wt% of TMVS shows a generated power of 10.77 and 8.58 mW with an increment of 130.54 % and 122.26 % respectively. The light harvesting enhancement was also due to the anti-reflective properties of the coated polymer layer which increases the light transmission to the solar cell. As seen in the SEM image, the P(MMA-*co*-AA) with 1 and 3 wt% of TMVS consist of a thinner polymer layer compared to the other polymer with higher concentration of TMVS. The thinner layer allow higher amount light transmission to the solar cell. Therefore, the anti-reflective properties and the thinner layer of coated polymer enhance the light harvesting efficiency. The P(MMA-*co*-AA) with 1 and 3 wt% of TMVS shows the similar trend as the

P(MMA-co-AA) control because no increment of power output after the first peeling test. It was observed that, the P(MMA-*co*-AA) with 1 wt% of TMVS have a higher increment compared to 3 wt% of TMVS because the polymer with 3 wt% of TMVS has a thicker coated polymer layer approximately 2 times as seen in the SEM image. The thick layer of polymer blocked the transmission of light to the solar cell which reduces the power output of the solar cell. As the peeling goes on, the power output of the solar cell decreases. The power output of the solar cell after the fourth peeling were 8.57 and 7.09 mW which shows a decrease of 47.03 % and 38.52 % compared to the result before peeling was done.

The solar cell with coating of P(MMA-*co*-AA) with 5, 7 and 9 wt% of TMVS shows an increase in the power output of the solar cell but comparably lesser to P(MMA-*co*-AA) without TMVS. This provide an evident that with the incorporation of TMVS it would affect the light transmission properties of the polymer sample. The solar cells with coating of P(MMA-*co*-AA) varied in TMVS concentration of 5, 7 and 9 wt% show a generated power of 8.83, 8.97 and 6.03 mW with an increment of 90.73, 83.25 and 50.73% respectively. The result obtained were compare with the P(MMA-*co*-AA) control which shows that the polymer with TMVS generate a lower power output value. The reason is that the incorporation of TMVS into the polymer sample promote the formation of multilayer polymer on the surface of the solar cell because of the cross-linking between polymer nanosphere.

The high degree of cross-linking between polymer nanospheres result in a thicker coating of P(MMA-*co*-AA) on the solar cell. The results show that, the thickness of the P(MMA-*co*-AA) layer on the solar cell would affect the generation of power output. After the first peeling, the power output of the solar cell increases by 140.87 %, 158.88 % and 106.54 % for P(MMA-*co*-AA) with 5, 7 and 9 wt% of TMVS respectively. The first peeling remove the thick multilayer to form a thinner layer of P(MMA-*co*-AA) nanospheres on the solar cell. Thus, the formation of thinner coating result in the higher light harvesting efficiency. Further peeling causes a gradual decrease in the power output after each peeling was done. The power output of solar cell coated with P(MMA-*co*-AA) with 5, 7 and 9 wt% of TMVS after the fourth peeling are 7.64, 9.02 and 6.20 mW. The result shows that the P(MMA-*co*-AA) with 5 wt% decrease by 28.30 % while for P(MMA-*co*-AA) with 7 and 9 wt% shows an increment of 0.9 and 4.35% compared to the newly coated solar cell with its respective concentration. This shows that the monolayer of P(MMA-*co*-AA) layer were remain intact on the surface of the solar cell.

The solar cell coated with P(MMA-*co*-AA) with the incorporation of TMVS shows two general trend firstly a gradual decrease in the power output as the peeling test proceed. Secondly, the power output increases after the first peeling then as the peeling proceed the power output decreases gradually. The result obtained was concluded that P(MMA-*co*-AA) with 7 wt% to be the best light harvesting enhancement properties with a sufficient adhesion strength. The P(MMA-*co*-AA) with 1 and 3 wt% of TMVS have a low adhesion strength due to the insufficient

adhesion on the solar cell. The P(MMA-*co*-AA) with 5 wt% shows similar trend as polymer with 7 and 9 wt% but with weaker adhesion strength because the power output is considerably lower compare to P(MMA-*co*-AA) with 7 wt% of TMVS because most of the polymer layer was being peeled off which reduces the anti-reflective properties on the solar cell. As with the P(MMA-*co*-AA) with 9 wt% of TMVS shows a higher adhesion strength compared to P(MMA-*co*-AA) with 7 wt% of TMVS. Therefore, the high amount of adhesion strength resist the peeling test much stronger which retained much of it multilayer polymer on the solar cell. Thus, P(MMA-*co*-AA) with 7 wt% shows a sufficient adhesion strength with high efficiency in light harvesting.

CHAPTER 5

CONCLUSIONS

5.1 Conclusions

This study, showed that incorporation of TMVS coupling agent as adhesion promoter has increase the adhesion performance of P(MMA-*co*-AA) on the glass substrate. Acrylic acid monomer were added to increase the wettability properties on the glass substrate but the result reveal, it has the lowest adhesion strength compare to the polymer with TMVS. Polymer with different amount of TMVS was synthesized in this study to determine the amount of TMVS which give the best adhesion performance. The polymer with 9 wt% of TMVS was found to give the strongest adhesion among the other polymer (1, 3, 5 and 7 wt%). The reason was owing to the high amount of active site which is capable of reacting with the hydroxyl group on the glass substrate forming strong Si-O-Si covalent bonds. Besides that, the adhesion increases when the coated glass slides were subjected for curing at 60^{o}C because it help to remove by-product water and increase the number of firmly bounded polymer chain on glass substrate.

The thermal characterization of P(MMA-*co*-AA) with and without the TMVS shows that the result does not change the thermal properties much. The TGA

thermogram showed that there are two degradation stages which occur at 186.85 and 389.00^{o}C. The first degradation is caused by the decomposition of AA side chain through the decarboxylation reaction whereas the second degradation is caused by the breakdown of polymer back bone. The first degradation occurred above 100^{o}C which is considerably a good material to be use for outdoor purpose. From DSC characterization, it shows that the T_g increases as the amount of TMVS increases because the amount of crosslinking increases between the polymer chains. Besides that, the SEM result shows that the thickness increases as the amount of TMVS incorporated into the polymer increases. The amount of cross-linking would increase the thickness of the polymer on the coated glass susbtrate.

The particle size distribution of the synthesize polymer have a distribution range from 52 to 240 nm with the average particle size of 106 nm. The distribution range of the polymer particle size obtained is considerable wide with a difference of 188 nm between the largest and the smallest polymer particles that can be found in the emulsion. The characterization of P(MMA-*co*-AA) with TMVS using ATR-FTIR shows the absent of C=C peak at 1600-1700 cm^{-1} indicating that the carbon double bond were open and reacted to form polymer chain. Besides that, the presence of Si-OH peak proved that the TMVS were successfully incorporated into the polymer chain and the presence of hydrolysable Si-OH group indicate that there is available active site for the condensation reaction of silane coupling agent onto the hydroxylated glass substrate.

The P(MMA-*co*-AA) coated on solar cell increases the light harvesting efficiency by acting as the anti-reflective layer on the solar cell surface which increases the light transmission to the solar cell. The result shows that, P(MMA-*co*-AA) with 7 wt% have the sufficient adhesion strength which give the highest light harvesting efficiency on the solar cell.

5.2 Future perspective

Some future study were suggested below:

1. To further increase the amount of TMVS to determine the maximum adhesion that could be obtain.

2. To carry out a comprehensive study of the effect TMVS on the light harvesting efficiency of solar cell by using different types of coupling agent.

3. To test the adhesion of polymer coating by exposing the coated solar cell to outdoor weathering for a certain period of time with monitoring.

REFERENCE

Adhikari, R. (2013). Atomic Force Microscopy of Polymer/Layered Silicate Nanocomposites (PLSNs): A Brief Overview. *Macromolecular Symposia*, 327(1), pp.10-19.

Alkan, C., Aksoy, S. and Anayurt, R. (2015). Synthesis of poly(methyl methacrylate-co-acrylic acid)/n-eicosane microcapsules for thermal comfort in textiles. *Textile Research Journal*, 85(19), pp.2051-2058.

Andrews, R. and Kazama, Y. (1967). Rheo-optical Properties of Polyvinyl Chloride Films: Unplasticized Homopolymer. *Journal of Applied Physics*, 38(11), pp.4118-4123.

Blum, F., Meesiri, W., Kang, H. and Gambogi, J. (1991). Hydrolysis, adsorption, and dynamics of silane coupling agents on silica surfaces. *Journal of Adhesion Science and Technology*, 5(6), pp.479-496.

Chand, N. and Dwivedi, U. (2006). Effect of coupling agent on abrasive wear behaviour of chopped jute fibre-reinforced polypropylene composites. *Wear*, 261(10), pp.1057-1063.

Cleary, J., Bromberg, L. and Magner, E. (2004). Adhesion of Polyether-Modified Poly(acrylic acid) to Mucin. *Langmuir*, 20(22), pp.9755-9762.

Coast, R., Pikus, M., Henriksen, P. and Nitowski, G. (1996). Vibrational Spectroscopic Observation of Acrylic Acid Coadsorbed in Dissociated and Molecular Forms on Oxidized Aluminum. *The Journal of Physical Chemistry*, 100(37), pp.15011-15014.

Eshel, G., Levy, G., Mingelgrin, U. and Singer, M. (2004). Critical Evaluation of the Use of Laser Diffraction for Particle-Size Distribution Analysis. *Soil Science Society of America Journal*, 68(3), p.736.

Faghihi, M. and Shojaei, A. (2009). Properties of alumina nanoparticle-filled nitrile-butadiene-rubber/phenolic-resin blend prepared by melt mixing. *Polymer Composites*, 30(9), pp.1290-1298.

Gelest.com. (2018). [online] Available at: https://www.gelest.com/wp-content/uploads/Goods-PDF-brochures-couplingagents.pdf [Accessed 26 Jun. 2018].

Ghaffari, M., Naderi, R. and Ehsani, M. (2014). Effect of silane as surface modifier and coupling agent on rheological and protective performance of epoxy/nano-glassflake coating systems. *Iranian Polymer Journal*, 23(7), pp.559-567.

Gibbs, P. (1996). *Is glass liquid or solid?*. [online] Math.ucr.edu. Available at: http://math.ucr.edu/home/baez/physics/General/Glass/glass.html [Accessed 26 Jun. 2018].

Hertl, W. (1968). Mechanism of gaseous siloxane reaction with silica. II. *The Journal of Physical Chemistry*, 72(12), pp.3993-3997.

Jörg, F. (2017). Functional Groups at Polymer Surface and Their Reactions. *Metal-Polymer Systems*, pp.135-172.

Kalita, D. and Netravali, A. (2015). Interfaces in Green Composites: A Critical Review. *Reviews of Adhesion and Adhesives*, 3(4), pp.386-443.

Kaynak, C., Celikbilek, C. and Akovali, G. (2003). Use of silane coupling agents to improve epoxy–rubber interface. *European Polymer Journal*, 39(6), pp.1125-1132.

Kendall, K. (1971). The adhesion and surface energy of elastic solids. *Journal of Physics D: Applied Physics*, 4(8), pp.1186-1195.

Khursheed, A. (2006). Scanning electron microscope design for quantitative multicontrast. *Scanning*, 18(2), pp.81-91.

Laskowski, C. (1998). *Acrylic Acid Production*. [online] Owlnet.rice.edu. Available at: http://www.owlnet.rice.edu/~ceng403/gr1498/AcrylicAcid.htm [Accessed 26 Jun. 2018].

Lee, C. L., Goh, W. S., Chee, S. Y., Yik, L.K. (2017) Enhancement of light harvesting efficiency of silicon solar cell utilizing arrays poly(methyl methacrylate-*co*-acrylic acid) nano-spheres and nano-spheres with embedded silver nano-particles. *Photonics and Nanostructures – Fundamentals and Apllications, 23, pp.36-44*

Lee, C., Goh, W., Chee, S. and Yik, L. (2017). Augmentation of power conversion efficiency of amorphous silicon solar cell employing poly(methyl methacrylate-co-acrylic acid) nanospheres encapsulated with gold nanoparticles. *Journal of Materials Science*, 53(7), pp.5183-5193.

Lee, S. and Wang, S. (2006). Biodegradable polymers/bamboo fiber biocomposite with bio-based coupling agent. *Composites Part A: Applied Science and Manufacturing*, 37(1), pp.80-91.

Liu, H. and Du, J. (2006). Synthesis and characterization of MoO2/P(St-co-MMA-co-AA) microspheres via microemulsion by γ-ray radiation. *Solid State Sciences*, 8(5), pp.526-530.

Liu, Q., Ding, J., Chambers, D., Debnath, S., Wunder, S. and Baran, G. (2001). Filler-coupling agent-matrix interactions in silica/polymethylmethacrylate composites. *Journal of Biomedical Materials Research*, 57(3), pp.384-393.

Miller, A. and Berg, J. (2003). Effect of silane coupling agent adsorbate structure on adhesion performance with a polymeric matrix. *Composites Part A: Applied Science and Manufacturing*, 34(4), pp.327-332.

Monticelli, F., Toledano, M., Osorio, R. and Ferrari, M. (2006). Effect of temperature on the silane coupling agents when bonding core resin to quartz fiber posts. *Dental Materials*, 22(11), pp.1024-1028.

Nachtigall, S., Cerveira, G. and Rosa, S. (2007). New polymeric-coupling agent for polypropylene/wood-flour composites. *Polymer Testing*, 26(5), pp.619-628.

Oh, S., Cho, B., Jeong, M. and Ko, J. (2016). Evaluation of the isothermal curing process of UV-cured resin in terms of elasticity studied through micro-Brillouin light scattering. *Journal of Information Display*, 17(2), pp.87-91.

Park, S. and Jin, J. (2001). Effect of Silane Coupling Agent on Interphase and Performance of Glass Fibers/Unsaturated Polyester Composites. *Journal of Colloid and Interface Science*, 242(1), pp.174-179.

Plueddemann, E. (1991.). *Silane Coupling Agents*. 2nd ed. New York: Plenum Press, pp.1-6.

Reynolds, W. (1949). Emulsion polymerization. *Journal of Chemical Education*, 26(3), p.135.

Rsc.org. (2018). *Silicon - Element information, properties and uses | Periodic Table*. [online] Available at: http://www.rsc.org/periodic-table/element/14/silicon [Accessed 26 Jun. 2018].

Said, H., Nik Salleh, N., Alias, M. and El-Naggar, A. (2013). Synthesis and characterization of hard materials based on radiation cured bio-polymer and nanoparticles. *Journal of Radiation Research and Applied Sciences*, 6(2), pp.71-78.

Schneider, M., Graillat, C., Guyot, A. and McKenna, T. (2002). High solids content emulsions. III. Synthesis of concentrated latices by classic emulsion polymerization. *Journal of Applied Polymer Science*, 84(10), pp.1916-1934.

Shefer, A. and Gottlieb, M. (1992). Effect of crosslinks on the glass transition temperature of end-linked elastomers. *Macromolecules*, 25(15), pp.4036-4042.

Simal, F., Demonceau, A. and Noels, A. (1999). Highly Efficient Ruthenium-Based Catalytic Systems for the Controlled Free-Radical Polymerization of Vinyl Monomers. *Angewandte Chemie International Edition*, 38(4), pp.538-540.

Smith, N., Antoun, G., Ellis, A. and Crone, W. (2004). Improved adhesion between nickel–titanium shape memory alloy and a polymer matrix via silane coupling agents. *Composites Part A: Applied Science and Manufacturing*, 35(11), pp.1307-1312.

Sood, A. (2004). Particle size distribution control in emulsion polymerization. *Journal of Applied Polymer Science*, 92(5), pp.2884-2902.

Sterman, S. and Marsden, J. (1966). SILANE COUPLING AGENTS. *Industrial & Engineering Chemistry*, 58(3), pp.33-37.

Wang, J., Chen, C., Buck, S. and Chen, Z. (2001). Molecular Chemical Structure on Poly(methyl methacrylate) (PMMA) Surface Studied by Sum Frequency Generation (SFG) Vibrational Spectroscopy. *The Journal of Physical Chemistry B*, 105(48), pp.12118-12125.

Wang, L., Liu, Y. and Liu, G. (2017). Hydrophobic coating of mica by piranha solution activation, silanization grafting, and copolymerization with acrylate monomers. *Journal of Applied Polymer Science*, 134(25).

Wu, J., Li, P., Ma, X., Liang, Q., Yuan, T. and Ma, G. (2015). Synthesis and characterization of polyacrylate composite with thiol-modified nanosilica as chain transfer agent. *Journal of Applied Polymer Science*, 132(45), pp. 42756

Xie, Y., Hill, C., Xiao, Z., Militz, H. and Mai, C. (2010). Silane coupling agents used for natural fiber/polymer composites: A review. *Composites Part A: Applied Science and Manufacturing*, 41(7), pp.806-819.

Yeon, K., Jin, N., Kwon, Y. and Ryu, K. (2003). Workability and Strength Properties of MMA-Modified Up Polymer Concrete. *Journal of Polymer Engineering*, 23(5).

Appendices

Appendix A

The total solid content for each polymer sample (1st trial)

Polymer sample	m1 (mg)	m2 (mg)	TSC (mg/mL)
P(MMA-*co*-AA)	482.7	280.7	202.0
P(MMA-*co*-AA) 1 g TVMS	458.1	248.0	210.1
P(MMA-*co*-AA) 3 g TVMS	485.4	287.0	198.4
P(MMA-*co*-AA) 5 g TVMS	448.8	243.0	205.8
P(MMA-*co*-AA) 7 g TVMS	517.4	306.3	211.1
P(MMA-*co*-AA) 9 g TVMS	485.5	283.9	201.6

Appendix B

The total solid content for each polymer sample (2nd trial)

Polymer sample	m1 (mg)	m2 (mg)	TSC (mg/mL)
P(MMA-*co*-AA)	494.0	285.0	209.0
P(MMA-*co*-AA) with 1 g of TVMS	479.6	275.6	204.0
P(MMA-*co*-AA) with 3 g of TVMS	510.8	310.3	200.5
P(MMA-*co*-AA) with 5 g of TVMS	420.2	212.4	207.8
P(MMA-*co*-AA) with 7 g of TVMS	513.5	304.0	209.5
P(MMA-*co*-AA) with 9 g of TVMS	470.2	268.2	202.0

Appendix C

Table 4.3: The total solid content for each polymer sample (3rd trial)

Polymer sample	m1 (mg)	m2 (mg)	TSC (mg/mL)
P(MMA-*co*-AA)	483.4	277.7	205.7
P(MMA-*co*-AA) 1 g TVMS	458.1	254.3	203.8
P(MMA-*co*-AA) 3 g TVMS	517.1	318.9	198.2
P(MMA-*co*-AA) 5 g TVMS	474.4	268.4	206.0
P(MMA-*co*-AA) 7 g TVMS	500.0	289.7	210.3
P(MMA-*co*-AA) 9 g TVMS	441.6	236.8	204.8

Appendix D

Infrared spectra of P(MMA-co-AA) with 1 wt% of TMVS

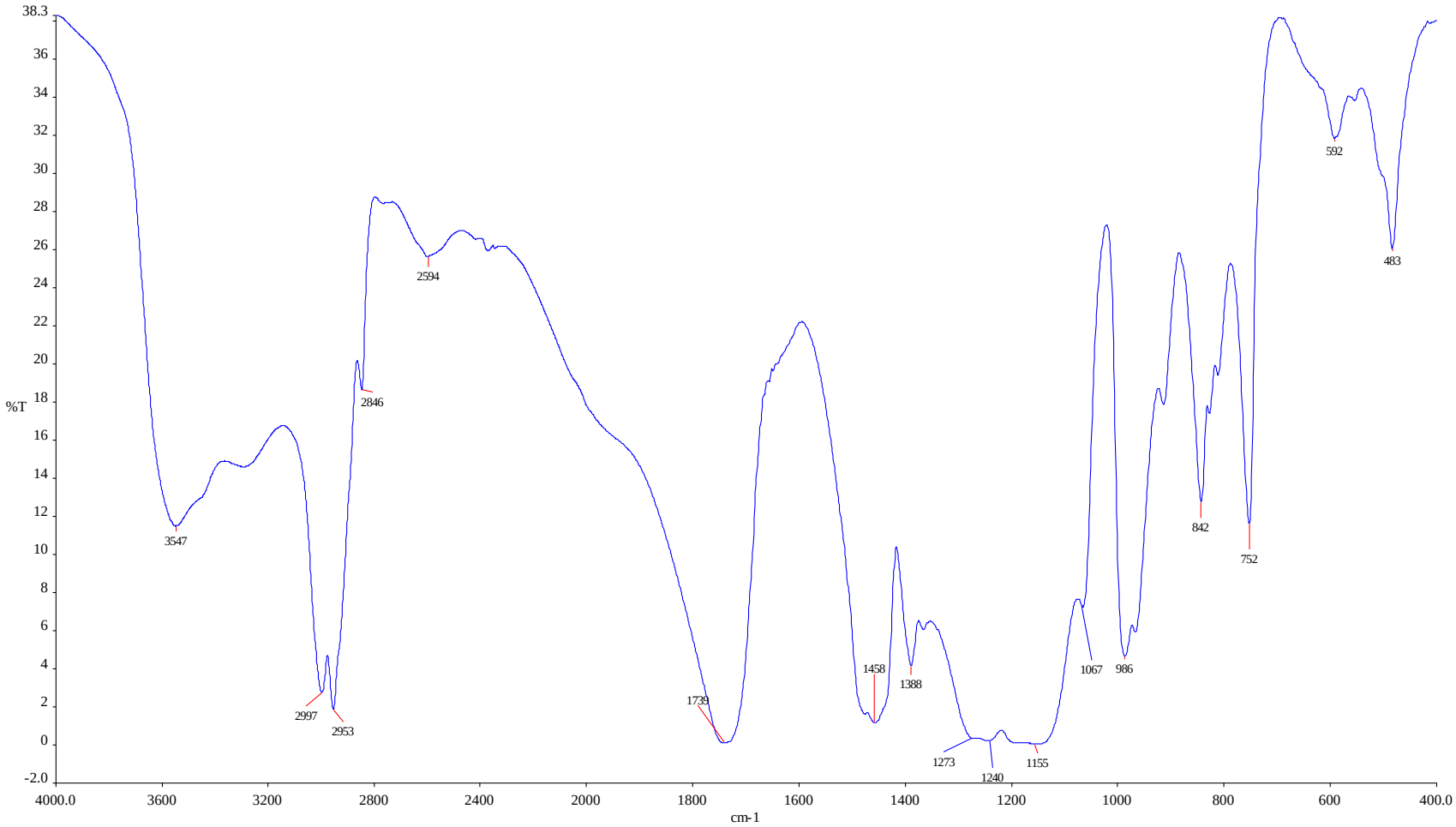

Appendix E

Infrared spectra of P(MMA-co-AA) with 3 wt% of TMVS

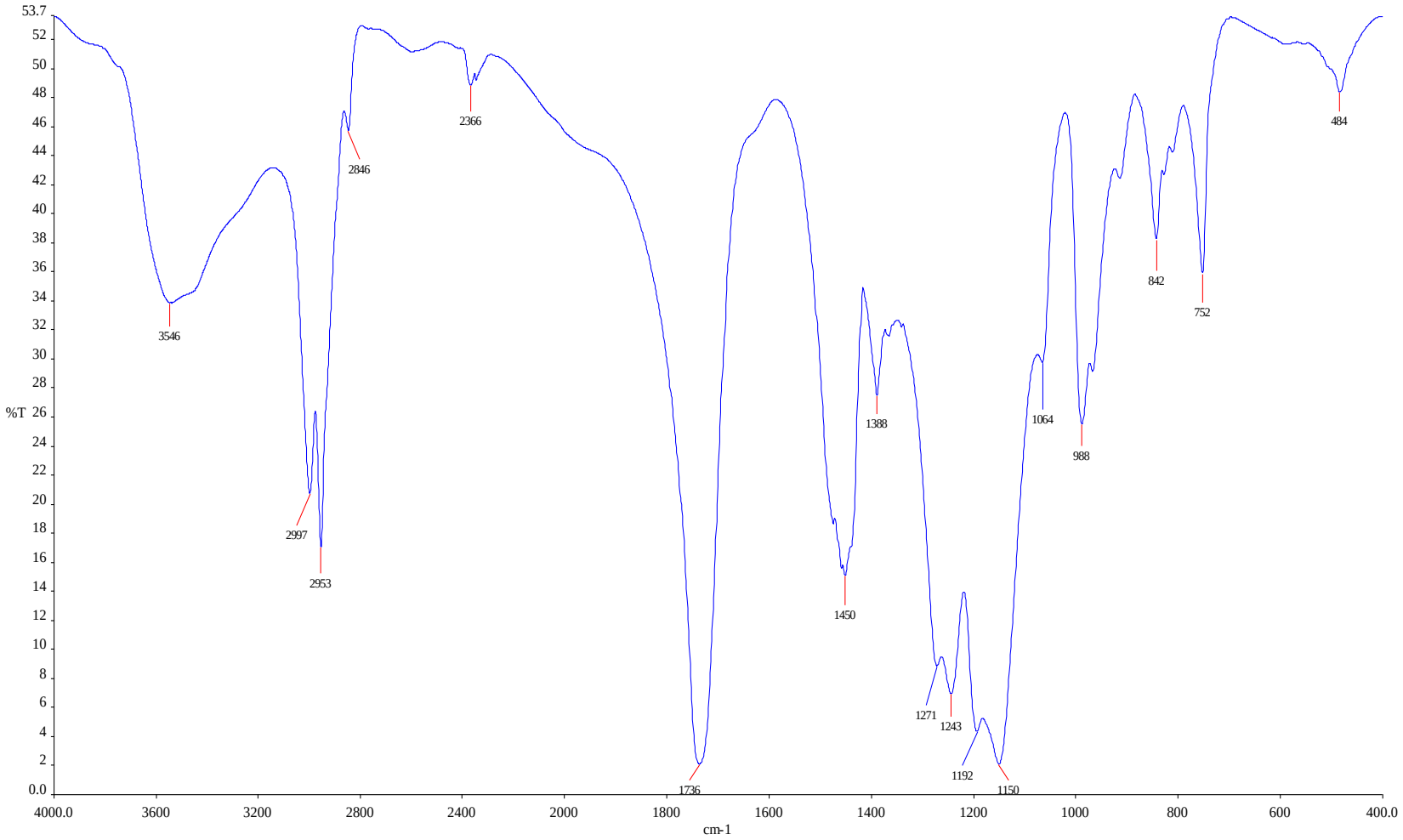

Appendix F

Infrared spectra of P(MMA-co-AA) with 5 wt% of TMVS

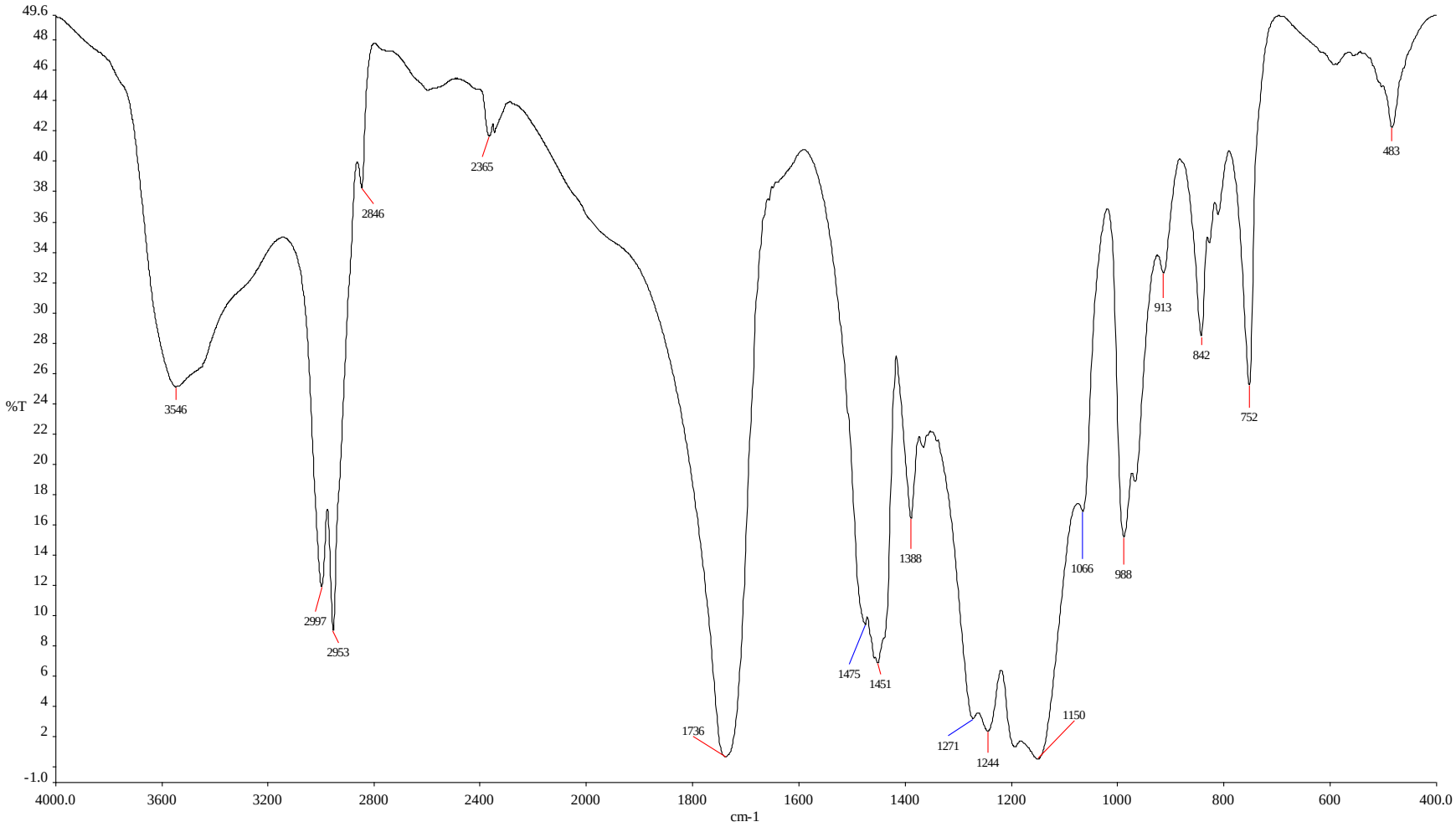

Appendix G

Infrared spectra of P(MMA-co-AA) with 7 wt% of TMVS

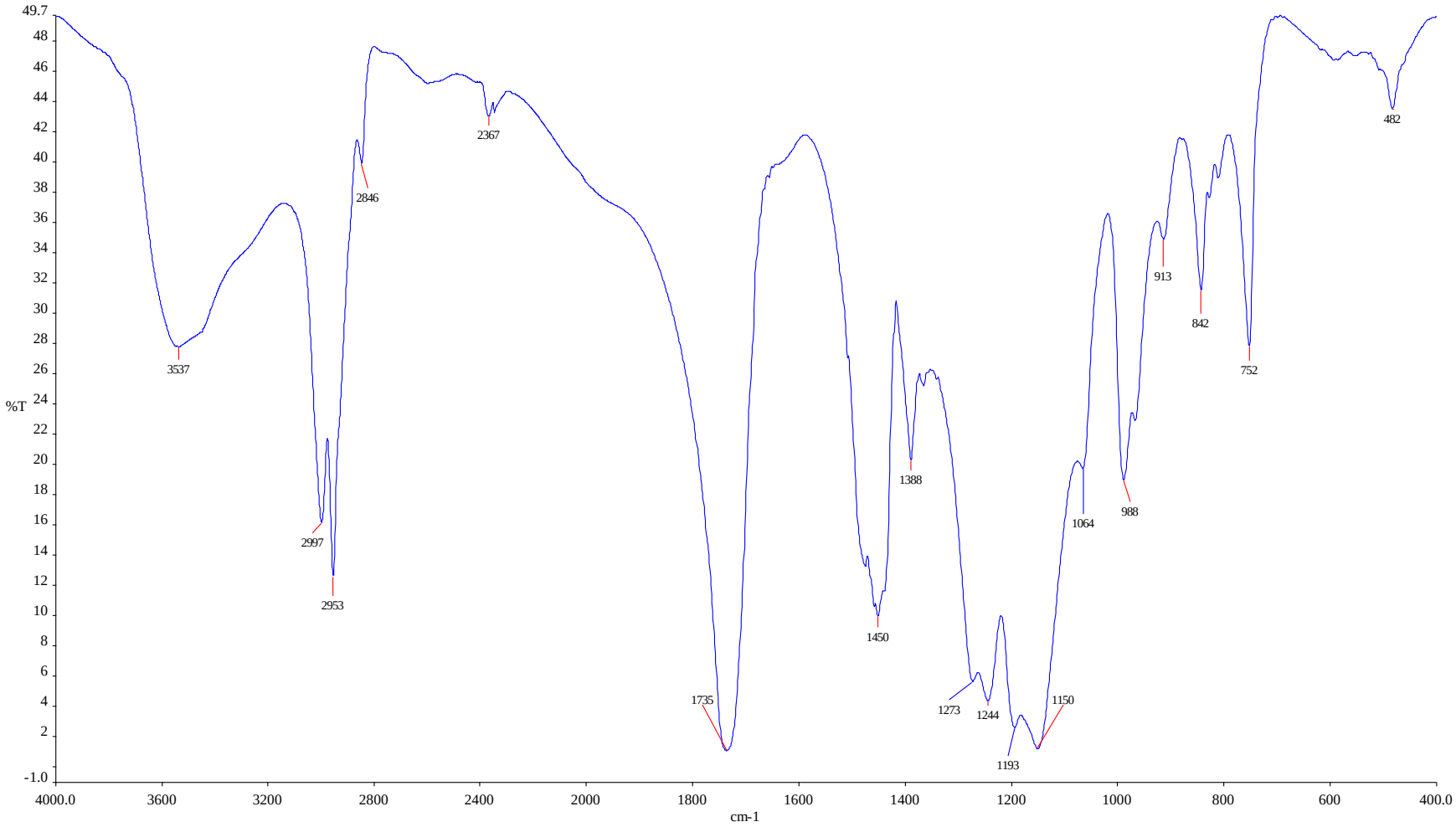

Appendix H

TGA thermogram of P(MMA-*co*-AA) with 1 wt% of TMVS

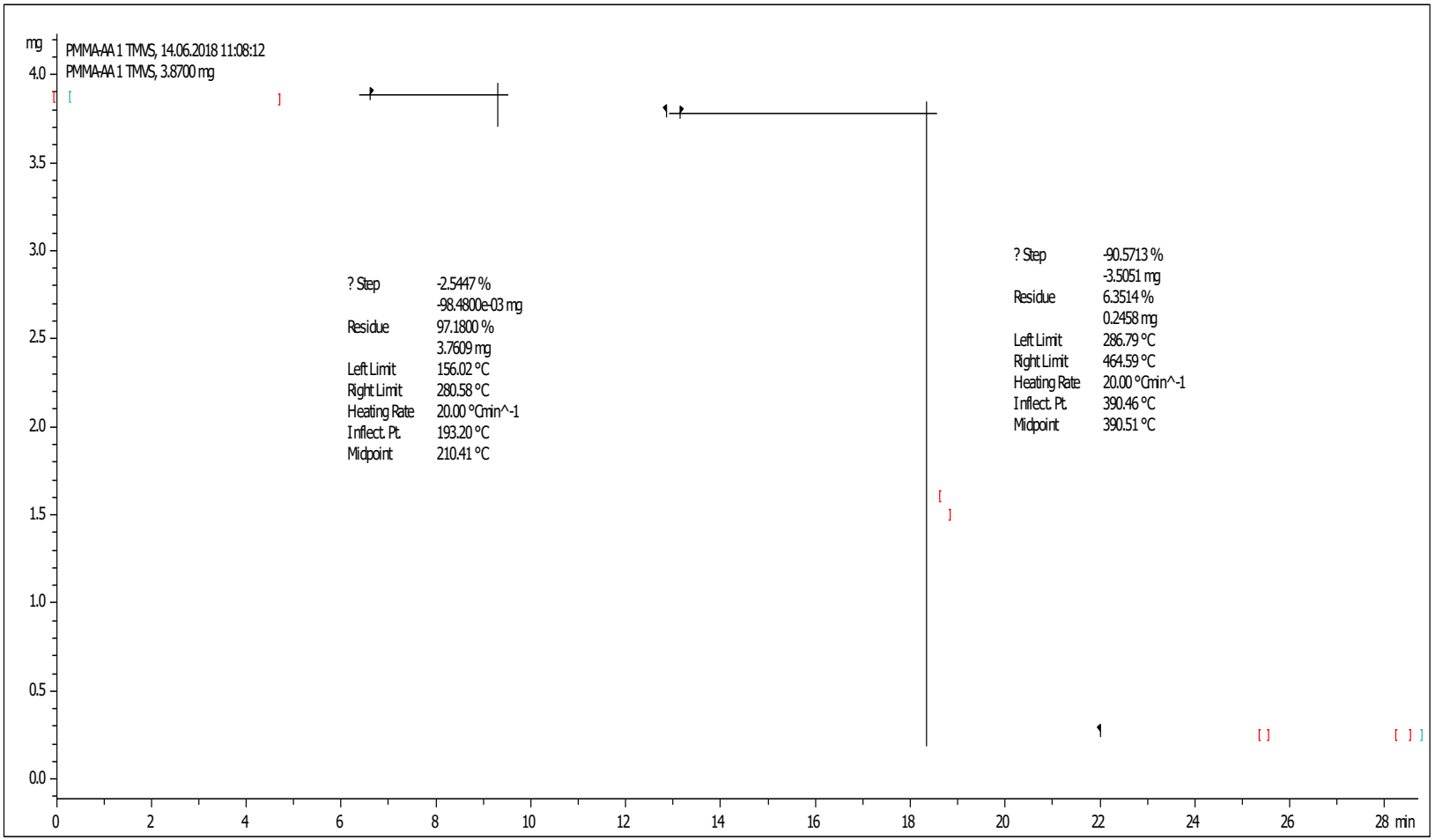

Appendix I

TGA thermogram of P(MMA-*co*-AA) with 3 wt% of TMVS

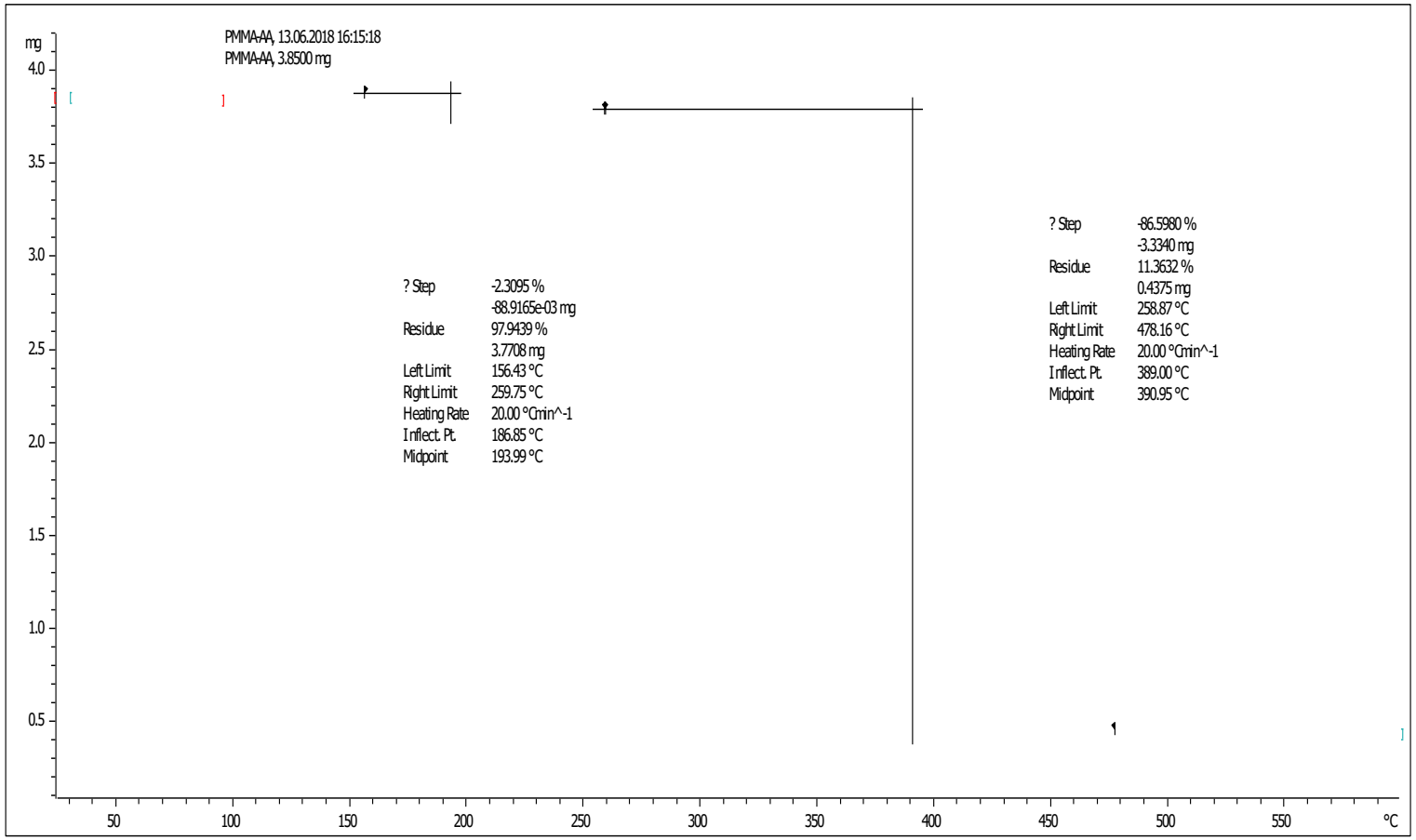

Appendix J

TGA thermogram of P(MMA-*co*-AA) with 5 wt% of TMVS

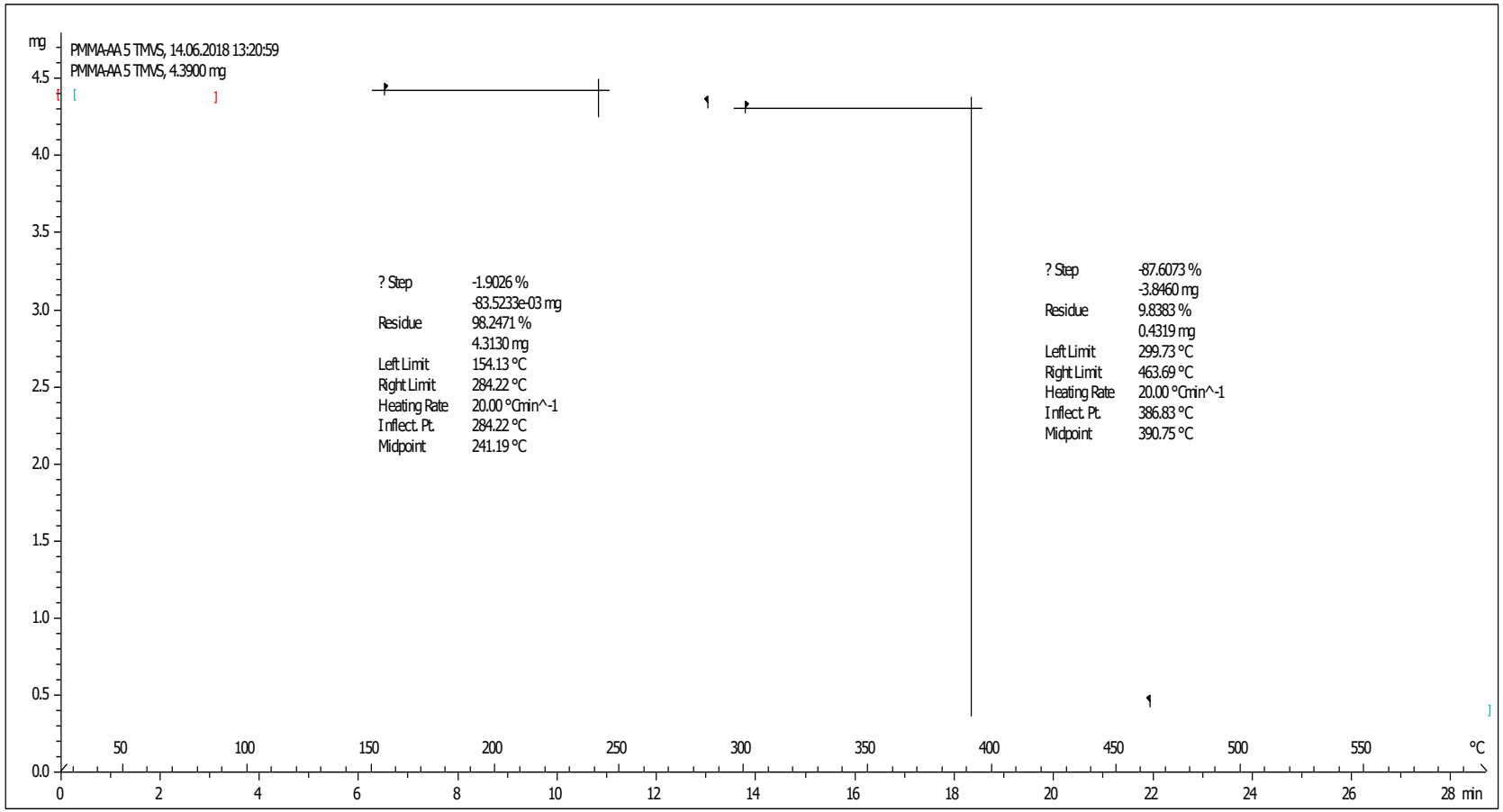

Lab: METTLER STARe SW 10.00

Appendix K

TGA thermogram of P(MMA-*co*-AA) with 7 wt% of TMVS

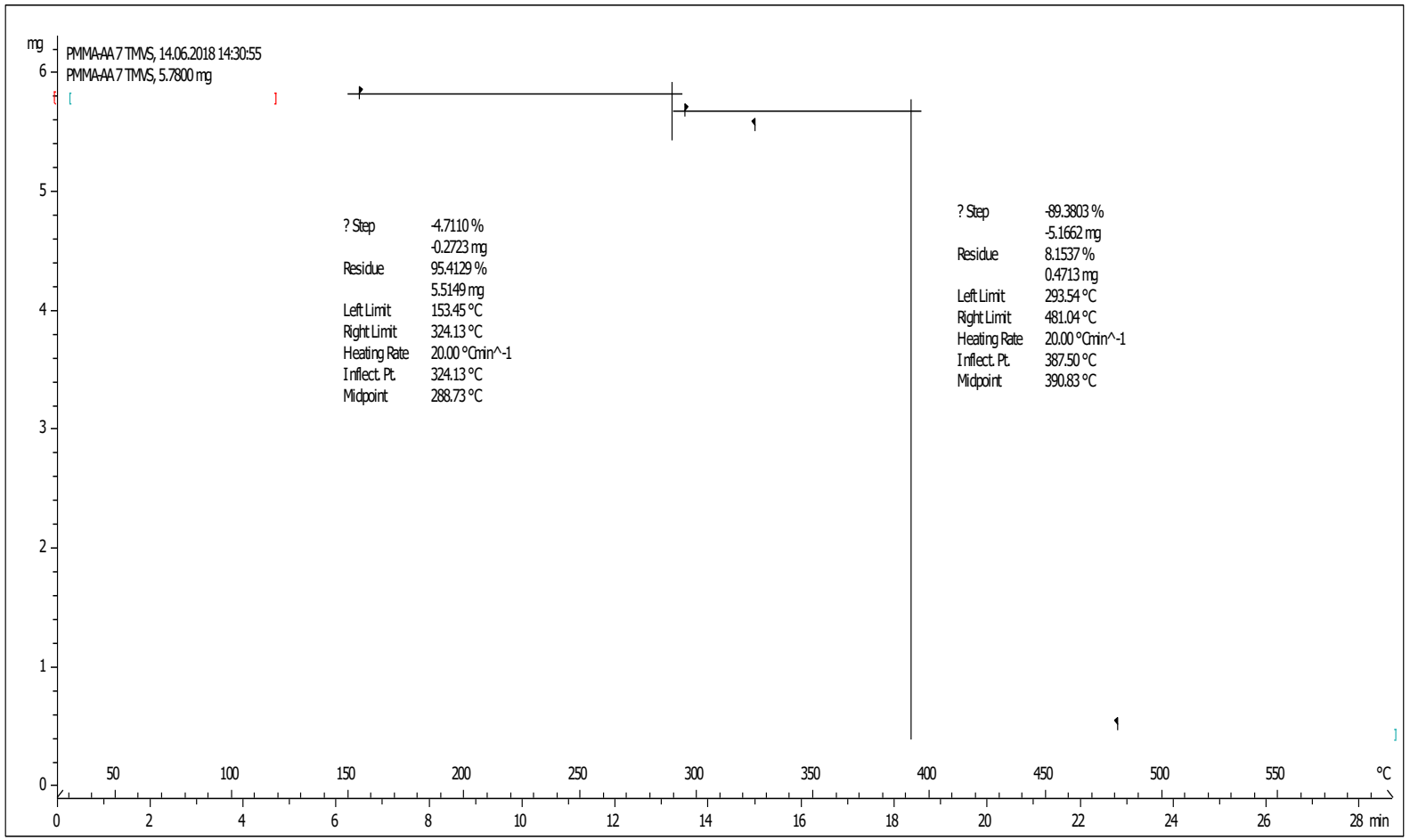

Appendix L

DSC Thermogram of P(MMA-co-AA) with 1 wt% of TMVS

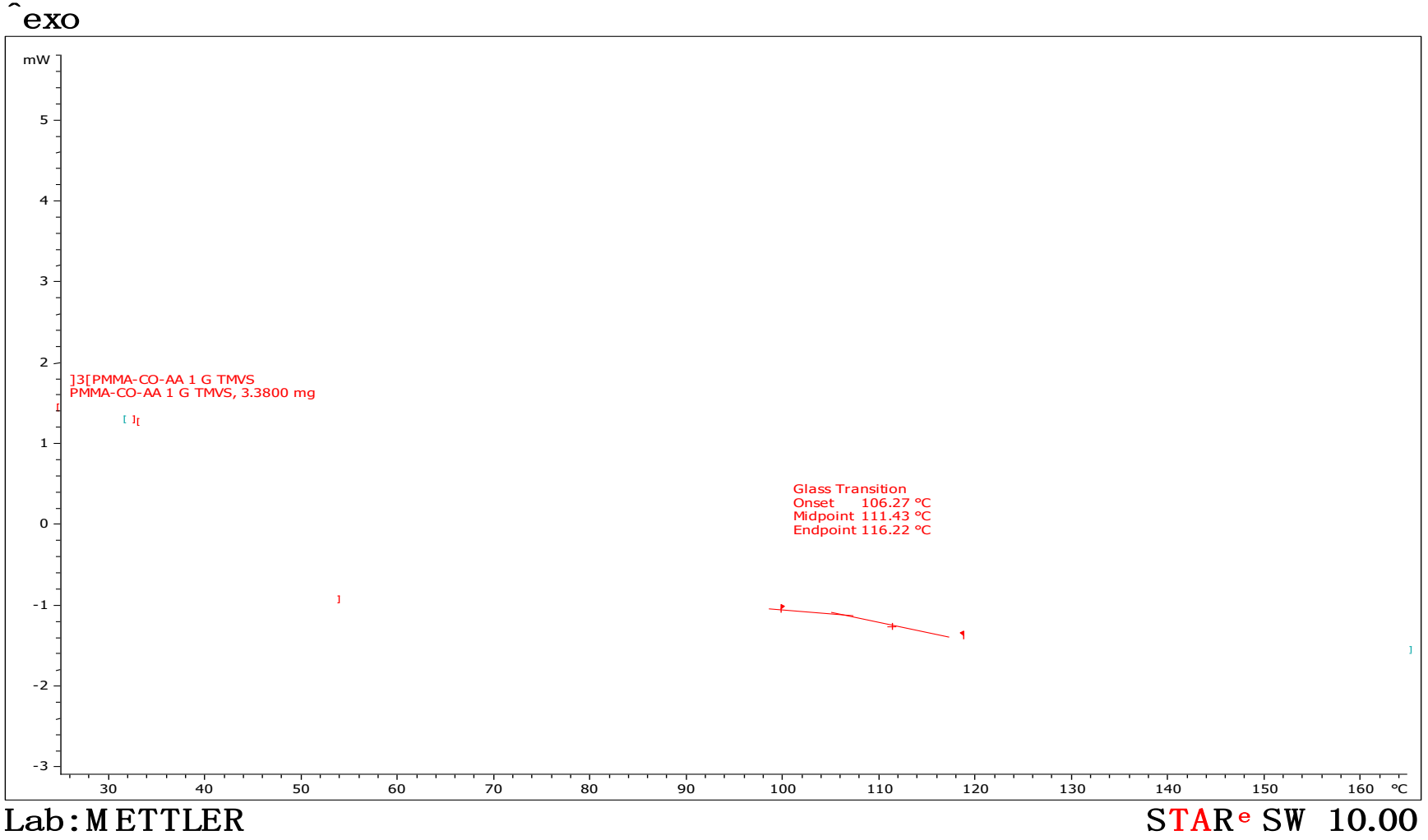

Appendix M

DSC Thermogram of P(MMA-co-AA) with 3 wt% of TMVS

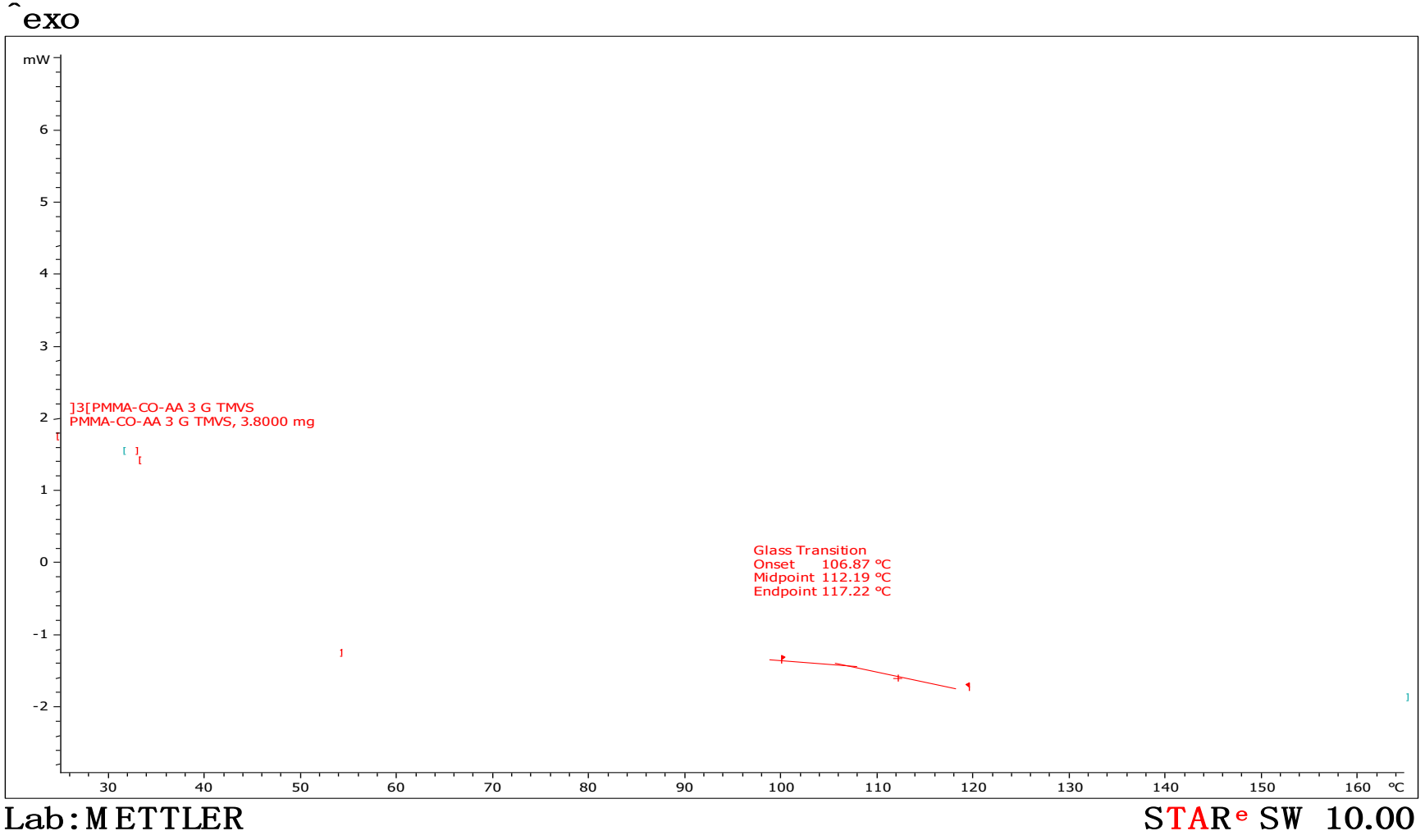

Appendix N

DSC Thermogram of P(MMA-co-AA) with 5 wt% of TMVS

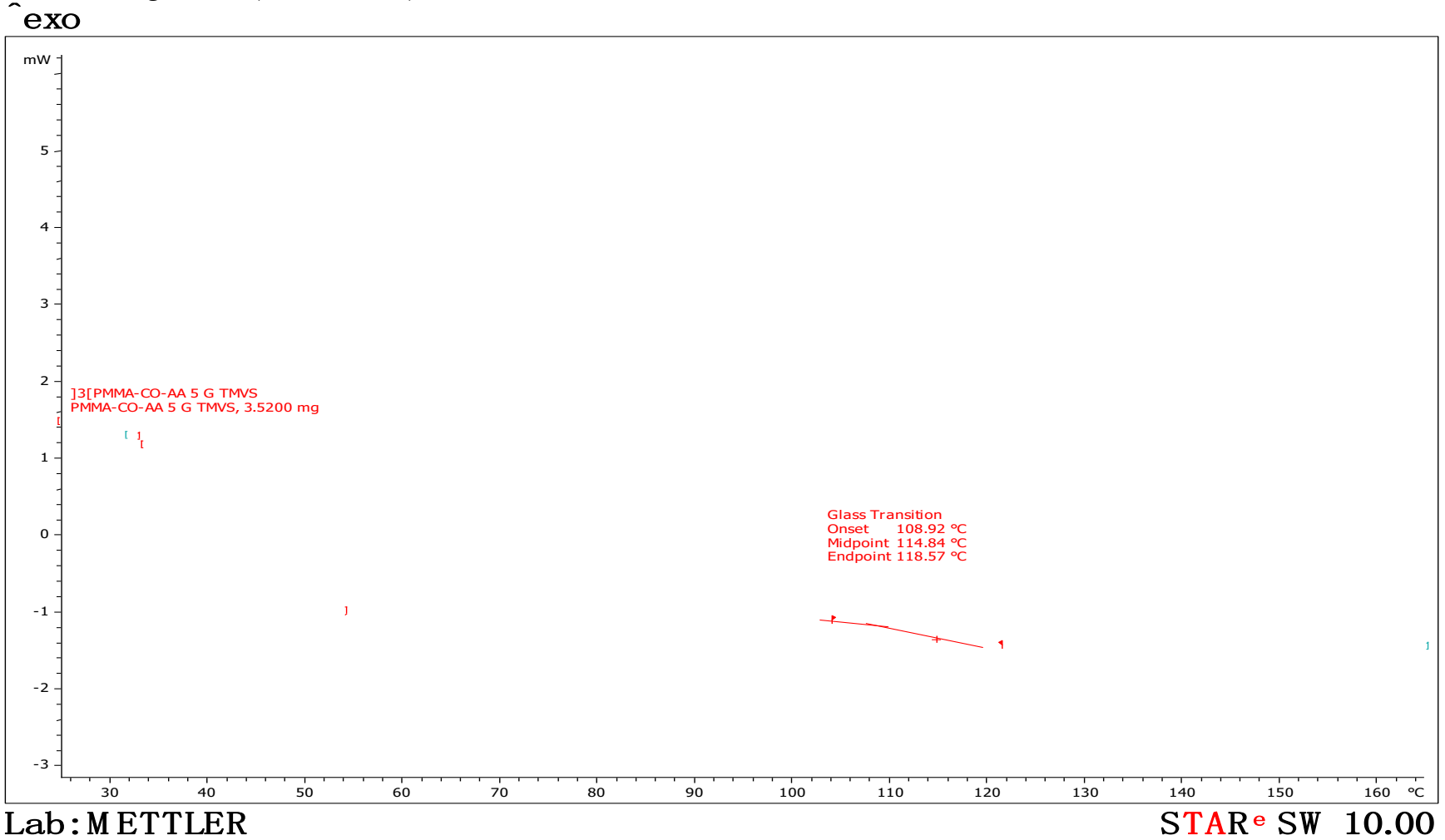

Appendix O

DSC Thermogram of P(MMA-co-AA) with 7 wt% of TMVS

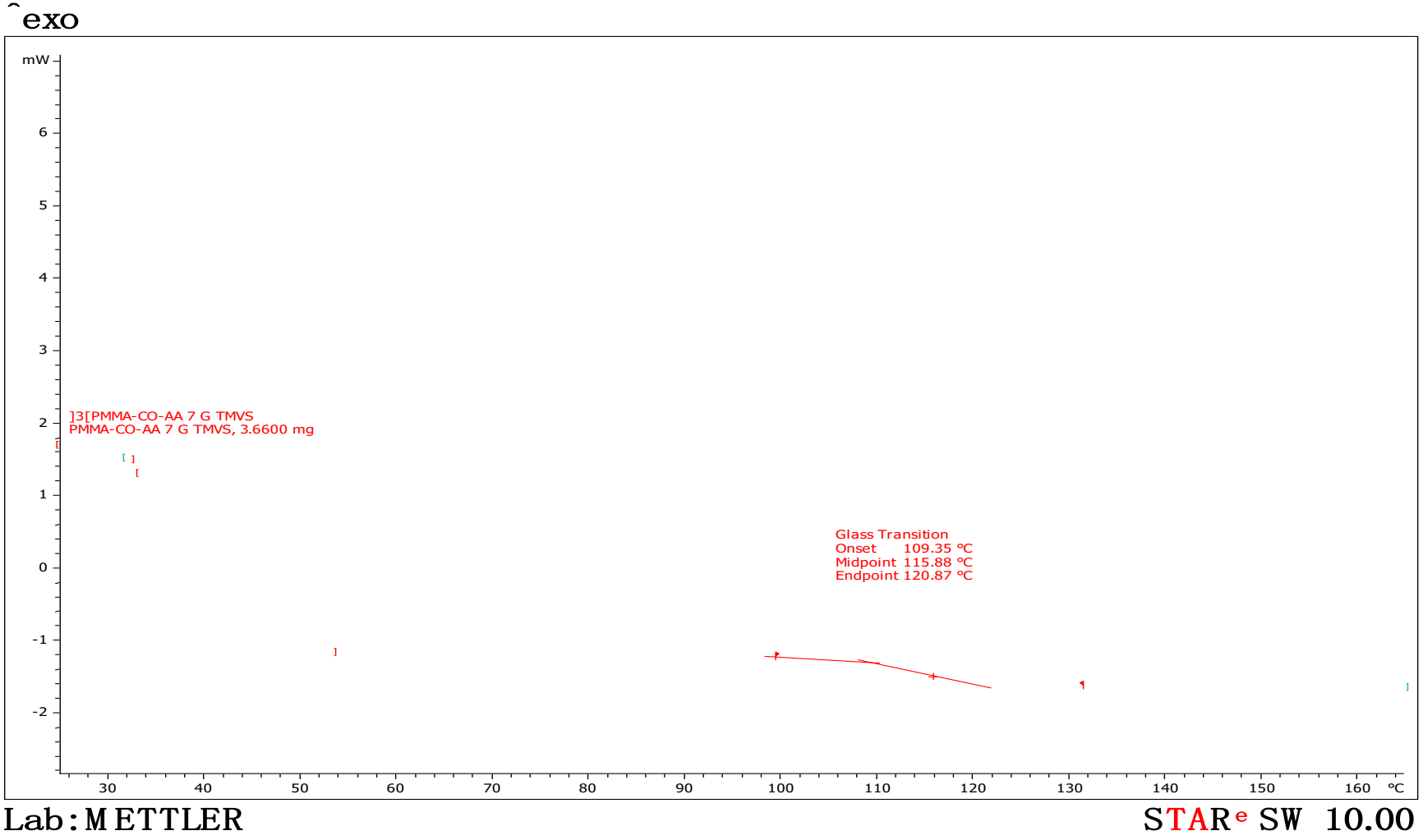

Appendix P

Side view of SEM image of P(MMA-co-AA) incorporated with 1 wt% of TMVS

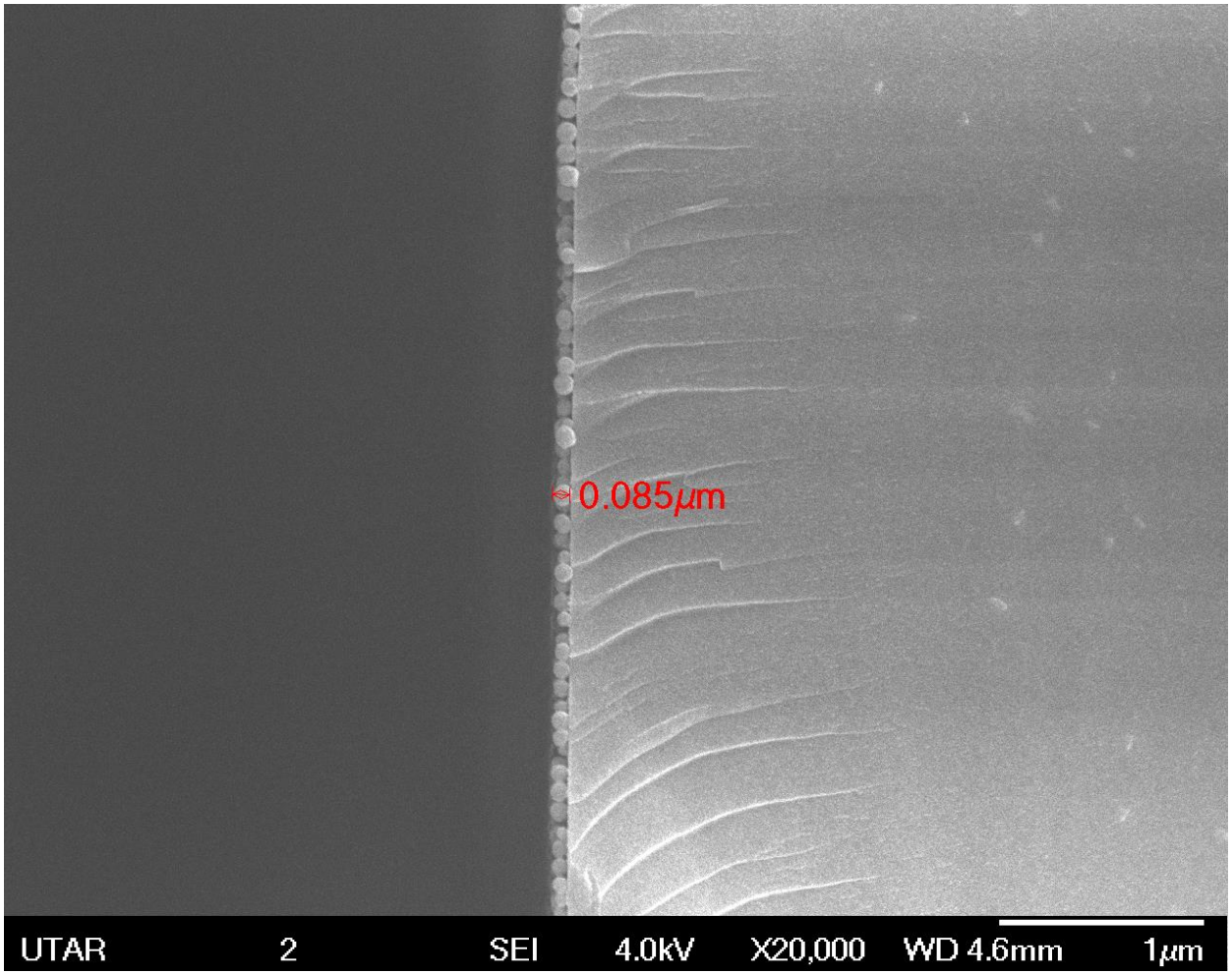

Appendix Q

Side view of SEM image of P(MMA-co-AA) incorporated with 3 wt% of TMVS

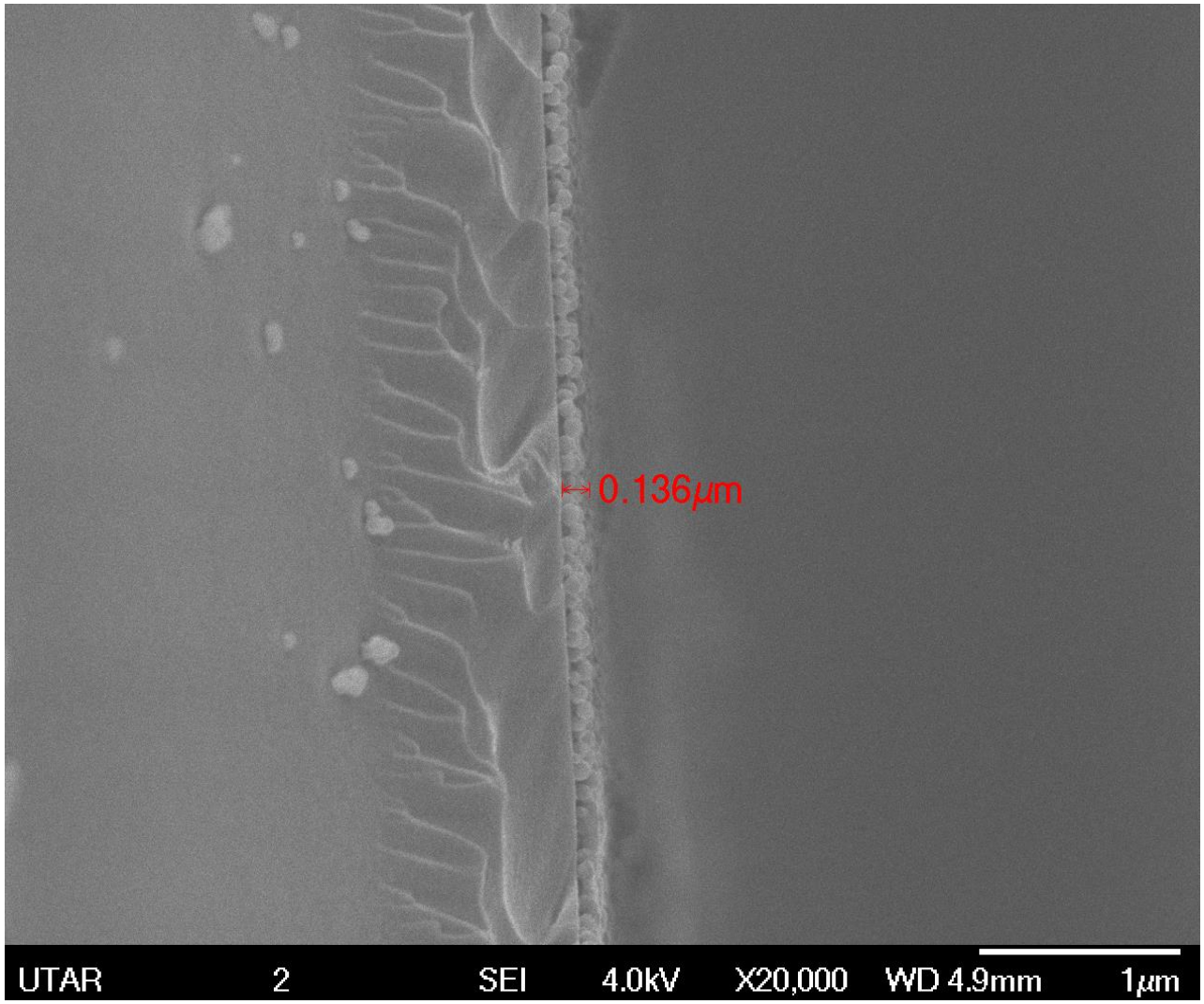

Appendix R

Side view of SEM image of P(MMA-co-AA) incorporated with 5 wt% of TMVS

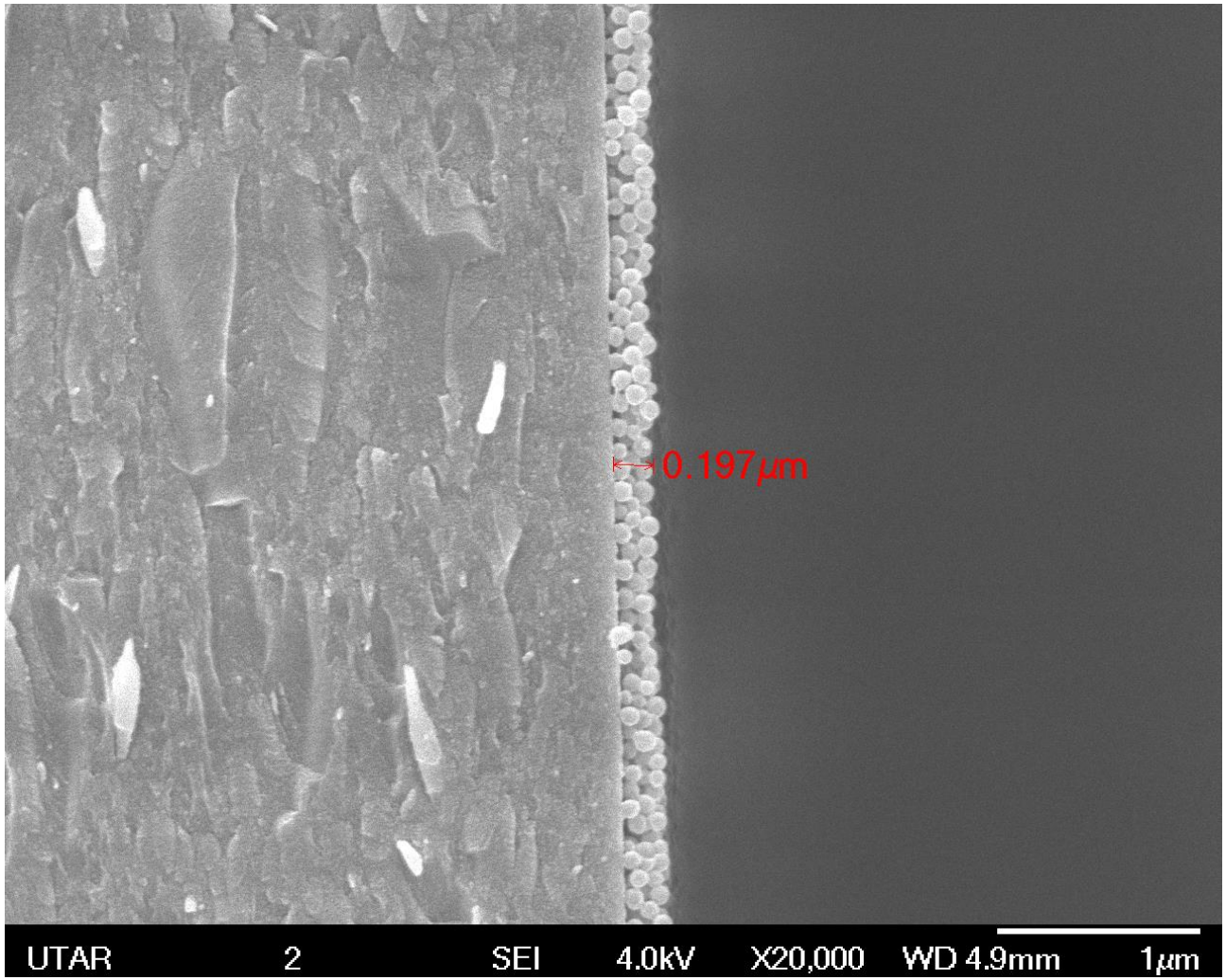

Appendix S

Side view of SEM image of P(MMA-co-AA) incorporated with 7 wt% of TMVS